Department of Mechanical Engineering
University of New Brunswick
Fredericton, N.B.

CA1
DTC 801
85
T11
c.2

TP 6809E

TANK CAR THERMAL RESPONSE ANALYSIS: EXECUTIVE SUMMARY: VOLUME 1

J.E.S. Venart

Prepared for:

TRANSPORT CANADA
TRANSPORTATION DEVELOPMENT CENTRE
Montreal, Quebec H3A 2R3

Prepared By:

University of New Brunswick
Department of Mechanical Engineering
P.O. Box 4400
Fredericton, N.B. E3B 5A3

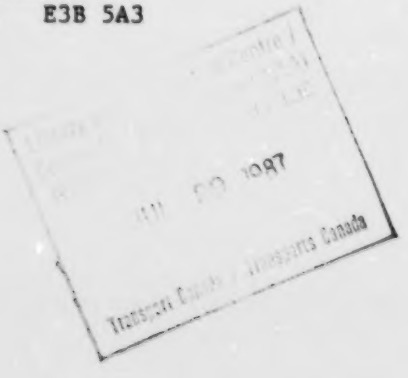

THE CONTENTS OF THIS REPORT REFLECT
THE VIEWS OF THE CONTRACTOR AND NOT
NECESSARILY THE OFFICIAL VIEWS OR
POLICIES OF THE TRANSPORTATION
DEVELOPMENT CENTER

Egalement dispunible en francais: TP 6809 F

REPORT DOCUMENTATION FORM

1. Transport Canada Report No.	2. TDC Project No.	3. Recipient's Catalogue No.
TP 6809E	4727	

4. Title and Subtitle	5. Report Date
TANK CAR THERMAL RESPONSE ANALYSIS:	March 1985
	6. Performing Organization Report No. UNB ME TF 24
7. Author(s)	8. Transport Canada File No.
J.E.S. Venart	D1465-302-2
9. Performing Organization Name and Address Fire Science Centre University of New Brunswick P.O. Box 4400 Fredericton, N.B. E3B 5A3	10. DSS File No. 11SD.T8200-2-2509 11. DSS or Transport Canada Contract No. OSD82-00085
12. Sponsoring Agency Name and Address Transportation Development Centre (TDC) Guy Favreau Complex 200 Dorchester Blvd. West, Suite 601, West Tower Montreal, Quebec H2Z 1X4	13. Type of Report and Period Covered Technical; May 82-May 85 14 Sponsoring Agency Code TDC 4727
15. Supplementary Notes	16. TDC Project Officer D.W. Dibble

17 Abstract

The work reported in this document is concerned with the experimental and analytical simulation of the fire induced heat transfer to rail tank cars containing liquified petroleum gases (propane). The study was undertaken with the purpose of generating a better understanding of the thermal-hydraulic behavior of the lading, tank, pressure relief valve, and a specific internal protection scheme, EXPLOSAFE.

A tank simulator was designed, developed, and used to obtain pressure, temperature, level, and thermal fluid behavior results with heat addition and pressure relief over a wide range of experimental conditions with Refrigerant 11 (R11). The phenomena of free convective liquid stratification and subcooled core heating were analyzed and experimentally confirmed. The effects of surface orientation and enhancement were studied in order to assess their influence on nucleate pool boiling with and without EXPLOSAFE. Analyses of tank geometry and initial liquid level, pool fire - flare interaction, and thermodynamic and transport properties of propane were made. A determination of the vapour space heat transfer was attempted. The thermal conductivity and thermal contact conductance of EXPLOSAFE were measured.

18. Key Words	19. Distribution Statement
Accidents, BLEVE, Boiling, Fires, Pool Fires, Propane, Railway Tank Car Thermal Response, Fire Protection	Limited number of copies available from the Transportation Development Centre

20. Security Classification (of this report)	21. Security Classification (of this page)	22. No. of Pages	23. Price
Unclassified	Unclassified	113	—

TDC CDT 79-005

FORMULE DE DOCUMENTATION POUR RAPPORT

1. N° du rapport Transports Canada	2. N° de l'étude — CDT	3. N° de catalogue du destinataire
TP 6809E	4727	

4. Titre et sous-titre	5. Date du rapport
TANK CAR THERMAL RESPONSE ANALYSIS: Executive Summary	Mars 1985
	6. N° du rapport de l'organisme exécutant: UNB ME TF 24
7. Auteur(s): J.E.S. Venart	8. N° de dossier Transports Canada: D1465-302-2
9. Nom et adresse de l'organisme exécutant: Fire Science Centre, University of New Brunswick, C.P. 4400, Fredericton, N.B. E3B 5A3	10. N° de dossier — ASC: 11SD.T8200-2-2509
	11. N° de contrat — ASC ou Transports Canada: OSD82-00085
12. Nom et adresse de l'organisme parrain: Centre de développement des transports (CDT), Complexe Guy Favreau, tour ouest, 200 o., boul. Dorchester, suite 601, Montréal, Qué H2Z 1X4	13. Genre de rapport et période visée: Technique; mai 82-mai 85
	14. Code de l'organisme parrain: TDC 4727
15. Remarques additionnelles	16. Agent de projet — CDT: D.W. Dibble

17. Résumé

Ce rapport concerne les travaux d'expérimentation et de simulation analytique sur les transferts thermiques induits dans les wagons-citernes contenant du GPL (propane), et soumis à l'action des flammes. La recherche visait à une meilleure connaissance du comportement thermo-hydraulique de la cargaison, du récipient, des soupapes de sûreté et d'un agent antidéflagrant connu sous le nom de EXPLOSAFE.

Un récipient figurant le wagon-citerne a été étudié, construit et utilisé dans le but de faire des observations directes des pressions, températures, niveaux et comportements de la cargaison en phase liquide lorsqu'elle est chauffée et que la surpression est évacuée dans l'atmosphère, et ce dans des conditions expérimentales très variables, utilisant le frigorigène R11 à la place du GPL. Le phénomène de stratification du liquide due à la convection naturelle et au refroidissement de la partie interne du liquide a été analysé et confirmé expérimentalement. L'effet de l'orientation du récipient et de l'extension des surfaces d'échange a également été étudié afin de déterminer son influence sur le phénomène d'ébullition ponctuelle du liquide, avec et sans Explosafe. Des études analytiques ont été faites des divers paramètres en jeu: géométrie du récipient, niveau de remplissage, interaction effet torche-flammes enveloppantes, propriétés thermodynamiques et transferts thermiques du propane. Une détermination a été tentée des transferts thermiques dans l'espace vide au-dessus de la cargaison. La conductivité thermique de l'agent Explosafe et sa conductance thermique au droit des points de contact avec les parois ont également été mesurées.

18. Mots-clés	19 Diffusion
Accidents, explosion d'un gaz en ébullition, incendies, effet torche, propane, comportement thermique d'un wagon-citerne, protection incendie.	Le CDT dispose d'un nombre limité d'exemplaires

20. Classification de sécurité (de ce rapport)	21. Classification de sécurité (de cette page)	22. Nombre de pages	23. Prix
non-classifié	non-classifiée	113	-

TABLE OF CONTENTS

	Page
Summary	1
Introduction	1
Task Assignments and Status	9
TASK 1. Experimental Vessel with Heat Addition and Pressure Release	9
TASK 2. Heat Transfer and Thermal Stratificaitons in Liquid and Vapour with/without EXPLOSAFE	19
2.1 Liquid Stratification	19
2.1.1 Physical Phenomena	20
2.1.2 Modification of Flow Properties for a Porous Boundary Layer	24
2.1.3 Effects of External Stratification on the Boundary Level	26
2.1.4 Results and Discussion for the Integral Solution	26
2.2 A Finite Difference Solution	29
2.2.1 The Difficulties Associated with the Geometry and a Possible Approach	30
2.2.2 The Numerical Method	32
2.2.3 Solution Method	32
2.2.4 Test Runs	33
2.3 Vapour Stratification	42
TASK 3. Boiling and Liquid "Swelling" Process with/without EXPLOSAFE	43
3.1 Boiling as a Function of Surface Orientation	43
3.1.1 Electric Heater	48
3.1.2 Test Specimens	50
3.1.3 T-Vessel and Its Equipment	52
3.1.4 Experimental Results	55
3.2 Two-Phase Swelling Analysis	67
TASK 4. Alternate Protection Schemes	71
TASK 5. Supporting Literature and Analyses	71
5.1 Numerical Model	73
5.2 Thermodynamic Properties	73
5.3 Tank Car Geometry	77
5.4 Cylindrical Surfaced Calorimeter	77
5.5 Thermal Conductivity and Contact Conductance of EXPLOSAFE	80
5.5.1 Experimental	80
5.5.2 Test Samples	83
5.5.3 Theoretical Predictions	84
5.5.4 Results and Discussion	84

TASK 6. Pool Fire - Flare Interaction 87

TASK 7. R12 Test Programme 91

TASK 8. Audio Visual Presentation of Results 91

TASK 9. Test Data Presentation 91

Conclusion 91

Recommendations 94

References 96

Appendix A: Tables of Contents of Supporting Report Volumes [1-7]

A.1 Transient Natural Convection in a Partially Filled Horizontal Cylinder..... 98

A.2 Experimental Deterimation of the heat transfer in the Vapour Space of a Partially Filled Horizontal Cylinder. 100

A.3 Pool Boiling Heat Transfer: The Effects of Enhanced Surfaces and Inclination..... 103

A.4 Supporting Studies..... 105

A.5 Published Papers..... 107

A.6 Pool Fire - Flare Interactions..... 109

A.7 Tank Simulator Test Data..... 112

LIST OF FIGURES

Figure		Page
1	Photograph of Experimental Vessel	5
2	Schematic Diagram of Experimental Setup	6
3	End View of the Lava Housing for Electrical Heaters	7
4	Electrical Circuits for Heaters	8
5	An Example of the Grid Layout of Thermocouples	10
6	Pressure Relief Valve	11
7	Pressure of Vessel	14
8	Vessel Tilted by 65 Deg	15
9	Vessel Tilted by 65 Deg	16
10	Mass of Vessel	17
11	Partially filled horizontal cylinder heated from the side.	21
12	Stratified and unstable fluid zones	22
13	Transient development of vertical temperature profiles for 1=20 kW/sq.m, 92% fill, without EXPLOSAFE	25
14	Momentum boundary layer for various degrees of external stratification (curves 1,2,3, and 4 are defined in text, eqns. 3.19)	27
15	80% fill, with 1" EXPLOSAFE. Transient development of vertical temperature gradient (q=40 kW/m^2)	28
16	85% fill, without EXPLOSAFE. Transient development of vertical temperature gradient (q=20 kW/m^2)	28
17(a)	Physical plane	31
(b)	Mathematical plane	31
18	Velocity profiles for Pr=19950., Gr=1.1	34
19	Temperature profiles for Pr=19950., Gr=1.1	35
20	Temperature profiles for Pr=0.7, Gr=4.5 x 10^4	36
21	Velocity profiles for Pr=0.7, Gr=4.5 x 10^4	37
22	Stream lines in transient computation, Pr=6380., Gr=114, t=4.6 mins	39

23	Isothermals in transient computation, Pr=6380., Gr=114, t=4.6 mins	40
24	Flow pattern for Pr=6380., Gr=35	41
25	Vapour space mean temperature evaluation	45
26	Heat transfer coefficient vs time	46
27	Heat transfer coefficient vs time	47
28	Detailed cross sectional view of the electric heater (actual size)	49
29	Encapsulated heating element	51
30	Heater assembly with Explosafe	51
31	Schematic view of the apparatus	53
32	Detailed electric circuit	54
33	Pool boiling heat transfer with Freon-11 for copper surface at 2 bar	56
34	Effect of orientation for copper surface	57
35	Experimental data with UNB #2 surface in natural convection region and empirical correlation of Fujii and Imura[8]	59
36	Hysteresis effect for UNB #2 surface at 2 bar in R-11	60
37	Comparison of the present results with available data and predictions in film boiling region	63
38	Effect of Explosafe	64
39	Variation of the exponent 'r' in Rohsenow equation	65
40	Variation of the constant 'C_{sf}' in Rohsenow equation	65
41	Correlation of data from mild steel surface using modified Rohsenow equation	66
42	Idealized system for swelling	69
43	Heights at different regions	71
44	Simulation Block Diagram	75
45	Sample Program Output ... on HP 85B	76
46	Flow Diagram of Subroutine TDPROP	77

47	Tank pitch geometry as a function of fill.....	79
48	Views of torch fire wall heater.....	80
49	Views of boiling on torch fire wall heater.....	82
50	Guarded hot-plate apparatus.....	83
51	EXPLOSAFE styles and orientations.....	84
52	Heat transfer model for EXPLOSAFE.....	87
53	Apparent thermal conductivity of EXPLOSAFE.....	88
54	Apparent thermal conductivity of EXPLOSAFE as a function of pressure.....	88
55	Top view of the positions of the equipment in the pool fire for Tests 1 to 3.....	91
56	Top view of the positions of the equipment in the pool fire for Test 4 to 6.....	92

LIST OF TABLES

Table		Page
1	Task Assignments and Final Report Volume Number	3
2	Tank Car Thermal Response Analysis Personnel	4
3	Experimental Program	12
4	Average Heat Transfer Coefficients	44
5	Comparison of major parameters on various surfaces	58
6	Comparison in heat flux and heat transfer coefficient for given superheats with different surfaces	62
7	Comparison between the theoretical and experimental swelling heights for UNB tank with different tank fillings (q/A = 16 kW/m^2, at 2 bar)	73
8	True thermal conductivity of EXPLOSAFE	87
9	Heat flux to Calorimeters and Radiometer in Propanol Pool Fire and Propane Flare Interaction Studies	90

Summary

This document reports on the work performed under the terms of a contract between the University of New Brunswick Fire Science Centre and Transport Canada, Transportation Development Centre entitled "Tank Car Thermal Response Analysis". The work was initiated under DSS File OSD T8200-2-2509, May 15, 1982. This report summarizes the studies undertaken and serves as an executive summary of the work contained in the seven (7) accompanying volumes [1-7] listed below:

Vol 2 Transient Natural Convection in a Partially Filled Horizontal Cylinder [1]

Vol 3 Experimental Determination of the Heat Transfer in the Vapour Space of a Partially Filled Horizontal Cylinder [2]

Vol 4 Pool Boiling Heat Fransfer: The Effects of Enhanced Surfaces and Inclination [3]

Vol 5 Supporting Studies [4]

Vol 6 Published Papers [5]

Vol 7 Pool Fire - Flare Interactions [6]

Vol 8 Tank Simulator Test Data [7]

Introduction

This study has been concerned with the formulation, analysis, modeling, simulation and verification of the fire induced heat transfer to tanks containing liquefied petroleum gas (LPG) or other hazardous materials (eg. LCl_2, NH_3). The time dependent behavior of the contents (pressure, temperature, level (mass)), pressure relief valves(s) (open-close sequence, mass flow rate, discharge (single (vapour or liquid) or two-phase)), flare (strength and position), tank (temperature and stresses), fire surrounds (intensity and location) and protection (internal and external) has been experimentally simulated and analytical/numerical models developed in order to determine whether full sized tanks exposed to accidental pool or torch fire environments will explode or BLEVE (boiling liquid expanding vapour explosion).

The work, initiated and funded by the Transportation Development Centre (TDC) of Transport Canada, commenced May 15, 1982. It was undertaken with the express purpose of generating a better understanding of the thermal hydraulic behavior of tanks containing LPG in a fire accident when unprotected (uninsulated) or protected with EXPLOSAFE. Aspects of this study addressed the experimental observation of pressurized fluid behavior (R11) with heat addition and pressure relief with and without EXPLOSAFE, free convection thermal stratification in the liquid and vapour contents, the effects of orientation and surface preparation on the boiling process, the pool fire - flare interaction, vapour space heat transfer and ancillary subjects. A detailed listing of the tasks undertaken is provided in Table 1. The personnel associated with the work are given in Table 2. Details of these tables are discussed later in this report.

The study to date has been supported by both Transport Canada, through the Transportation Development Centre (TDC), and the Natural Sciences and Engineering Research Council of Canada (NSERC), the latter through a three year strategic grant which commenced its third year in November 1985. A contract proposal entitled "Tank Thermal Response Analysis: Phase II" (September 10, 1984) has been prepared and submitted for comment and possible consideration to Transport Canada for a continuation of some aspects of the project.

The major accomplishment of this work has been the design, fabrication, testing, and utilization of the primary experimental device. This facility consists of a instrumented 381 mm diameter x 330 mm long double walled electrically heated pressure vessel with associated pressure relief valve and 1" thick plexiglass viewing windows. R11 is used as the simulant lading fluid. Figure 1 is a photograph of the test vessel. A schematic diagram of

the facility is shown in Figure 2.

Testing has been conducted as a function of heat flux (20-80kW$_e$/m^2), fill level (78,55, and 23% by volume), pressure relief valve size and operation, and protection (EXPLOSAFE). The heat flux is provided from electric heaters (Figures 3,4) strapped to the inner thin walled stainless steel vessel inside an argon or dry nitrogen ballasted outer pressure vessel. The heaters are controlled by 3 - 3 phase 208 V variacs.

TABLE 1 - TASK ASSIGNMENTS AND FINAL REPORT VOLUME NUMBER

TASK	DESCRIPTION	VOLUME	REFERENCES
1.	a) Design, fabricate, develop, instrument and test an experimental system to study tank/fluid behavior with external heat addition and pressure release with/without EXPLOSAFE	1,8a,8b	[1,7]
	b) Experiments in support		
2.	Heat transfer and thermal stratification in liquid and vapour with/without EXPLOSAFE	1,2,8a,8b	[1,2,7]
3.	Boiling and liquid "swelling" process with/without EXPLOSAFE	3,8a,8b	[3]
4.	Alternative interior protection schemes	1	[2]
5.	Supporting analysis, information, literature and publications - Literature - Numerical model - External boundary conditions - pool fire characterization - Thermal Conductivity and Contact Conductance of EXPLOSAFE - Thermal Properties of Propane - Hot Spot Simulation Apparatus - Geometry - Publications	4,5	[4,5]
6.	Pool Fire-Flare interaction	7	[6]
7.	Audio Visual Data Presentation	8	[7]
8.	Final Report		Executive Summary

Table 2 - Tank Car Thermal Response Analysis Personnel

Personnel currently associated with the project and their status and affiliation:

Dr. J.E.S. Venart, P.Eng	Director & Co-principal Investigator	Mechanical Eng. & Fire Science Centre (FSC)	May 15/82 - present
Dr. F.R. Steward, P.Eng.	Co-Principal Investigator	Chemical Eng. & FSC	May 15/82 - present
Dr. A.C.M. de Sousa	Co-Principal Investigator	Mech. Eng. & FSC	May 15/82 - present
Dr. J.G. Lenard, P.Eng.	Co-Principal Investigator	Mech. Eng.	May 15/82 - Sept 15/84
Dr. R.C. Prasad	Assistant Investigator	Faculty of Eng., UNBSJ	Sept./82 - present
V. Magapu	Research Assistant (PT, Ph.D.Candidate)	Mech. Eng.	April/84 - present
G. Smith	Technician	Mech. Eng.	Nov./82 - present
E. Richard	Research Technician	Chem. Eng. & FSC	Sept./83 - Sept./84
R. Doyle	Assistant (MScE Candidate)	ME	Sept./83 - present
G. Qureshi	Assistant (MScE Candidate)	ME	Sept./82 - March/85
S. Smathaparla	Assistant (MScE Candidate)	ChE	Sept./83 - present
Q. Wang	Assistant (MScE Candidate)	ME	Sept./83 - present
P. Wentzell	Assistant (MScE Candidate)	ME	Sept./83 - present
S. Wong	Assistant (Ph.D. Candidate)	ChE	Sept./83 - present

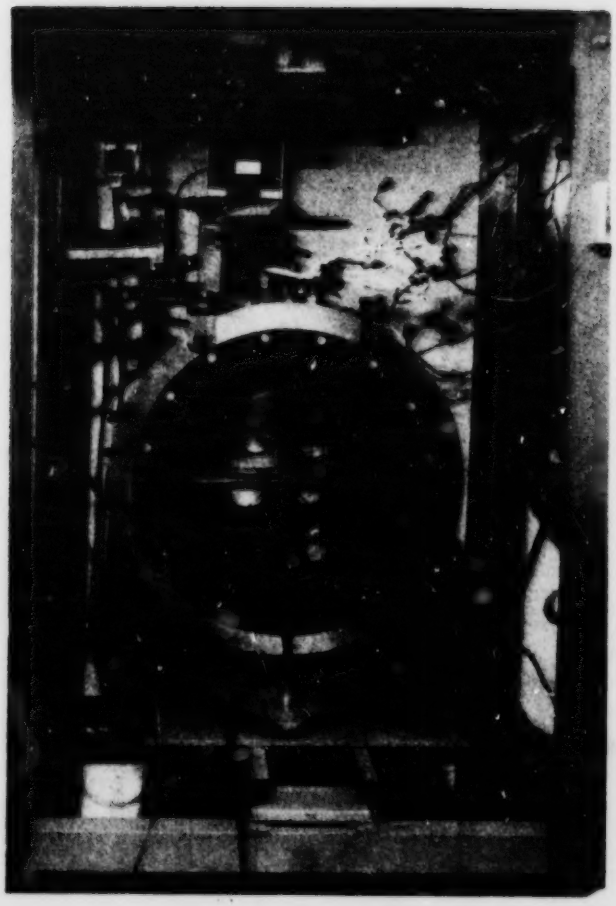

Figure 1. Photograph of Experimental Vessel

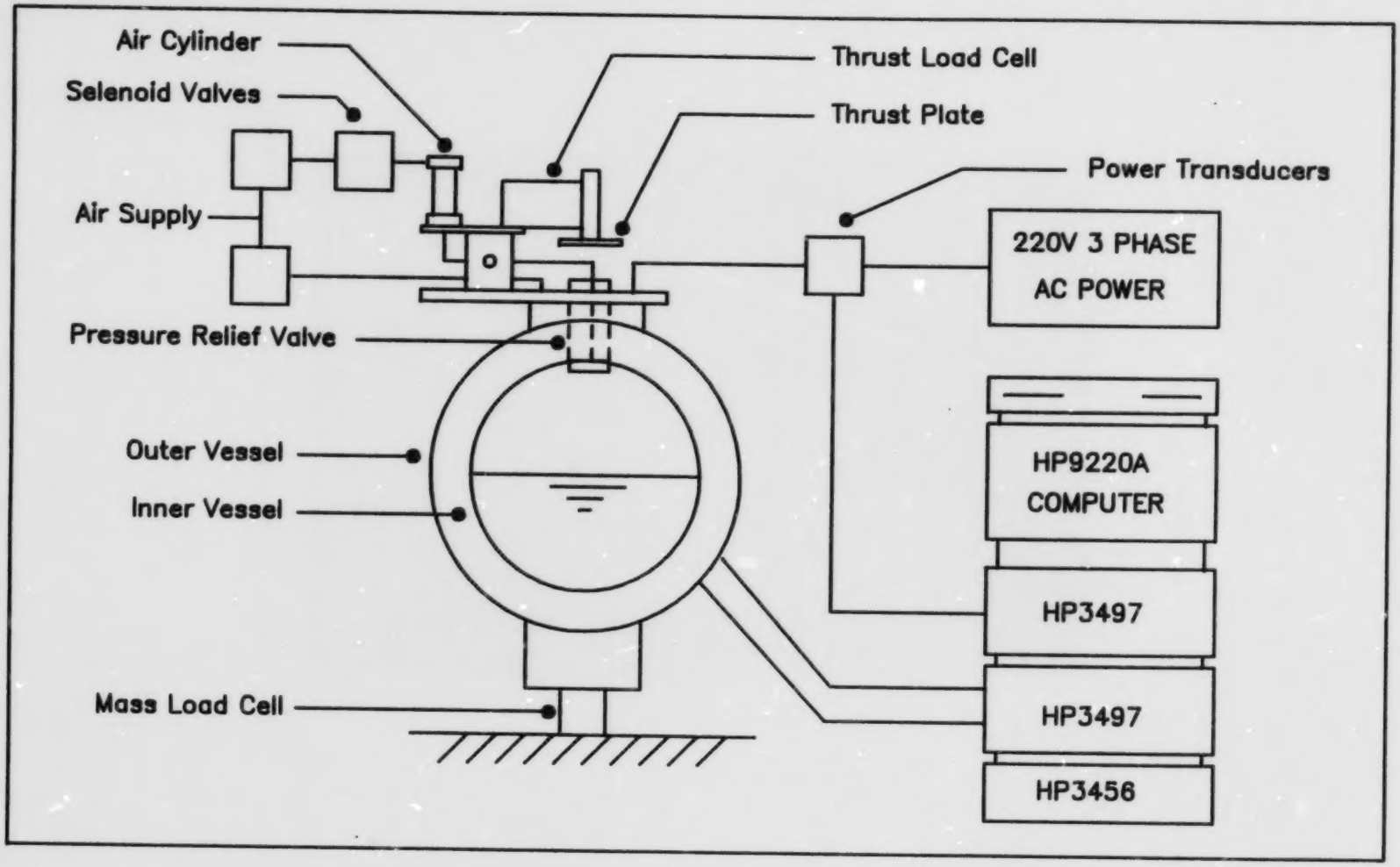

Figure 2. Schematic Diagram of the Experimental Setup

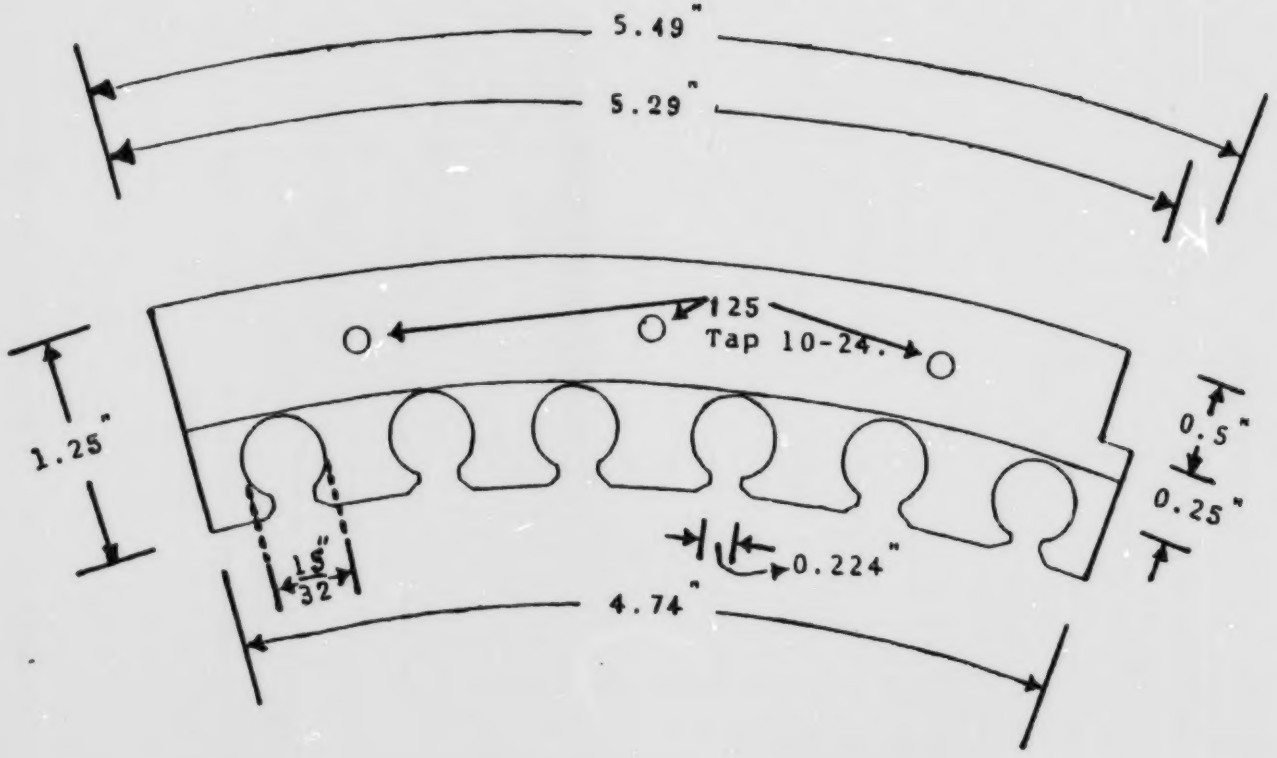

Figure 3. End View of the Lava Housing for Electrical Heaters

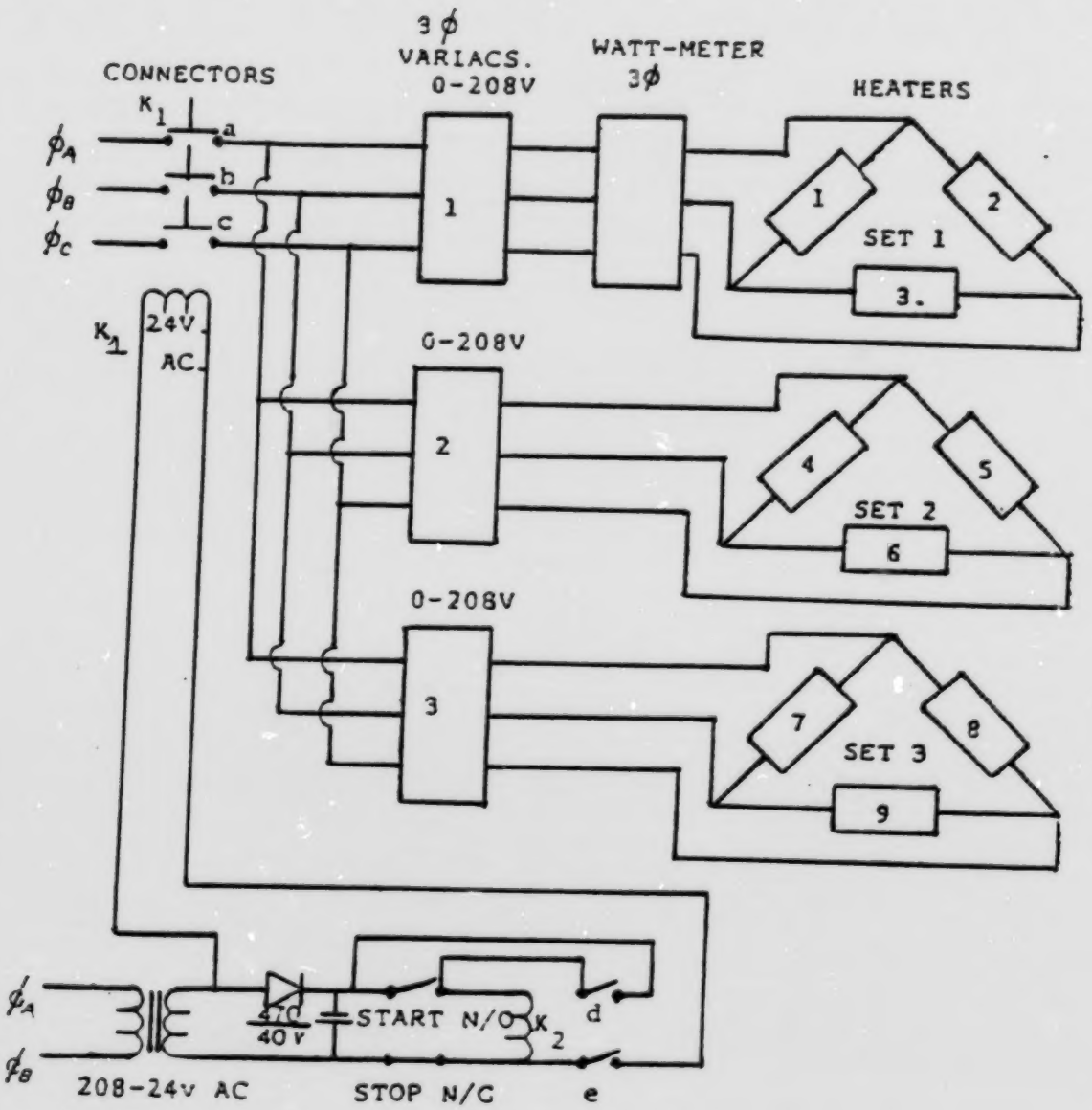

Figure 4. Electrical circuit for heaters.

Temperature (Figure 5) and pressure measurements as well as pressure relief valve action (Figure 6) are obtained/controlled via an HP-85B+3456, 3437, 3497 DVM, 120+ channel data acquisition and control unit (Figure 2). These units have now been supplemented to provide capability for the spatial and temporal determination of void fraction using capacitance measurements, mass discharge and PRV discharge thrust with new data acquisition and control equipment provided by an NSERC strategic equipment grant (November 1984).

The measurement programme undertaken in the present study is outlined in Table 3 and all the experimental results detailed in Volume 8 [7] of this report by the numerical and plotted data and their associated time synchronized video records.

Task Assignments and Status

The task assignments are outlined in Table 1. In the discussion that follows, each of the task assignments is considered in some detail along with a compilation of the pertinent results obtained so to summarize here the work.

A more detailed discussion of each task and its results may be obtained from a consideration of the relevant supporting volume(s) noted earlier.

TASK 1. Experimental Vessel with Heat Addition and Pressure Release.

The experimental facility and auxiliary systems (Figures 1 and 2) has been used in the test programme (Table 3) to obtain the experimental pressure, temperature, level and fluid behavior results given in [7]. These are reported as a function of heat flux, initial fill, pressure relief valve area, and internal protection (EXPLOSAFE).

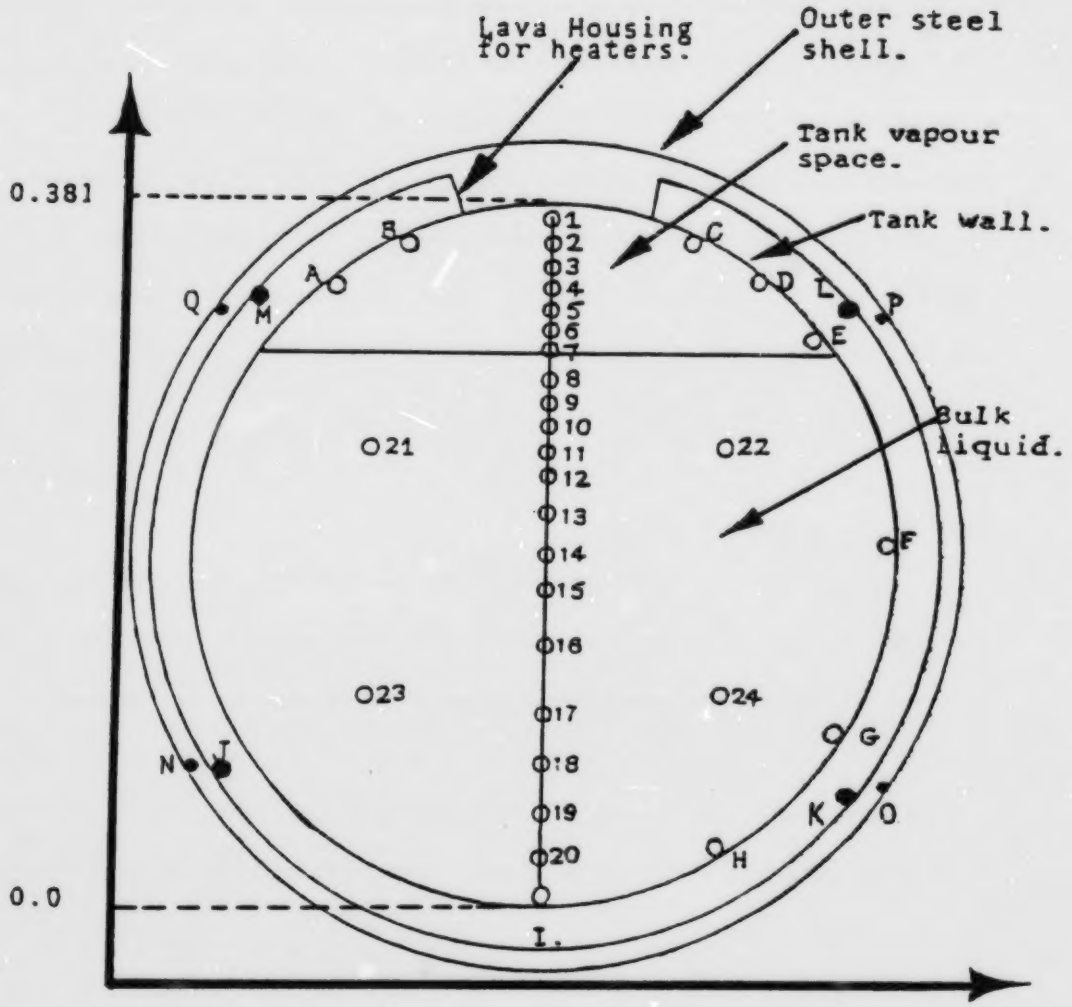

Inside wall thermocouples	-	9	Iron constantan	(A-I)
Lava housing	"	- 4	"	" (J-M)
Outer shell	"	- 4	"	" (N-Q)
Fluid	"	- 24	Copper	" (1-24)

Figure 5. An example of the grid layout of thermocouples.

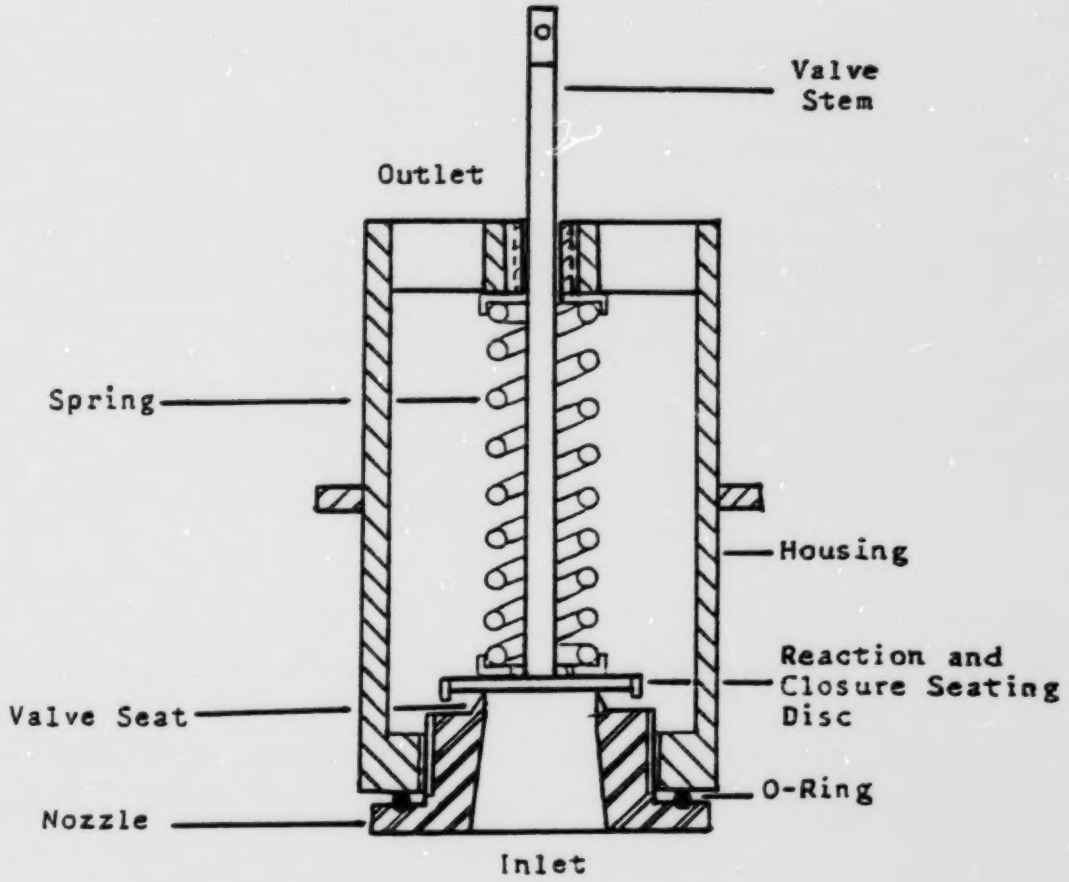

Figure 6. Pressure Relief Valve

Table 3. Experimental Program

	Type: Protected or Unprotected	Heat Flux (kW/m^2)	PRV Orifice Diameter	Liquid Level PRECENT
	PHASE I.			
1.	UNPROTECTED.	10.	3/8"(9.5 mm)	65.
2.	"	65.	1/4"(6.4 mm)	76.
3.	"	65.	"	58.
4.	"	65.	"	23.
5.	"	65.	3/8"(9.5 mm)	76.
6.	"	65.	"	58.
7.	"	65.	"	23.
	PHASE II.			
8.	EXPLOSAFE.	40.	3/8"(9.5 mm)	74.
9.	"	40.	"	58.
10.	"	40.	"	23.

The test programme used R11 as the simulant fluid, lading fills of 80, 55, and 25 percent, heater power levels of 25, 40 and 65 kW/m^2, pressure relief valve orifices of 6 and 9 mm for saturated initial conditions with and without an inner 25 mm thick EXPLOSAFE annulus wall protection for some tests.

To date the basic experiments in the test facility (Volume 2, [1] Volume 3 [2]) have indicated the very complex nature and interdependence

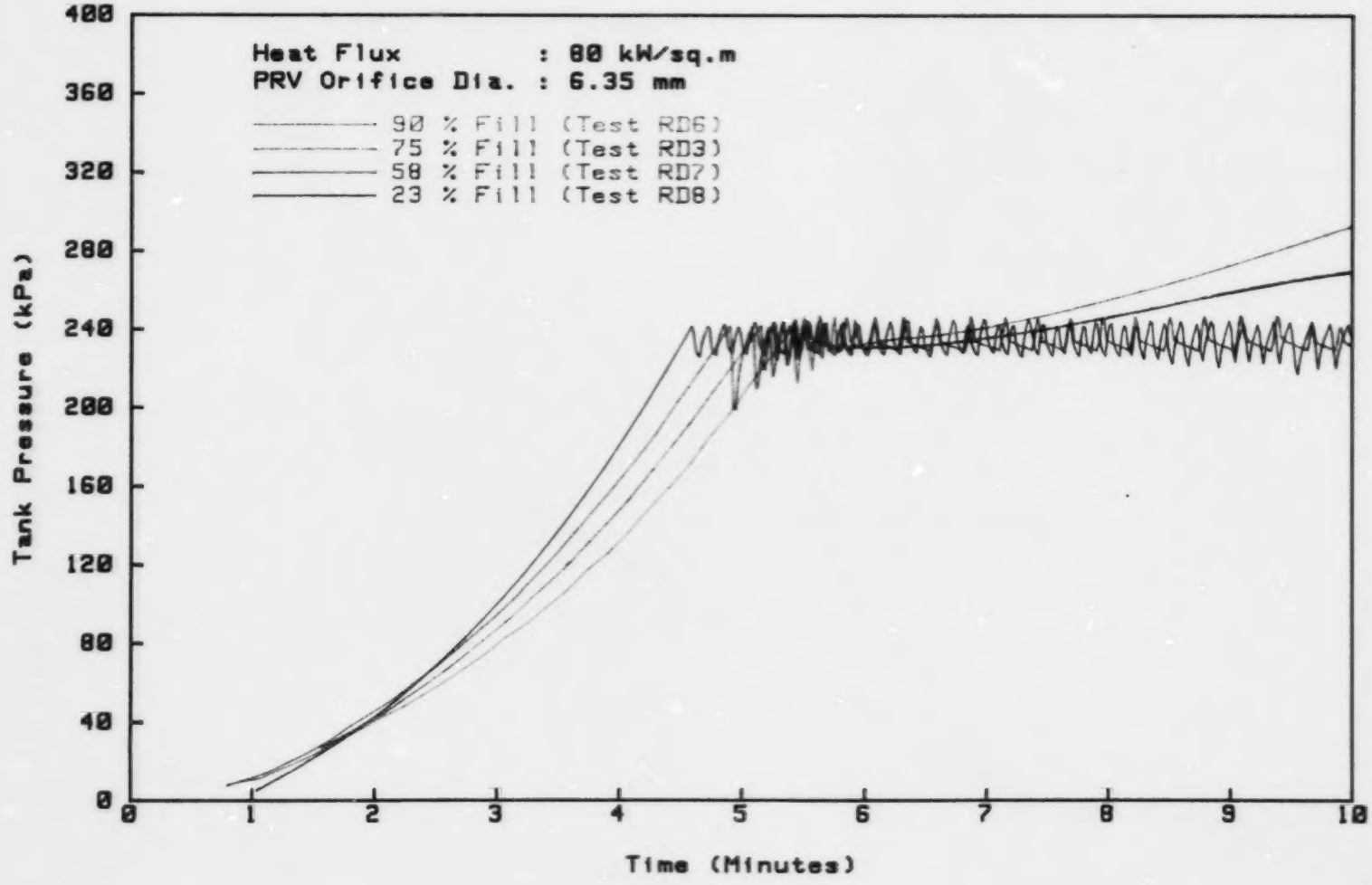

Figure 7. Pressure of Vessel

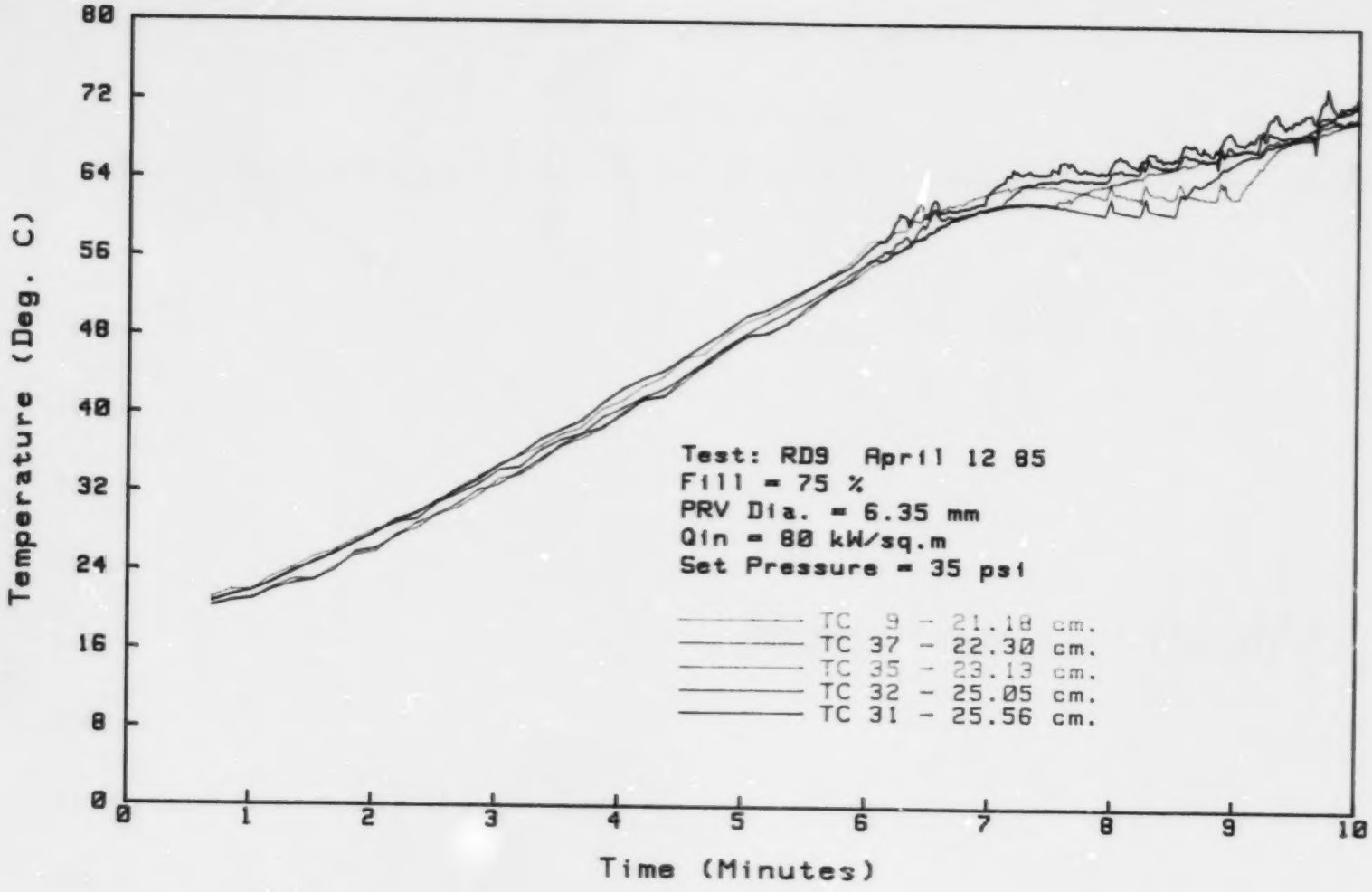

Figure 8. Fluid Temperatures - Vessel Tilted by 65 Deg.

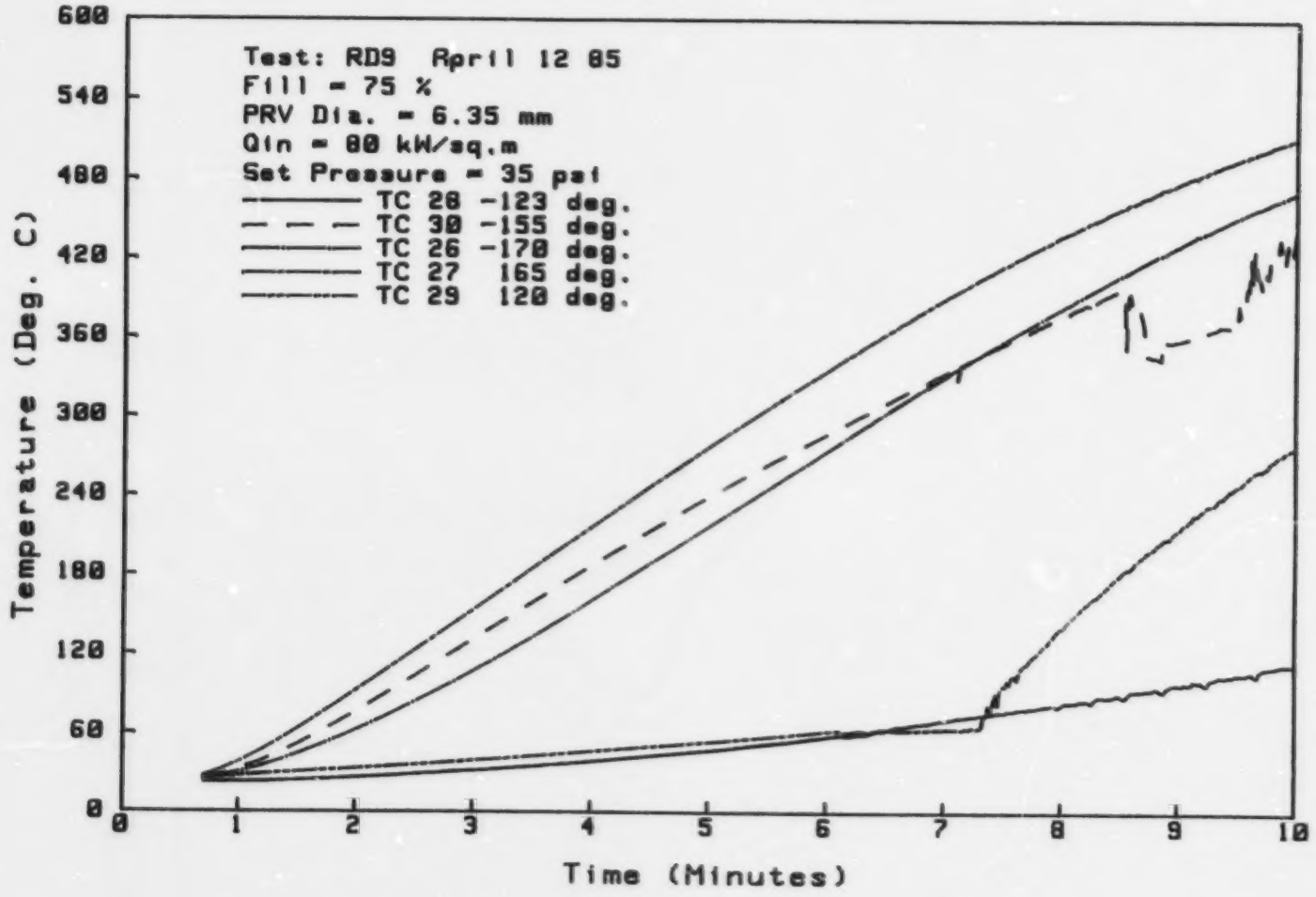

Figure 9. Wall Temperatures - Vessel Tilted by 65 Deg.

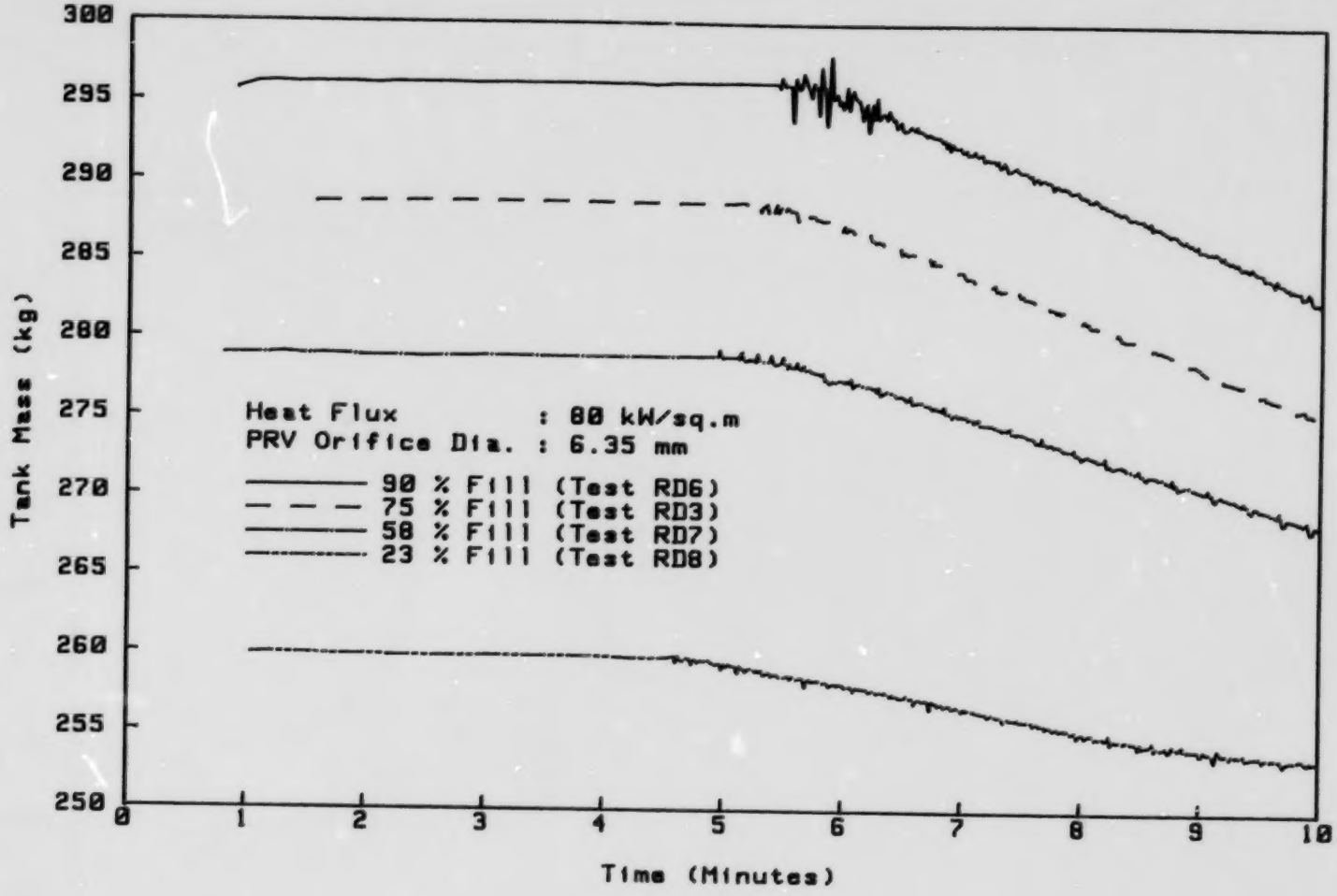

Figure 10. Mass of Vessel

of the thermohydraulic phenomena. The pressure (Figure 7), temperature (Figures 8 and 9), and mass (Figure 10) temporal response as a function of heat flux and level exhibit this complexity. These figures illustrate the tank response from tests later than those reported here. The elements that have the most profound effect on tank lading behavior are the amount of thermal stratification and hence subcooling and superheat, the pressure-time and temperature-time responses, and the boiling process as well as the unsteady flashing and two phase swelling processes which occur with changes in vent size and action. The thermal stratification and boiling phenomenon will be discussed later. Here we will only generally discuss the pressure and temperature response of the tank and its contents as well as the mass flow behavior of the pressure relief valve. More specific details and conclusions are to be found in the requisite volumes [2,3,7].

The rate of pressure rise increases significantly with increasing heat flux and decreasing volumetric fill (Figure 7). The pressure relief value behavior also alters from one of constant on-off cycling at low lading fills (23%) to intermittent close/open cycles with characteristic pressure reduction and recovery (55%), to the maintenance of continuous venting with either decreasing rate of pressure increase (75%) or increasing rate of pressure increase (90%).

Fluid temperatures rise with increasing time exhibiting the stratification patterns to be discussed later and the influence of value cycling, particularly on temperatures in the vicinity of the PRV vent. The surface temperature of the liquid sets the pressure and hence causes valve behavior. In particular the pressure recovery during valve action supplemented by detailed analysis of video records confirms the following sequence of events during valve cycling:

- the initial outrush of fluid is superheated vapour.

- as pressure falls the now superheated stratified fluid flashes to vapour with some time delay. The vapour generation rate may be less or greater than valve capacity.

- depending upon the depth of the superheated layer, which in turn is dependent upon the external heat flux and time, the pressure can either fall or rise depending upon valve capacity and the degree of two phase carry over to the vapour in the form of liquid droplets (mist flow) or vapour bubble carry under in the bulk liquid causing gross liquid "swelling" and hence two phase ingestation by the valve.

- If two phase ingestation is significant valve pressure relieving capacity is reduced and the pressure rises.

- If the heat flux to the liquid is sufficient vapour generation exceeds valve capacity and the pressure rises.

- As liquid level falls, vapour generation with constant heat input to the liquid, decreases eventually leading to valve closure and subsequent cycling until all the lading is vapourized.

During the above events, due to the very low vapour space heat transfer coefficients, tank wall temperatures increase significantly, > 600°C (Figure 9). Unless tank wall temperatures are reduced or tank contents relieved rapidly, tank failure and a BLEVE is imminent.

Mass releases through the valve (Figure 10) illustrate the effects of two phase discharge in the initial vents for lading fills of 90, 75, and 55%. Although, there was some visual evidence of liquid droplet discharge in the 23% fill there is little effect shown in the mass - time response.

TASK 2. Heat Transfer and Thermal Stratifications in Liquid and Vapour with/without EXPLOSAFE.

2.1 Liquid Stratification

The analysis and verification of wall free convection, subcooled core heating and stratification in the liquid space has been completed [1] and reported [4,5]. The problem considered the transient natural convection of fluid in a partially filled, uniformly heated horizontal cylinder. Two methods were used to solve the governing equations of motion. In the first the governing equations were rewritten in their integral form and closed form expressions obtained for the thermal stratification occurring in the vessel. This solution utilized a new stability criteria for the commencement of the wall boundary layer on the inner surface of a convex wall. The predictions obtained compared favorably with the experimental data both with and without EXPLOSAFE. In the second method the differential equations of motion were numerically integrated using finite differences after coordinate transformation. The computation results compare satisfactorily with experimental data for completely filled tanks and qualitative agreement in the experimental flow pattern in partially filled tanks was obtained. The objective of the work was to be able to predict the temperature time history of the lading and the fluid's surface temperature hence determining the rate of increase of pressure in the vapour, particularly if either external (insulation or water spray) or internal (EXPLOSAFE) protection is provided to the tank.

The problem in its simplified form, consists of a partially filled vessel and is a typical example for natural convection in enclosed spaces, as shown in Fig. 11.

In external problems, Prandtl's boundary layer theory is directly applicable and the complete equations of motion are reduced to the so called

"boundary layer equations", where it is presumed that the boundary layer flow does not affect the external medium.

Contrary to the above, flow in internal convection problems, the boundary layer affects the surrounding fluid therefore coupling the two regions. This coupling constitutes the main source of difficulty in obtaining analytical solutions to such enclosure problems.

The problem besides this possesses difficulties arising due to the partial filling. That is, the boundaries surrounding the liquid are not aligned with the coordinate system as in the case of a rectangular enclosure or a completely filled horizontal cylinder where Cartesian or polar coordinates can be used with ease.

The following qualitative descriptions are due to the experiments carried out with the 380 mm diameter stainless steel tank heated uniformly (excluding a small portion of approximately 30° chord angle at the top) whose ends are covered with plexiglass walls permitting clear visualization and video recording. The details of instrumentation control hardware and software along with the experimental procedure are discussed in [2].

2.1.1 Physical Phenomena

When the walls of the horizontal tank are suddenly exposed to uniform heating, heat is transferred to the fluid core mainly by conduction. After a short time delay, buoyancy forces overcome gravitational forces and the fluid adjacent to walls rises along the walls, up to the free surface, as depicted in Fig. 12. The heated fluid spreads towards the center as it reaches the surface and gradually forms a distinct warm layer in which a positive temperature gradient exists with a maximum at the interface. The flow inside the cylinder is

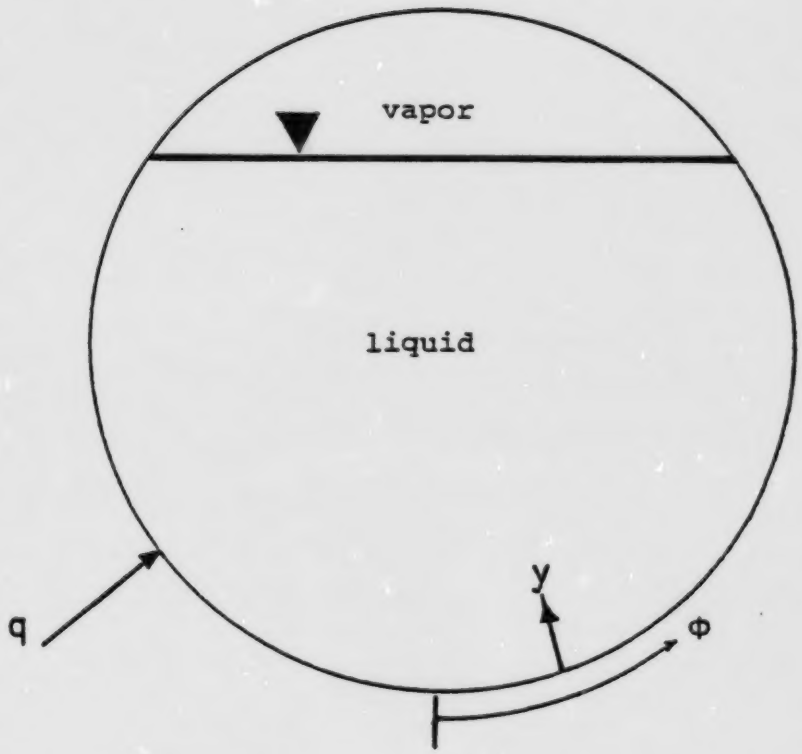

Figure 11. Partially filled horizontal cylinder heated from the side.

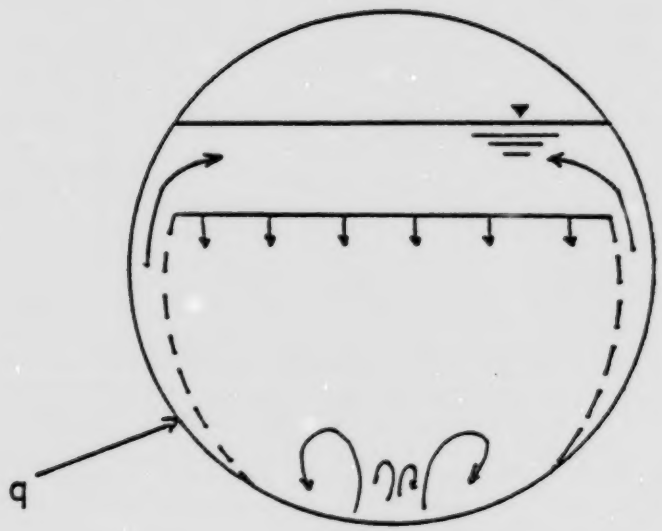

Figure 12. Stratifed and Unstable Fluid Zones

recirculating innature, but the magnitudes of the velocities inside the bulk of the liquid are essentially very much smaller than the boundary layer velocities. The stratification developed in this form is stable and the shape of the temperature profile in the vertical direction does not change significantly as time progresses, although the circulatory motion accelerates up to a point. The pressure in the vapor space is at a saturation condition consistent with the liquid interface temperature. That is, the interface temperature controls the pressure in the vapor space. The determination of time dependent stratification is, therefore, of considerable importance.

Another observation made from the experiments is that of an unstable region at the cylinder bottom. In this region, the heat transfer mechanism is similar to the case where a horizontal or nearly horizontal heated plate faces upwards. In this unstable region mixing between heated and core fluid occurs contributing to the increase of bulk temperature. It is necessary, therefore, to predict the initiation of the stable wall boundary layer after this region and modify any analysis accordingly.

In summary, the following can be deduced from the above description:

(a) There exists a thin boundary layer where the velocities are much higher than the downward core velocities.

(b) The fluid layers in the stratified region are isothermal in a horizontal direction.

(c) Furthermore, relying on experimental data, for moderate heat fluxes of the order of 0-30 kW/m^2, such as will occur with insulated tanks or the initial phases of unprotected tanks, it can be stated that the core region below the stratified layer is in a quasi isothermal state. That is, the spatial temperature distribution in the core is uniform but the core temperature increases as time progresses. In Fig. 13 the region below the

dashed line indicates the presence of isothermal conditions in the core with almost vertical profiles (note that each profile is at a different time level), therefore justifying this assumption.

Item (a) stated above automatically uncouples the internal core from the boundary layer flow and allows a treatment similar to an external boundary layer problem while (b) permits the use of a single temperature profile in the stratified layer in the vertical direction. In (c) it is suggested that influence of external stratification can be neglected at the early stages of heating such as warm liquid injection into the core from the boundary layer. The effects of this case have been determined in a separate analysis and examined for various degrees of stratification after an integral analysis. The details of the analysis and solution techniques are presented in [1].

2.1.2 Modification of Flow Properties for a Porous Boundary Layer

To deal with the physical situation in which EXPLOSAFE, covers the inside walls of the tank, the following modifications to the fluid properties are made.

(a) The thermal conductivity is calculated based on the configuration of the aluminum mesh immersed in Freon 11 at stagnation conditions. A general methodology for this is given in an appendix of [1] where the effective conductivity (solid and stagnant liquid) are given versus various void fractions at several solid to liquid conductivity rations.

(b) The heat capacity and thermal expansion coefficient is unchanged.

(c) The density of the mesh/fluid combination is the weighted average.

(d) The effective kinematic viscosity is 1.8 times larger than that of Freon 11 based on the assumption of similarity between heat and momentum diffusion.

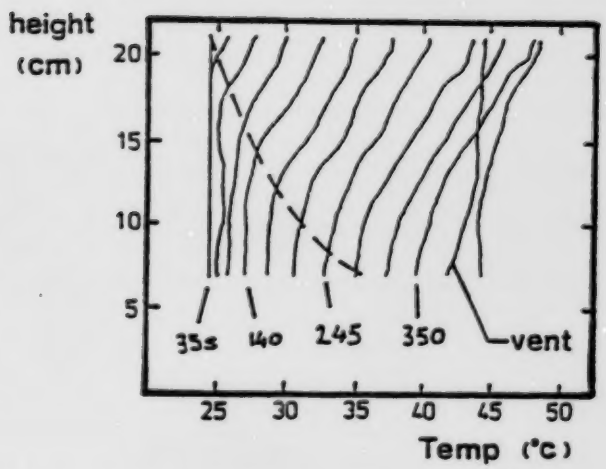

Figure 13. Transient development of vertical temperature profiles for q-20 kW/m^2, 92% fill, without EXPLOSAFE.

The proposed approach is very simple but a reasonable one since the EXPLOSAFE saturated fluid possesses a very low void fraction (~ 0.03). Its role is mainly to conduct heat away from the wall further into the core, essentially accelerating the stratification process since a larger amount of fluid is entrained in the boundary layer (due to the augmentation in the conductivity).

2.1.3 Effects of External Stratification on the Boundary Layer

The effect of external stratification shows itself with the injection of warm liquid into the surrounding medium, thus resulting in the thinning of momentum boundary layer. In Fig. 14 this thinning is shown to become greater as the temperature gradient outside the boundary increases.

The external temperature gradient has a deaccelerating effect on the boundary layer, similar to an adverse pressure gradient in forced flow. Naturally, the driving force in free convection is the temperature difference between the core and the point of interest. Once this difference becomes smaller in the downstream direction, the flow deaccelerates.

In the analysis presented in [1] an isothermal core is considered but once the liquid is completely stratified, this approach is not sufficient and one must solve the perturbation equations along with the energy and mass equations.

2.1.4 Results and Discussion for the Integral Solution

Data from experiments with R11 for two different fill heights are plotted along with the analytical predictions in Figs. 15 and 16 with and without the internal protection material EXPLOSAFE. The proposed approach leads to very close agreement despite the simplifying assumptions utilized in

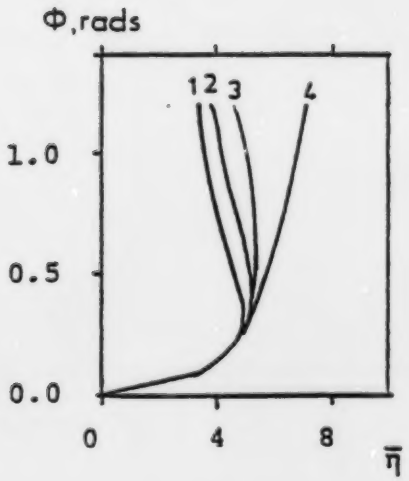

Figure 14. Momentum boundary layer for various degrees of external stratification.

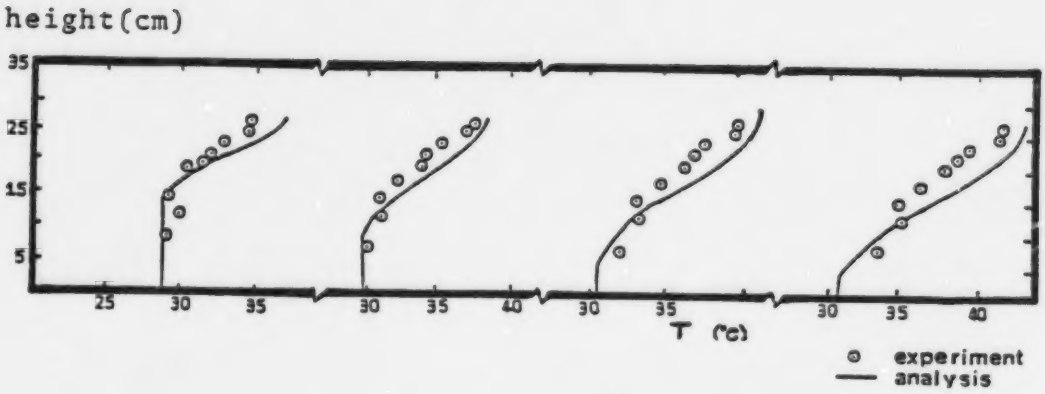

Figure 15. 80% fill, with 1" EXPLOSAFE. Transient development of vertical temperature gradient (q=40 kw/sq. m).

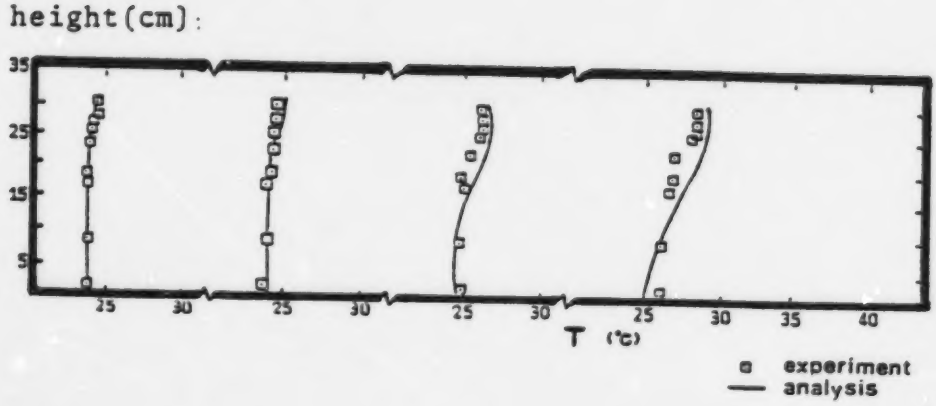

Figure 16. 85% fill, without EXPLOSAFE. Transient development of vertical temperature gradient (q=20 kw/sq. m).

its development. The third order polynomial temperature profile appears to represent the thermal stratification profile adequately for both cases. For filling ratios below 30 percent by volume, a lumped analysis can be made since this angle approximately represents the stability for side wall boundary layer commencement.

In the present analysis, the liquid-vapor interface is assumed adiabatic due to the experimentally observed temperature profiles and the very small amount of condensation or evaporation taking place resulting from the vapor being compressed due both to heating and from liquid thermal expansion.

Boundary layer heat loss due to external stratification and due to eddy mixing are quite distinct. The first is a result of decreasing buoyancy forces while the latter mechanism is caused by the reverse shear between the core and boundary layer.

In the partially filled horizontal cylinder large downward velocities are absent due to the mixing of the core fluid with the fluid issuing from the unstable region located on the concave bottom of the cylinder. In this region the heated fluid moves directly vertically upwards to mix with the downward moving fluid from the stratified layer, reducing the effect of reverse shear and enhancing the mixing to provide a near isothermal but time dependent core temperature. This latter effect is accounted for in the presented analysis by the instability analysis since this provides the primary energy content to the core.

2.2 A Finite Difference Solution

A numerical approach is necessary to have a qualitative as well as more detailed quantitative information. The integral technique presented earlier cannot meet this requirement although it can give good predictions in an averaged sense.

2.2.1 The Difficulties Associated with the Geometry and A Possible Approach

Although the governing equations are solvable with a suitable finite difference method, there are difficulties associated with the geometry of the solution domain. Due to the partial filling the coordinate system used does not coincide with the boundaries of the region, hence there will be some trouble in locating the control volume boundaries at the interface. The polar coordinate system as well as any others commonly used will fail to give regular mesh points in this region. One is therefore forced to choose the coordinate system such that it will exactly fit the boundaries of the solution domain. That is, one has to use a special transform.

The method used is to stretch the X-coordinate by normalizing it using the cord length associated with the Y-coordinate of an arbitrary point. In this way, an orthogonal system can be obtained in the transformed plane (ξ,η) where

$$\zeta = \frac{X}{\sqrt{(1-y)^2}} \quad \text{and} \quad \eta = Y$$

The result of this transformation can be seen in Figure 17, where the original circle is mapped onto a square or the partially filled region to a rectangle. It can be seen that

$$L(Y) = \sqrt{(1-Y^2)} \times 2$$

is the associated cord length which varies with height.

In [1] this method has been extended to consider other tank cross section geometries.

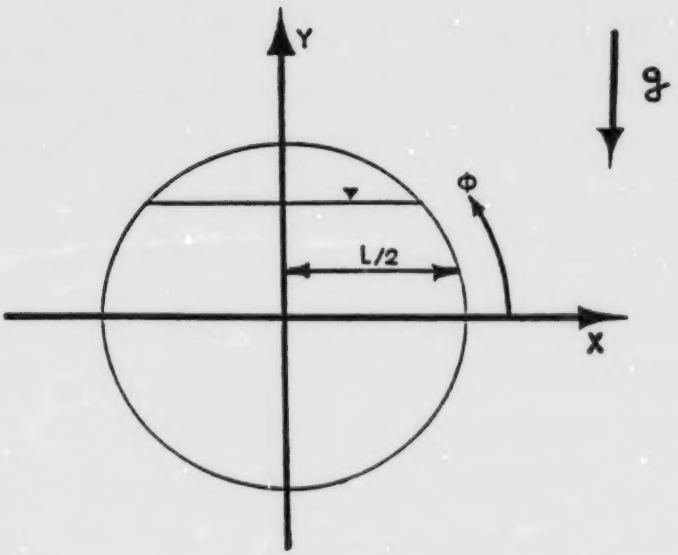

Figure 17a. Physical Plane

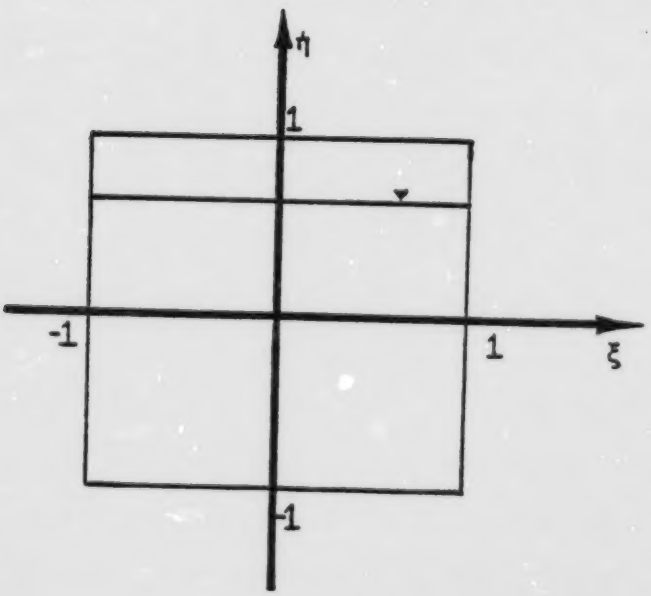

Figure 17b. Mathematical Plane

2.2.2 The Numerical Method

The governing partial differential and their associated boundary conditions are transformed to vorticity-steam function equations and these in turn transformed according to the constraints of the geometric transformation. Complete details of the transformation techniques required are given in Appendix C of [1].

The transformed equations are discretized using central differences with an implicit representation in time. The scheme is unconditionally stable for all time steps. Throughout the computation the vorticity transport equation utilized a relaxation coefficient of one although the stream function-vorticity equation required very heavy underrelaxation.

Despite this, the advantages brought by the transformation are obvious:

1) It is possible to choose a rectangular grid throughout the domain without any difficulty at the interface.
2) One can use central differences with conventional orders of accuracy. That is, since the coordinate system is orthogonal, the Taylor series expansions are valid in their original form but in ξ and η.
3) One has the freedom to choose $\Delta\xi = \Delta\eta$ so that the truncation error introduced by the Taylor series expansion is minimized.

2.2.3 Solution Method

The discretized equations given in Appendix D of [1] are solved both with a line by line (a combination of Gauss-Seidel and TDMA methods) and the Gauss-Seidel point by point method. The traversing direction in the former was chosen to be from bottom to top with horizontal lines (i.e. TDM was written in a horizontal direction).

In the point by point Gauss-Seidel method left to right sweeps from bottom to top are made. No significant im rovement was noted with respect to the computation time between the two methods.

2.2.4 Test Runs

Published experimental data for completely filled cylinders are available with Prandtl numbers 19950 and 0.7 (silicone oil and air, respectively). Data are given for a case where the walls of the cylinder were kept at constant temperature with a saw-tooth distribution. The computed steady state velocity and temperature profiles are plotted against the experimental values in Fig. 18 and Fig. 19. The comparison is good considering the assumptions made in the model equations. The mathematical plane was chosen to be $-1<\xi<1$ with $-0.99<\eta<0.99$ to exclude the singularities.

The results of the temperature and velocity profiles with Pr = 0.7, Gr = 4.5 10^4 are shown in Fig. 20 and Fig. 21 where they are compared with experimental data. In this case, the cylinder halves were kept at two different temperatures. The agreement with the steady state velocity profiles is not as good as for the temperature profile.

For the case of the partially filled vessel, glycerine, was chosen for the simulation runs in order to conserve computation time. It should be noted that now the solution domain is $-1<\xi<1$, $-0.99<\eta<0.4$ where $\eta = 0.4$ corresponds to a 75% filling.

The flow conditions are such that $Gr^*_R = 114$ and Pr = 6380. Since the properties are assumed constant along with the heat flux, these values do not change during the computation.

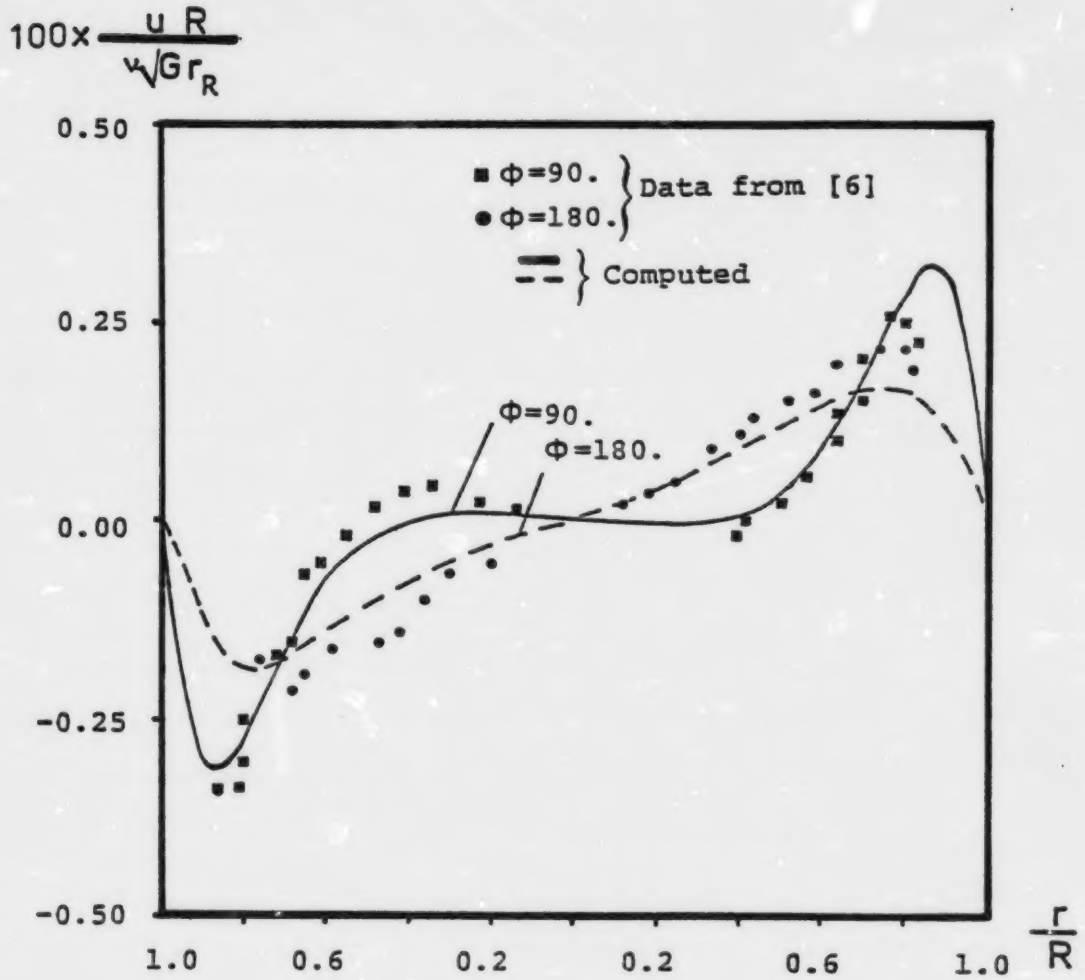

Figure 18. Velocity Profiles for Pr=19950., Gr=1.1

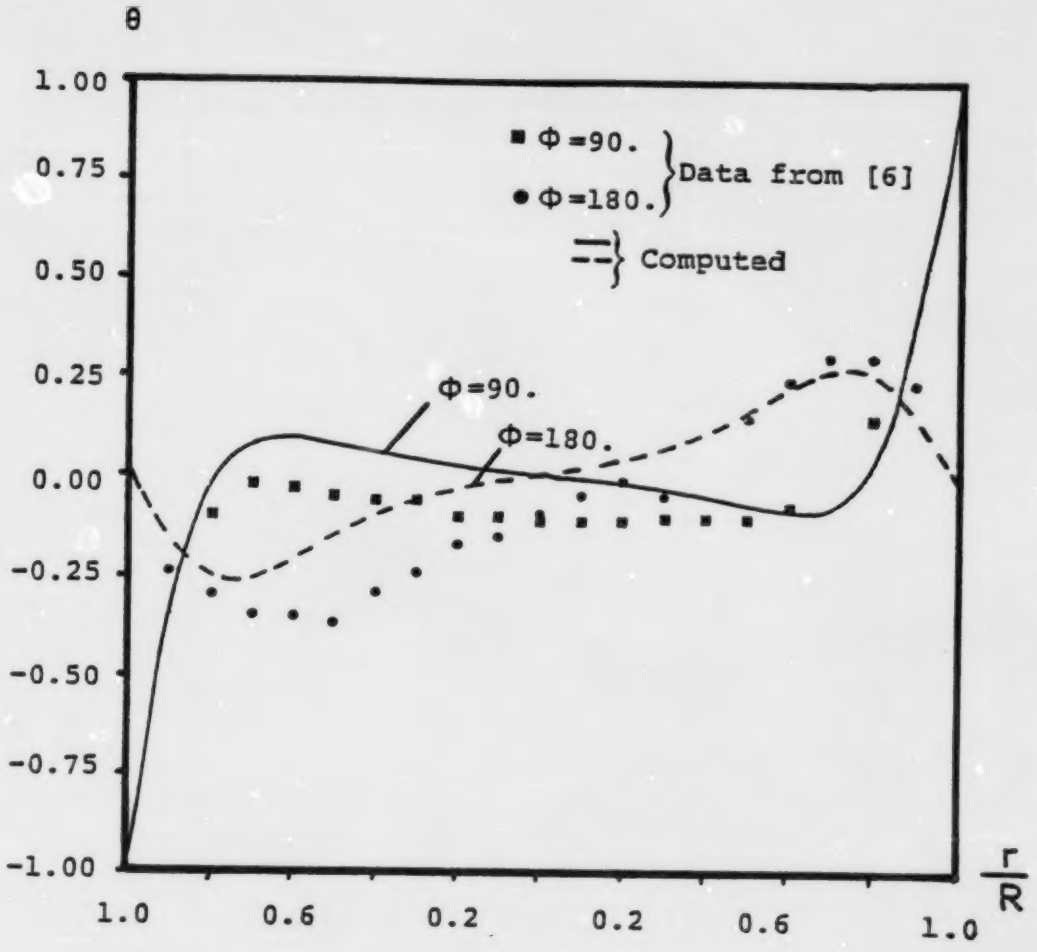

Figure 19. Temperature Profiles for Pr=19950., Gr=1.1

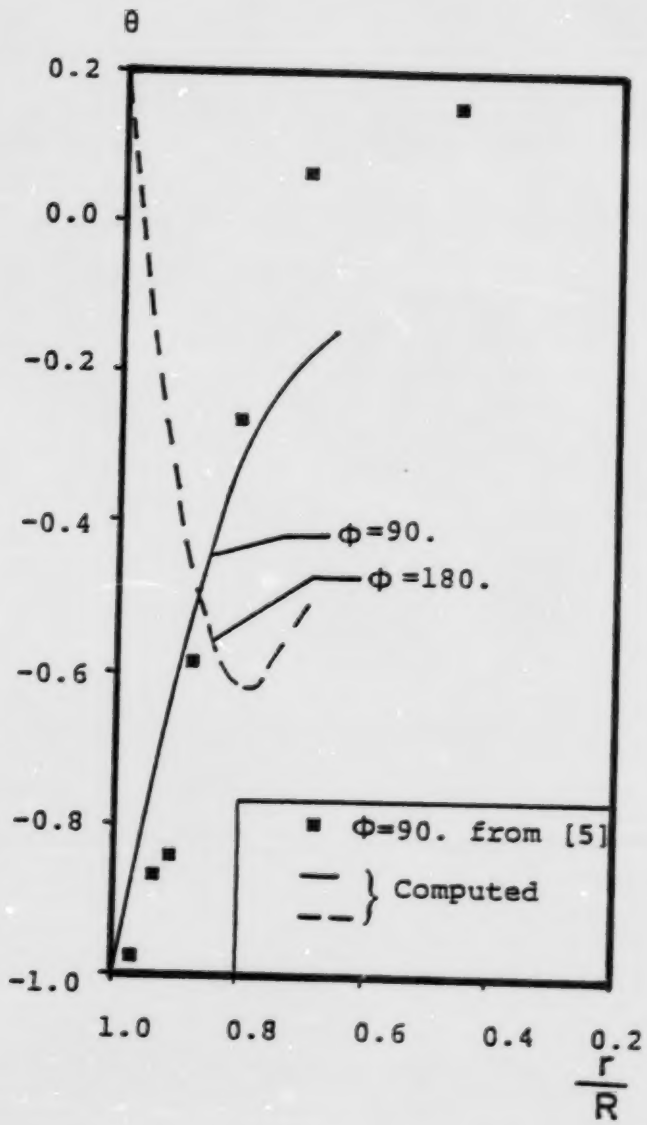

Figure 20. Temperature Profiles for Pr=0.7 Gr=4.5 x 10^4.

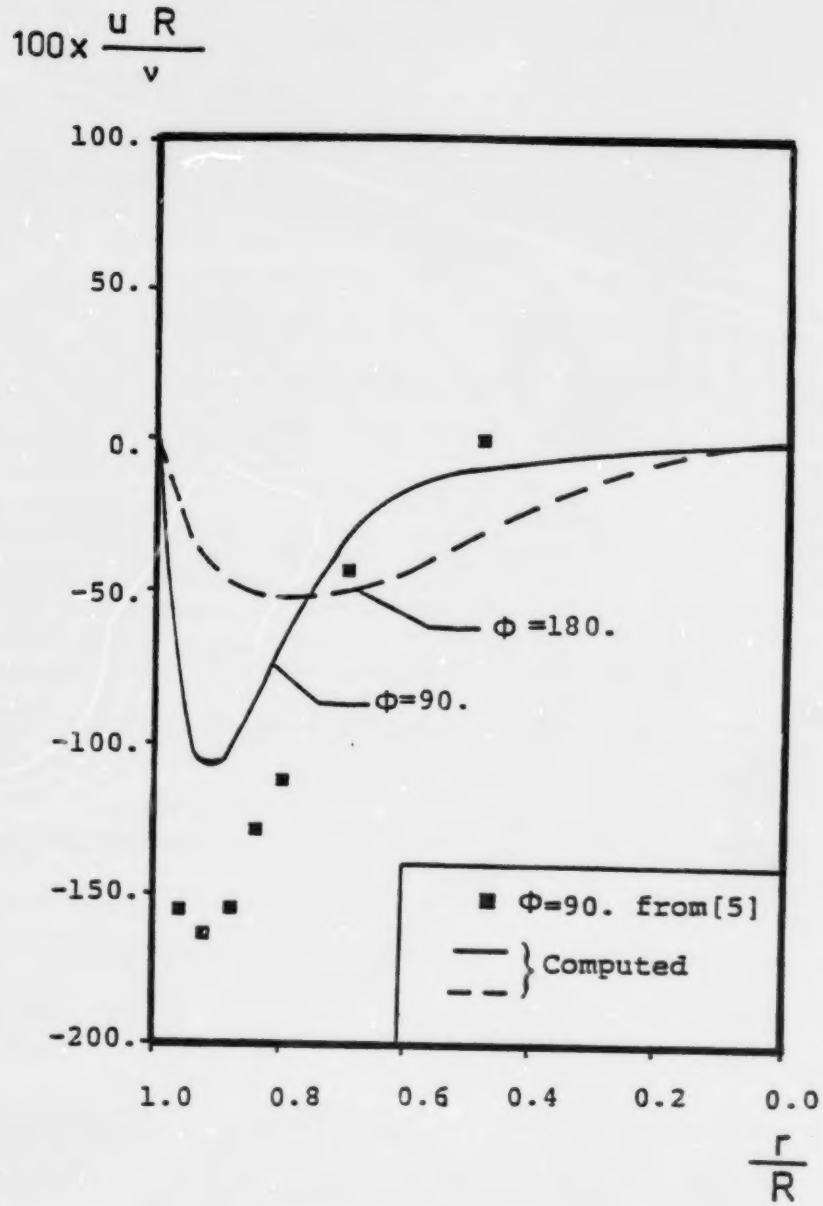

Figure 21. Velocity Profiles for Pr=0.7, Gr=4.5 x 10^4.

The simulated flow starts with two small eddies at the tank walls close to $\phi = 90°$. Eventually the two rotating cells join at the centre and a distortion is observed along the line of their contact (Fig. 22).

The shape of the inner most eddies before and after the contact can be explained as follows: consider only one-half of the cylinder, say the left, the developing cell in this region would continue to grow indefinitely with the flow velocities increasing if there were no other cell in the other half of the cylinder. However when they meet at the centre since the other is rotating in the opposite direction, they cannot grow further, hence the flow must adjust itself to the new situation. Being more explicit, we can say that the inward expansion of the streamlines at the centre is merely due to the increase in effective downward flow area so that the cell, being restricted in its growth, will compensate for this by expanding inwards. Note that the heat flux is always constant and so the flow has to accelerate somehow. Once the above is considered, it is easy to deduce that the flow cannot take any other shape.

The isotherms shown in Fig. 23 are for the corresponding time of Figure 22 and indicate the thermal stratification of the surface region liquid and also the isothermal nature of the core temperatures in the horizontal direction. This was a presumed condition in the previously discussed integral analysis.

A flow visualization, (Figure 24) qualitatively verifies the above results. Here a tracer was injected into a glass vessel of aspect ratio (length to diameter) of 2, allowed to diffuse and mix uniformly with the glycerine inside. The vessel was filled to about 60% compared to the 75% in the numerical simulation. The photograph shows a similar development of the streamlines which appear to buckle inwards.

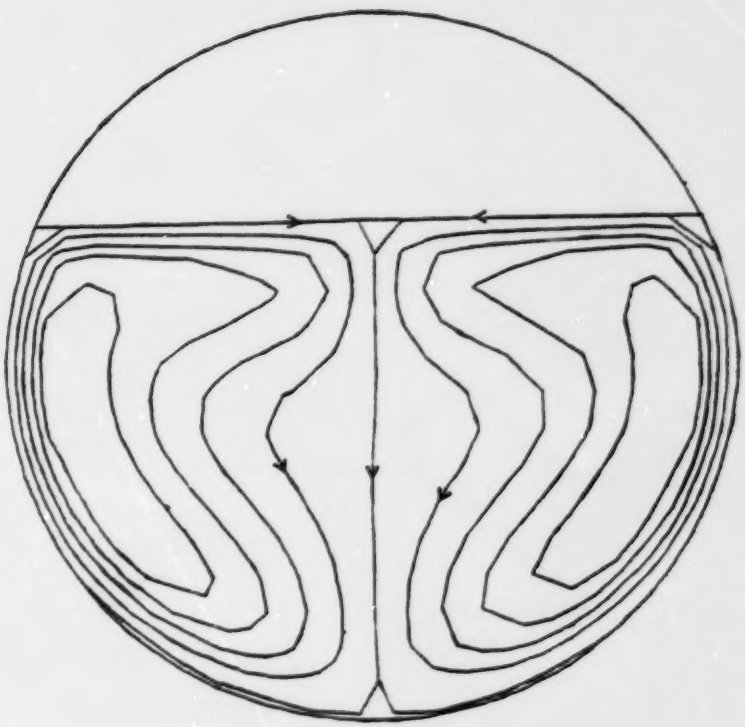

Figure 22. Stream lines in transient computation, Pr-6380., Gr=114., t=4.6 mins.

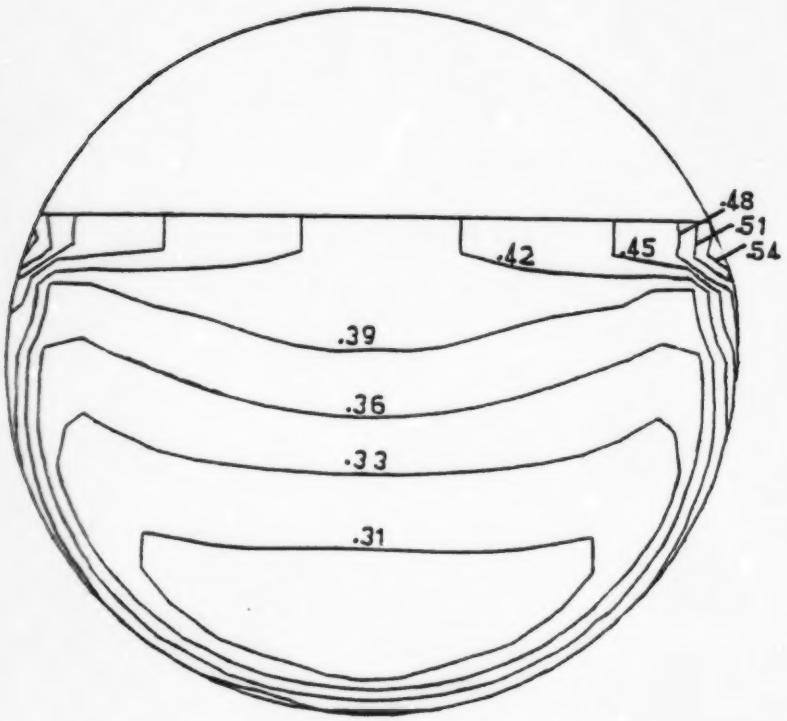

Figure 23. Isothermals in transient computation, Pr=6380., Gr=114., t=4.6 mins.

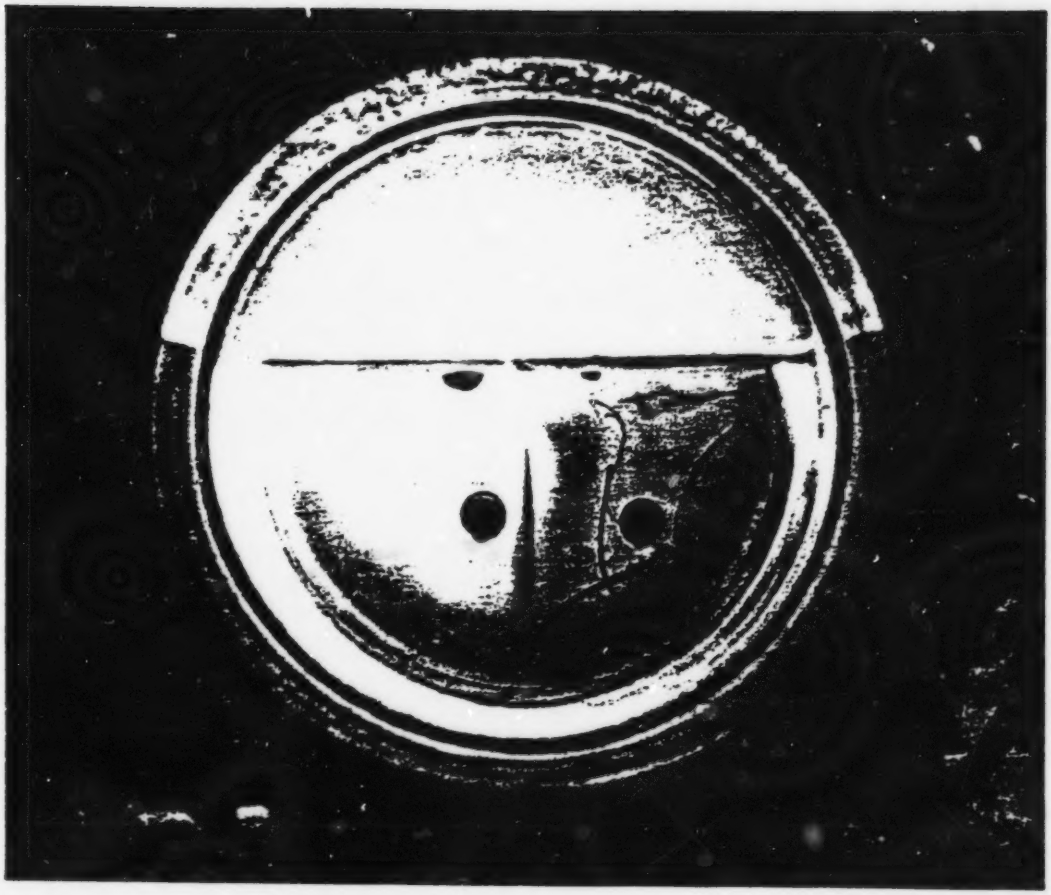

Figure 24. Flow pattern for Pr=6380., Gr=35

2.3 Vapour Stratification

In the vapour space a stratification analysis similar to that used above cannot be verified due to the very small heat transfer coefficients existing while the pressure relief valve is closed. In the valve open position the two phase swell that occurs in the lading due to the depressurization brought about by PRV opening causes transitions in the vapour space and liquid wall heat transfer coefficients. In the vapour space, liquid carry over may wet the wall and result in cooling whereas in the liquid space the decreased density of the now two-phase fluid, coupled with the additional wall heat transfer caused by circumferential conduction results in an interface heat flux spike which may trigger an early onset to film like boiling in the interface region.

A preliminary assessment of the vapour space heat transfer prior to vent has been completed [3]. The test data for the six experiments at 65 kW_e/m^2 conducted without EXPLOSAFE with PRV set pressures of 343 kPa were analyzed. Three of the tests had 6.35 mm PRV orifices and the others a 9.52 mm orifice. Temperatures were evaluated from thermocouples located on the walls and vapour space of the tank as detailed in [2]. The results presented are based upon the following conditions and/or assumptions and as shown in Figure 25.

1. The liquid/vapour interface is adiabatic.
2. The average vapour phase temperature is a weighted average as shown.
3. The wall temperatures are determined from the arithmetic mean of the four (4) measured points of the inner stainless steel vessel.
4. The physical properties of the vapour were calculated using standard relations and tables available for R11.

5. The vapour volume was calculated taking into consideration the change in liquid level with time as determined from video recordings.
6. The heat transfer area was calculated by subtracting the topmost unheated area around the PRV from the vapour space wall.

Five points were averaged for the 23% liquid fill. The fifth point is shown as X in Figure 25.

The average heat transfer coefficient determined in this manner are shown in Table 4 and detailed in Figures 26 and 27. It can be seen that in all but one test, test 18, curve C, Figure 27, the mean heat transfer coefficients are quite small and can be represented as being time invariant up to the point of PRV opening at 2.6 W/m^2K (0.46 $BTU/ft.^2hr.°F$). Detailed comments on these preliminary results are made in [2]. Considerable more work is now necessary to predict vapour space and indeed liquid space wall temperatures in the interface region particularly with depressurization due to the non equilibrium effects of "flashing".

A discussion of the effects of EXPLOSAFE upon vapour space heat transfer is included in [2]. The experimental results of these tests indicated little increase in vapour space heat transfer except that due to fin effects.

TASK 3. Boiling and Liquid "Swelling" process with/without EXPLOSAFE".

This work, which considers enhanced surfaces as well as smooth and EXPLOSAFE covered mild steel and copper surfaces is reported in [3] and considers the effects of surface inclination of the boiling processes.

3.1 Boiling as a Function of Surface Orientation.

An examination of pool boiling heat transfer in R11 with different surfaces was carried out. Surfaces consisting of copper, mild steel, Union

. Wall Thermocouples

x Wall Thermocouples used only for the 23% fill

x Vapour Phase Thermocouples

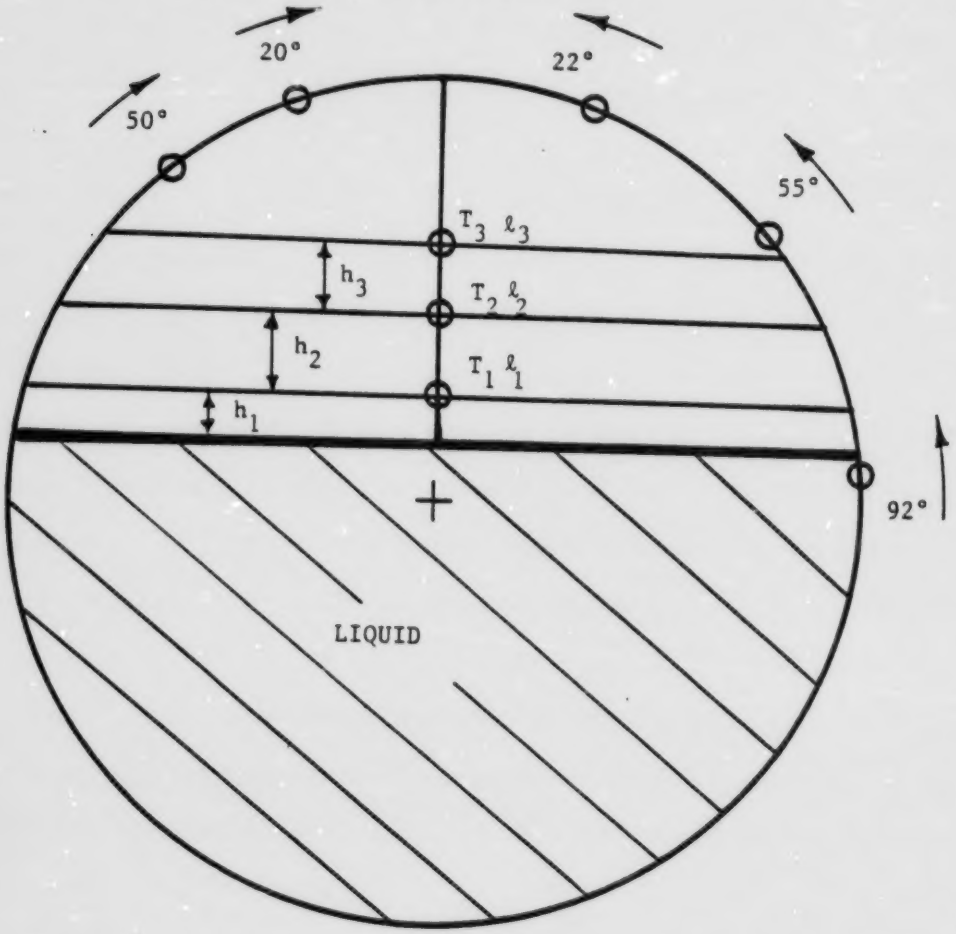

$$T_{ave} = \frac{T_1(h_1 + \frac{h_2}{2})\,\ell_1 + T_2(\frac{h_2}{2} + \frac{h_3}{2})\,\ell_2 + \ldots}{(h_1 + \frac{h_2}{2})\,\ell_1 + (\frac{h_2}{2} + \frac{h_3}{2})\,\ell_2 + \ldots}$$

Figure 25 Vapour Space Mean Temperature Evaluation.

Table 4

Average Heat Transfer Coefficients

Test	Mean-Heat-Transfer-Coeff.		Standard Deviation	
	kW/msq(°C)	BTU/ftsq(°D)Hr	kW/msq(°C)	BTU/ftsq(°F)Hr
13	0.002587	0.4558	0.000474	0.0834
14	0.003086	0.5435	0.000582	0.1025
15	0.002692	0.4740	0.001290	0.2271
16	0.002644	0.4656	0.000970	0.1708
17	0.002070	0.3650	0.000923	0.1625
18	0.004195	0.7389	0.000923	0.1625

From All the Five Tests: (Excluding Test 18)

Mean-Heat-Transfer-Coeff.		Standard Deviation	
kW/msq(°C)	BTU/ftsq(°D)Hr	kW/msq(°C)	BTU/ftsq(°F)Hr
0.002627	0.4626	0.000957	0.1685

Carbide "Hi Heat Flux", EXPLOSAFE, and two flame sprayed metalized enhanced surfaces were investigated. An investigation of the effects of surface orientation, in both nucleate and film boiling was conducted with heat fluxes to 170 kW/m^2.

The developed experimental device permits replacement of the test section and enables data to be obtained at any heater surface orientation from facing vertically upwards to facing downwards. Photographic and profilemetoric studies of the enhanced surfaces were utilized in an attempt to explain the experimental observations. All tests were performed at 2 bar except for the copper surface in which data were obtained at three different system pressures to confirm that the boiling system behaved according to well established patterns. The data were correlated using Rohsenow's nucleate pool boiling equation as a function of orientation and pressure.

It was concluded that surface orientation is important in nucleate and film boiling. For nucleate boiling inclination angles of 160° to 180° (i.e. facing downward) result in severe increases in the wall-fluid temperature difference.

The experimental apparatus is composed of five components: an electric heater, test specimens (copper and mild steel surfaces, four types of enhanced surface (EXPLOSAFE, UNB surface #1, #2, and Union Carbide High Heat Flux), a glass T-vessel and its equipment, an electric circuit panel, and thermocouples along with a HP-85 computer and data acquisition system (HP 3456A and 3497A digital voltmeters).

3.1.1 Electric heater

To achieve a uniform temperature field on the surface, a coil heater was used. Fig. 28 illustrates the detailed cross sectional view of a coil

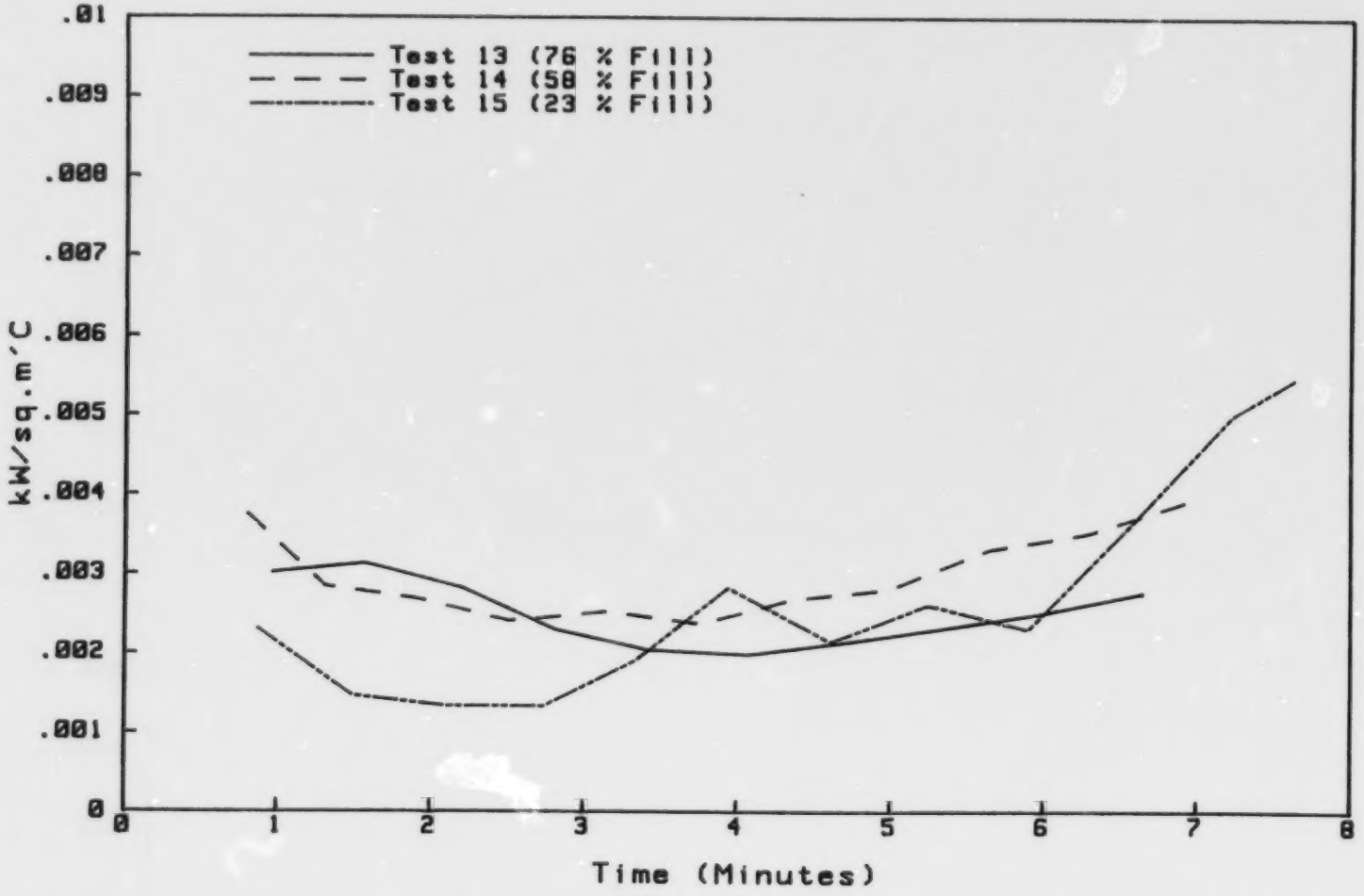

Figure 26. Heat Transfer Coefficient Vs Time

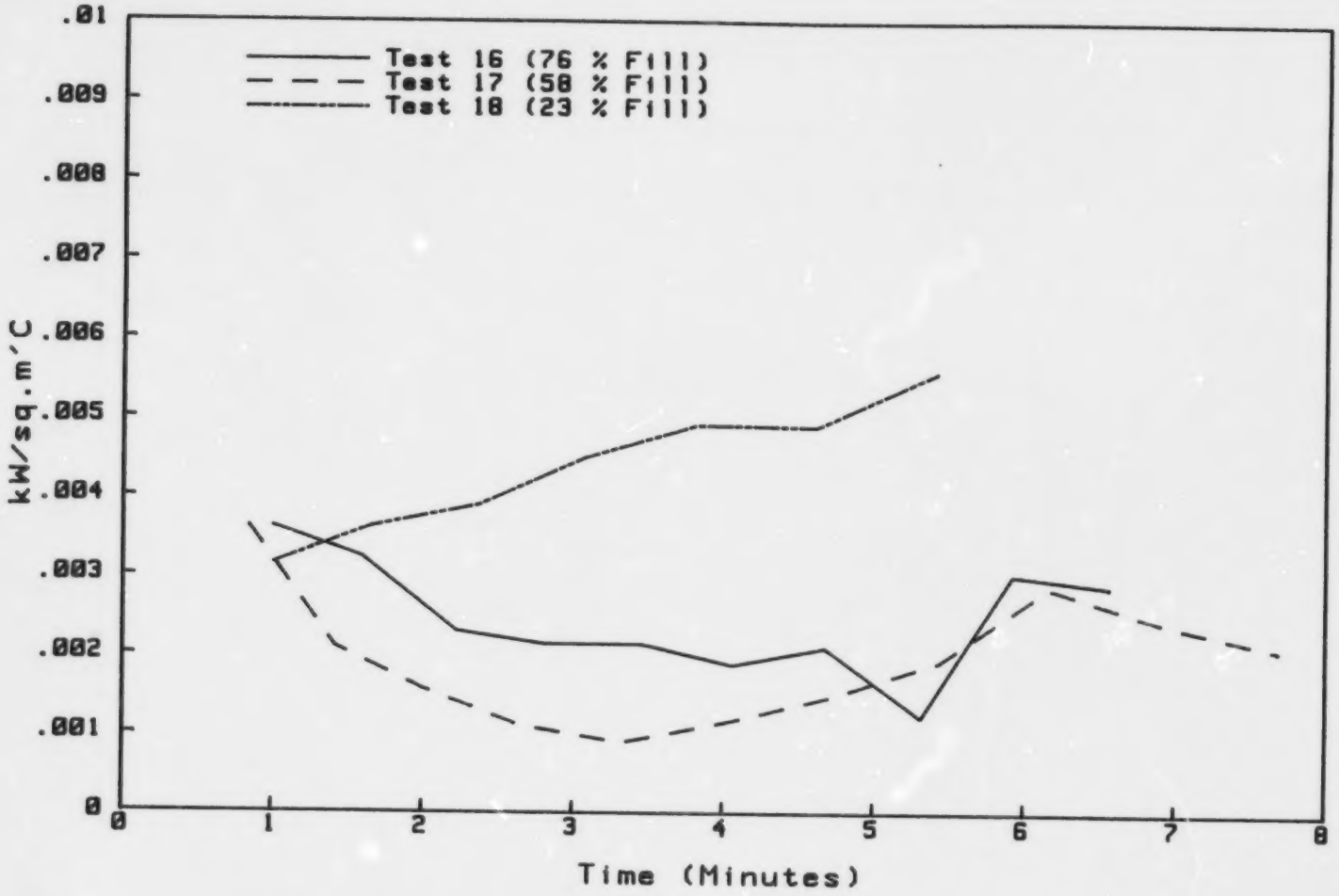

Figure 27. Heat Transfer Coefficient Vs Time

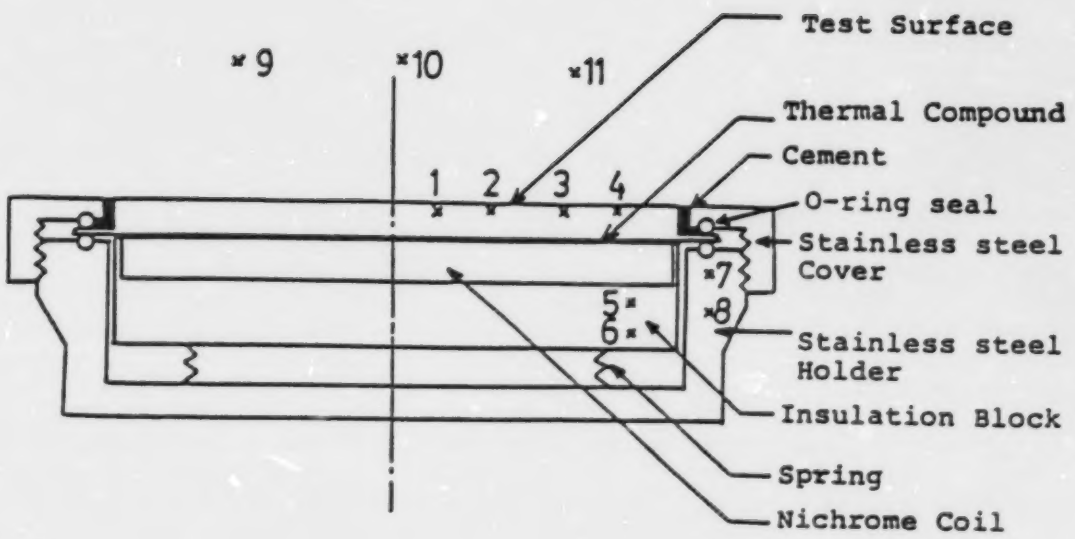

Thermocouple No. 1-8 Iron-Constantan
Thermocouple No.9-11 Copper-Constantan

Figure 28. Detailed cross sectional view of the electrical heater (actual size).

electric heater. Spiral grooves for the coil were machined in a machinable ceramic block to limit the heat transfer to one side of the heating plate. The coil, (16 gauge, 3.3 mm dia, nichrome wire), was placed in the grooves and spaces between the grooves and coils and inside coils were filled with Al_2O_3 cement.

Four holes were drilled radially on the spiral grooves to insert four surface temperature thermocouples. (Fig. 29). The encapsulated heater was ground flat to promote good contact with the test surface and a thin thermally conductive high temperature grease applied between the test suface and the heating element.

The heating element plate and attached surface thermocouple assembly was mounted with sealing O-rings in a stainless steel holder by a stainless steel cover. A low conductivity cement, the O-rings and the geometric reduction of the circumference caused by the machined lip of the test surface decreased contact conductance and edge heat losses. Heat losses from the base of the heater were minimized by the use of only three high temperature springs in the air space between the encapsulated heater block and the specimen container. The springs ensured maintenance of good thermal contact between the heater and the test surface through the high temperature thermal grease.

For tests with Explosafe the material was cut in a circular shape and placed on the surface. To maintain good contact, six studs were used to secure stainless steel wires over the surface of the EXPLOSAFE. By adjusting the tension of the wire good thermal contact between the surface and EXPLOSAFE could be obtained. Fig. 30 illustrates the fully assembled heater with an EXPLOSAFE cover.

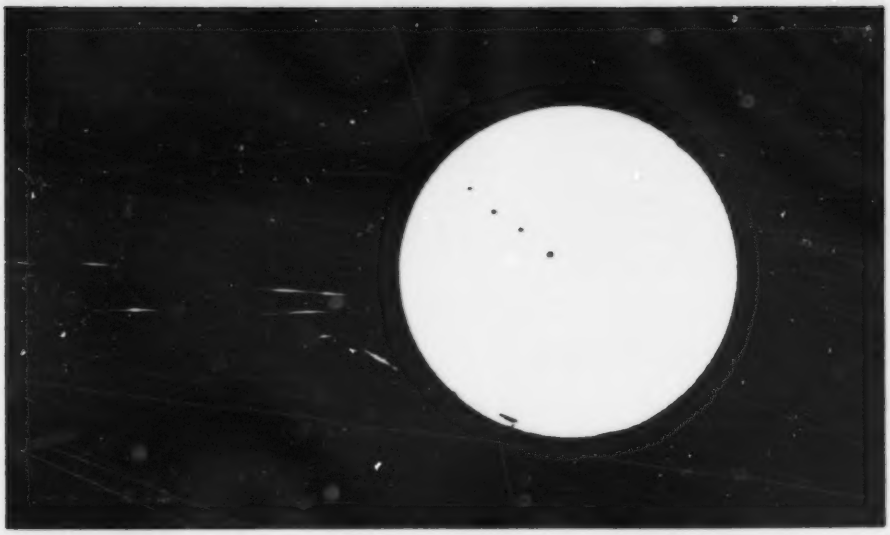

Figure 29. Encapsulated heating element

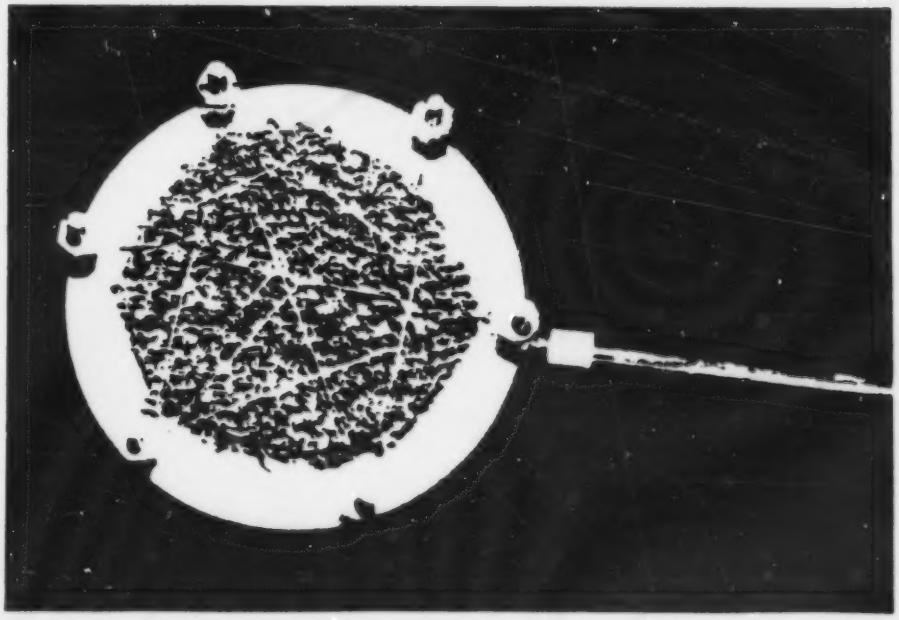

Figure 30. Heater assembly with EXPLOSAFE

3.1.2 Test specimens

Two flat machined and finished surfaces (copper and mild steel) and three enhanced surfaces (UNB #1, #2 and UC) 7.8 cm diameter were prepared.

The plain surfaces were polished with a coarse emery paper. The porous metal coatings on a mild steel surface were prepared by flame spraying. Detailed procedures are given in Appendix A of [3].

3.1.3 T-vessel and its equipment

As seen in Fig. 31, a pyrex glass T-section (43 cm tall, 15 cm x 15 cm x 10 cm diameter) was used as the test vessel. To preheat the liquid to desired temperatures and maintain the system pressure especially at low heat fluxes, three auxiliary heaters located on the lower closure plate were used. A constant pressure was maintained inside the T-vessel by using a water cooled reflux condenser.

The electric control and measurement circuit is shown in figure 32. AC heater current and voltage measurements were made utilizing standard resistors and a true RMS voltmeter along with a calibrated current transformer. With surface inclination, departure from nucleate boiling and transition to film boiling can occur with resulting heater burn-out. Surface temperatures were therefore monitored continuously and if the rate of temperature increase exceeded prescribed limits the power was automatically shut down by computer control.

Eight iron constantan thermocouples were used to measure the test surface temperature (4) and the temperatures of the encapuslated heater block (2) and stainless steel heater (2). The test plate surface thermocouples were tightly fitted into holes drilled to within 0.5 mm of the surface and filled with thermal compound. The thermocouples on the heater block and

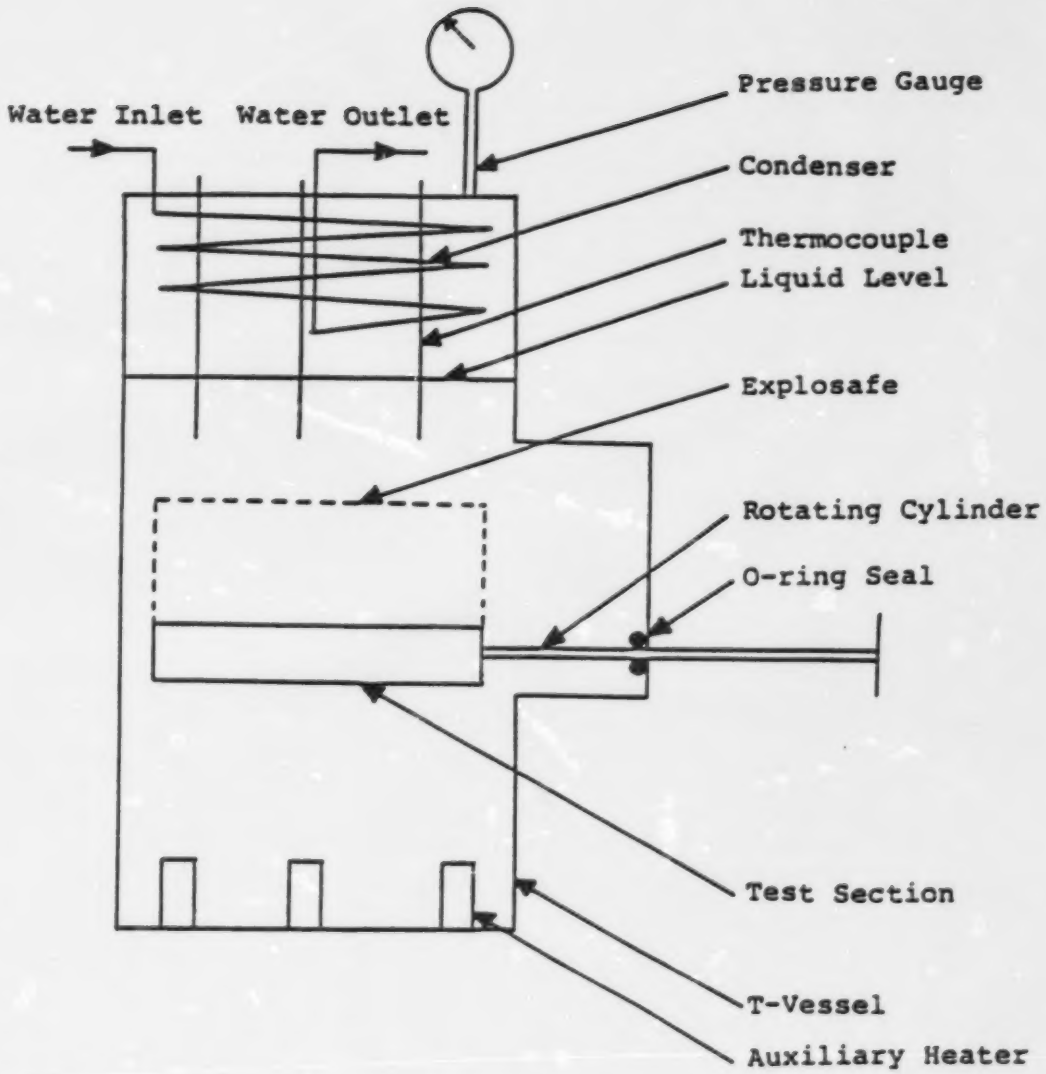

Figure 31. Schematic view of the apparatus

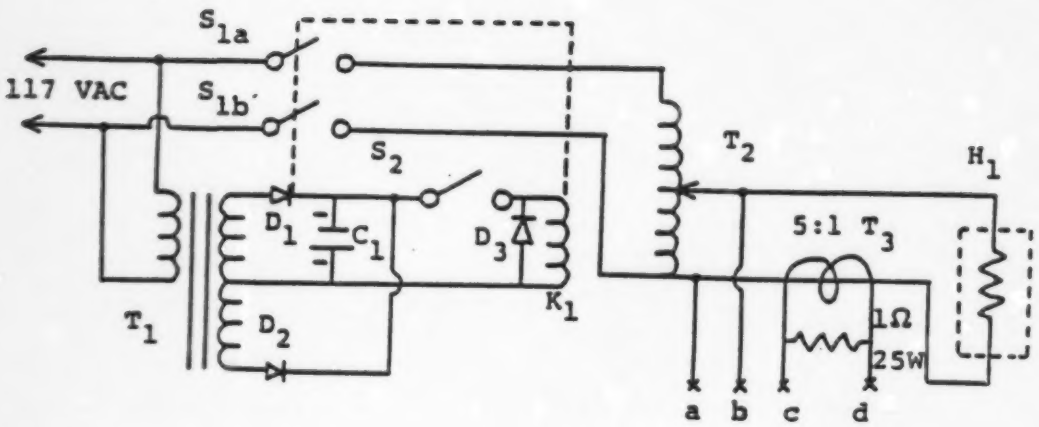

$D_{1,2,3}$	: 600V-1A Diode
C_1	: 470μf/35V
K_1	: 24 V Coil DPST Relay
$S_{1a,b}$	: DPST Relay 24 Volt DC Coil
S_2	: Remote control(HP-3497 voltmeter)
a,b	: E_1, Voltage through main heater
c,d	: E_2, Voltage through standard resistor
T_1	: 36VCT/117V
T_2	: 12A/0-140V, Voltage transformer
T_3	: 5:1, Current transformer
H_1	: Test heater

Figure 32. Detailed electric circuit.

stainless steel holder were used to assess heat losses. The liquid temperatures were determined from three thermocouples located in the pool as shown in figure 31.

The thermocouples were monitored using the HP85A controlled HP3497A voltmeter/data acquisition system with the AC voltages being measured using an HP3456A digital voltmeter.

Full details of the experimental procedure are given in [3].

3.1.4 Experimental Results

Pool boiling heat transfer experiments with two plain surfaces (copper and mild steel) and four types of enhanced surfaces (UC, UNB #1, UNB #2 and a surface with several thickness of EXPLOSAFE) were conducted in Freon-11. The surface orientation effect has been examined carefully. Figs. 33 and 34 represent these results and Table 5 illustrates the comparison of major parameters on the various surfaces. Film boiling tests were carried out only for the copper, UNB #1 and UNB #2 surfaces. The effects of orientation were studied for all surfaces except the UC surface.

To investigate the effectiveness of EXPLOSAFE, two pieces of EXPLOSAFE (3/4" and 2" thick) were tested on the copper surface at 2 bar.

Surface roughness tests and photographic studies of the surface cross sections were done in an attempt to explain the bubble nucleation mechanism and film boiling results. Finally, all results in nucleate boiling regime were correlated by using the Rohsenow's pool boiling equation. The complete results are given in Volume 4 [3].

The results (Fig. 33 and 34) indicate that in the natural convection regime (0-10 kW/m^2) an increase in surface inclination reduces liquid surface superheat. Fig. 35 compares the present results with those of Fujii and

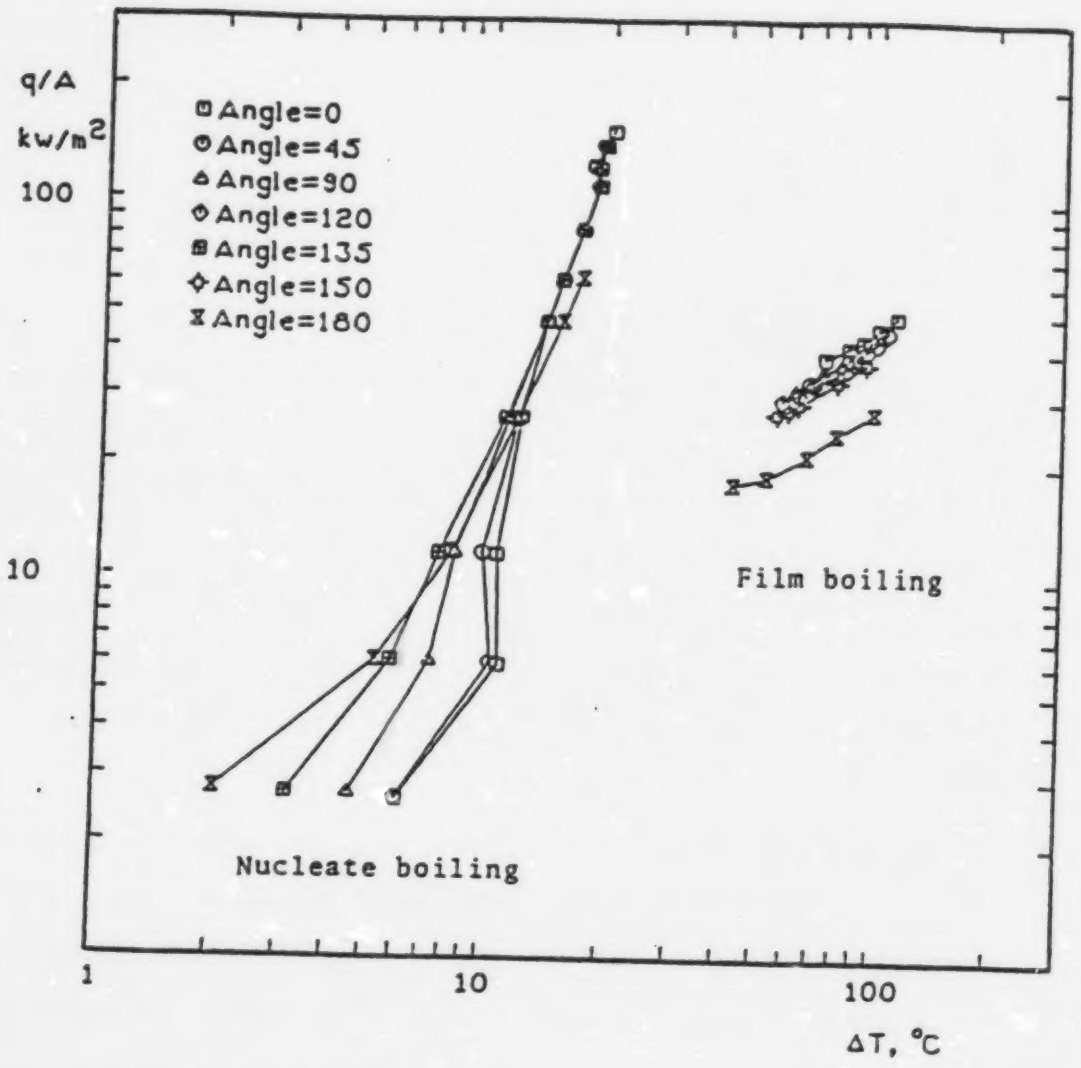

Figure 33. Pool boiling heat transfer with Freon-11 for copper surface at 2 bar.

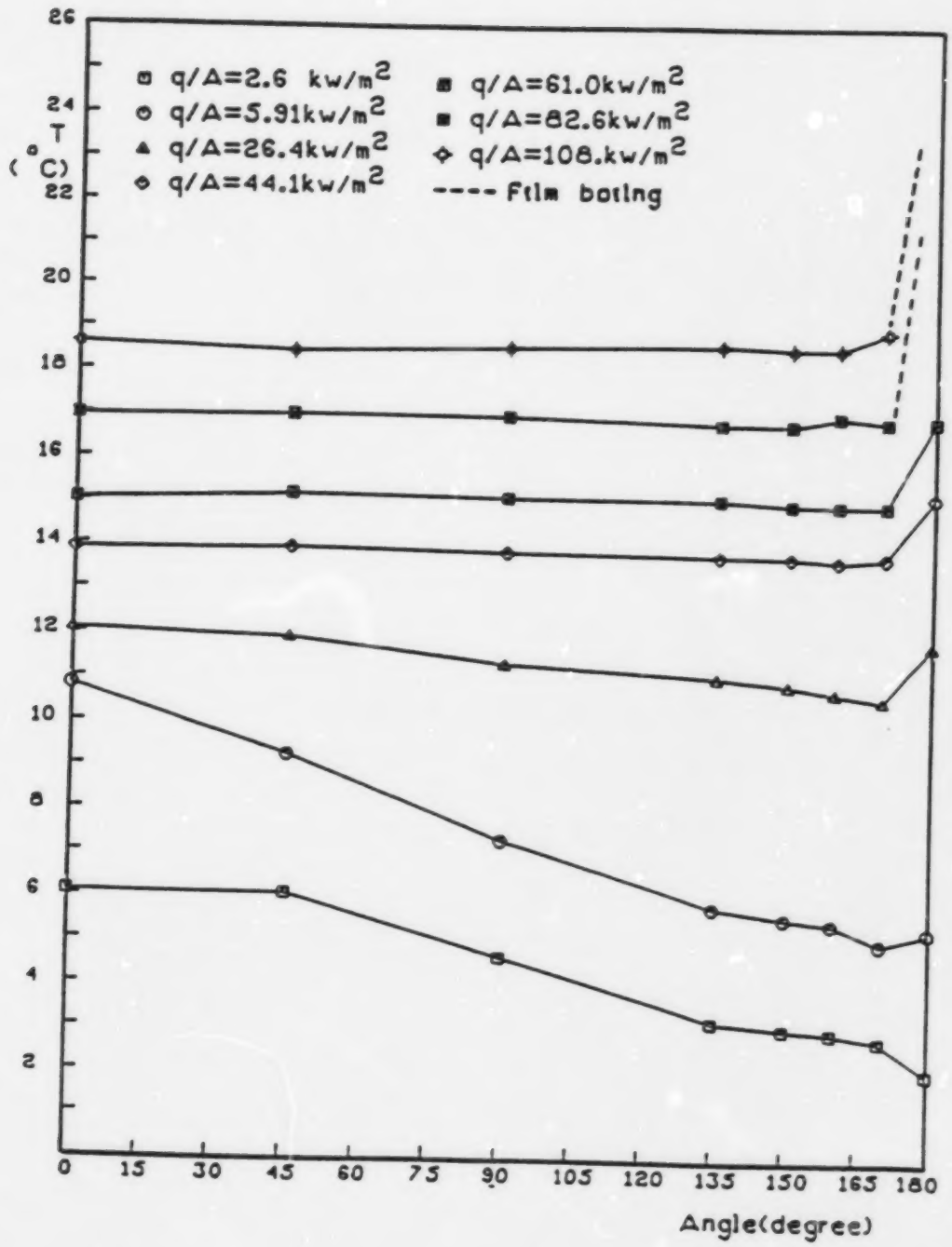

Figure 34. Effect of orientation for copper surface.

Table 5 Comparison of major parameters in various surfaces

parameters / surfaces	NP_n	NP_f	$(q/A)_\ell$ (kw/m^2)	$(\Delta T)_\ell$ (°C)	$(q/A)_i$ (kw/m^2)	$(\Delta T)_i$ (°C)	$(q/A)_h$ (kw/m^2)	$(\Delta T)_h$ (°C)	$(q/A)_{min}$ (kw/m^2)	$(\Delta T)_{min}$ (°C)
Copper (2 bar)	11	5	2.6	6.07	5.91	10.83	152.3	19.98	38.4	72.8
Copper (1 bar)	13	0	2.67	7.53	6.1	13.0	150.3	24.5		
Copper with 3/4" Explosafe	12	0	2.47	5.49	5.81	10.3	139.3	17.9		
Copper with 2" Explosafe	12	0	2.57	5.44	6.31	10.62	148.5	18.6		
Mild Steel	12	0	2.17	5.05	5.92	10.98	152.2	21.33		
UC	12	0	1.4	2.94			158.7	15.9		
UNB #1	12	3	1.36	2.97	5.5	9.88	137.3	15.15	41.4	123.2
UNB #2	15	5	1.62	3.95	24.8	11.1	174.6	8.18	68.8	151.9

(NP represents the number of data points and the subscripts n,f stand for nucleate and film boiling respectively and ℓ,i and h mean the lowest, incipient and highest boiling points in nucleate boiling and 'min' represents the minimum boiling point in film boiling.)

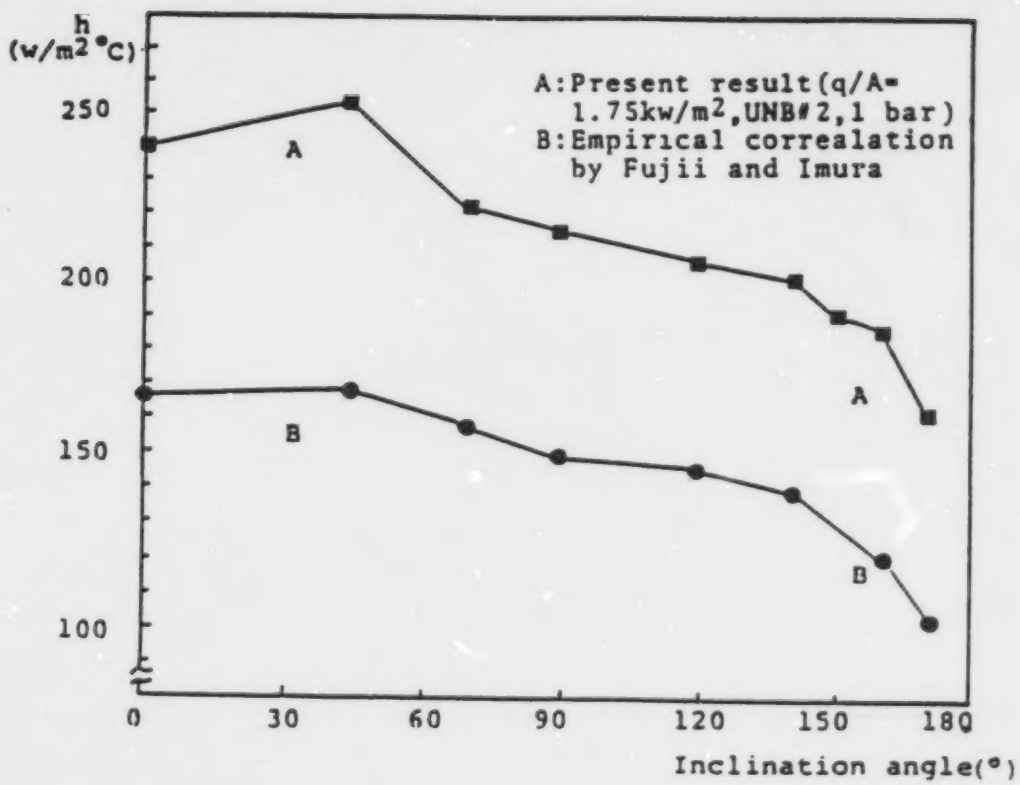

Figure 35. Experimental data with UNB #2 surface in natural convection region and an empirical correalation of Fujii and Imura (Ref. [8] of [3]).

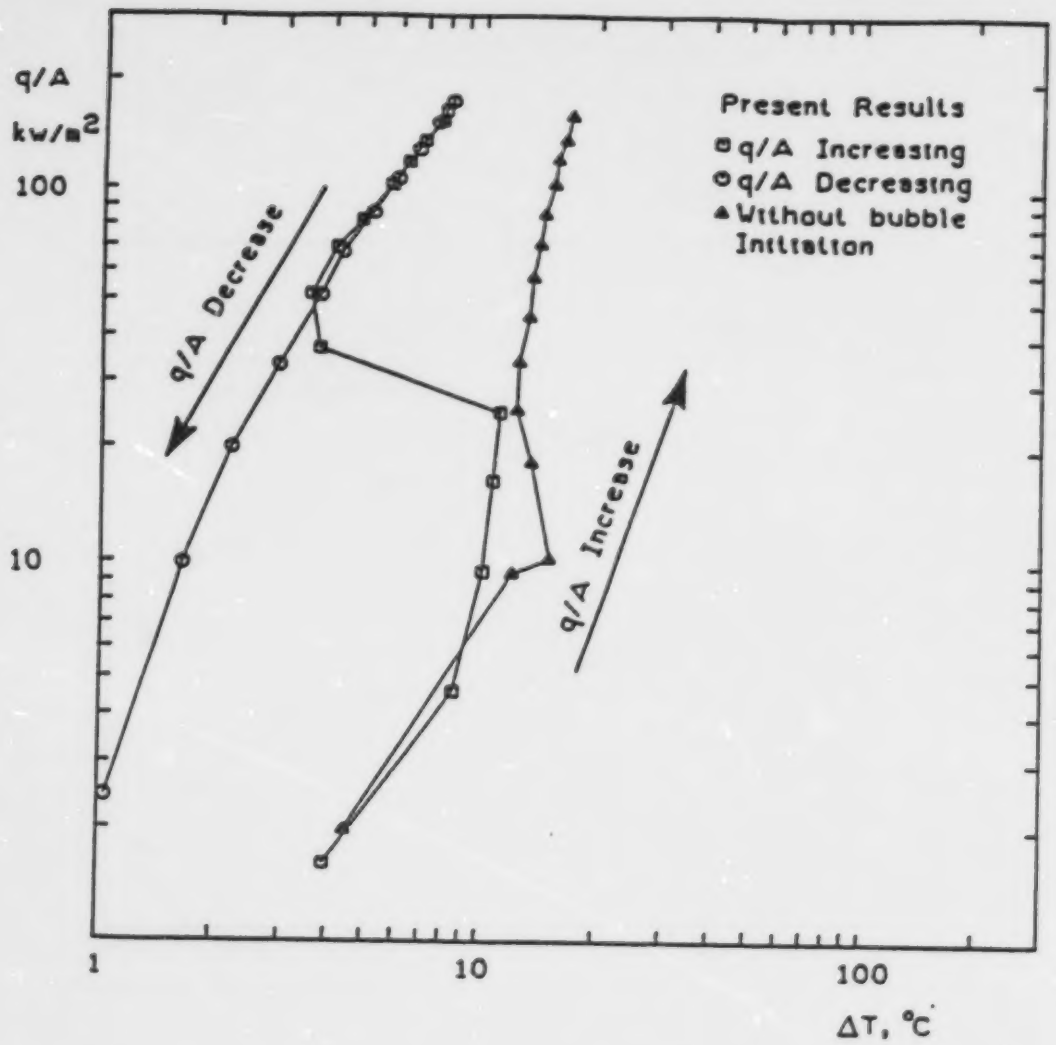

Figure 36. Hysteresis effect for UNB #2 surface at 2 bar in R-11.

Imura. Differences here are attributable to the surface enhancement of UNB2 however the shape of the two curves is similar.

In nucleate boiling, unless surfaces are preinitiated there are hysteresis effects or incipient boiling points and a marked "knee" in the boiling curve as shown for UNB#2 (Fig. 36). Once bubble sites are initiated boiling superheats are very much reduced and a steady boiling curve, $q = A\Delta T^b$, results. The slope b, from log-log coordinates is usually 2.9 for the upwards facing surface as it is here (Fig. 33). A comparison of surface heat fluxes and the required superheat temperatures is given in Table 6.

Due to the very considerable reduction in superheat caused by the enhanced surface UC and UNB#2 consideration must be made for using them inside tanks to initiate early boiling and hence provide vapour space protection especially when coupled with geyser systems such as proposed initially by UNB in 1981 [4].

Film boiling tests were also conducted for three surfaces as a function of inclination as shown in Figure 37 where the results are compared with the experimental and predictive work of others.

EXPLOSAFE, which is a honeycomb type expanded aluminum mesh, has been proposed for use as an internal protection device in case of accident inrailway tank cars. It was supposed that EXPLOSAFE would act as a fin to take the heat away from the point of application. The pool boiling results with this material however reveal that it does not cause any appreciable enhancement in nucleate boiling. As the thickness increases, the heat transfer was even retarded (Fig. 38). This can be explained by the introduction of a thermal contact resistance and existing bubble nucleation theories. Even though EXPLOSAFE maybe in good contact with the surface,

ΔT(°C)	Copper	Mild Steel	UC	UNB #1	UNB #2
			q/A (kw/m^2)		
5	2.1	2.1	14	15	84
8	4	4	40	42	170
16	68	56	160	160	
			h ($w/m^2 \cdot °C$)		
5	420	420	2800	3000	16800
8	500	500	5000	5250	21250
16	4250	3500	10000	10000	

Table 6. Comparison in heat flus and heat transfer coefficients for given superheats with different surfaces.

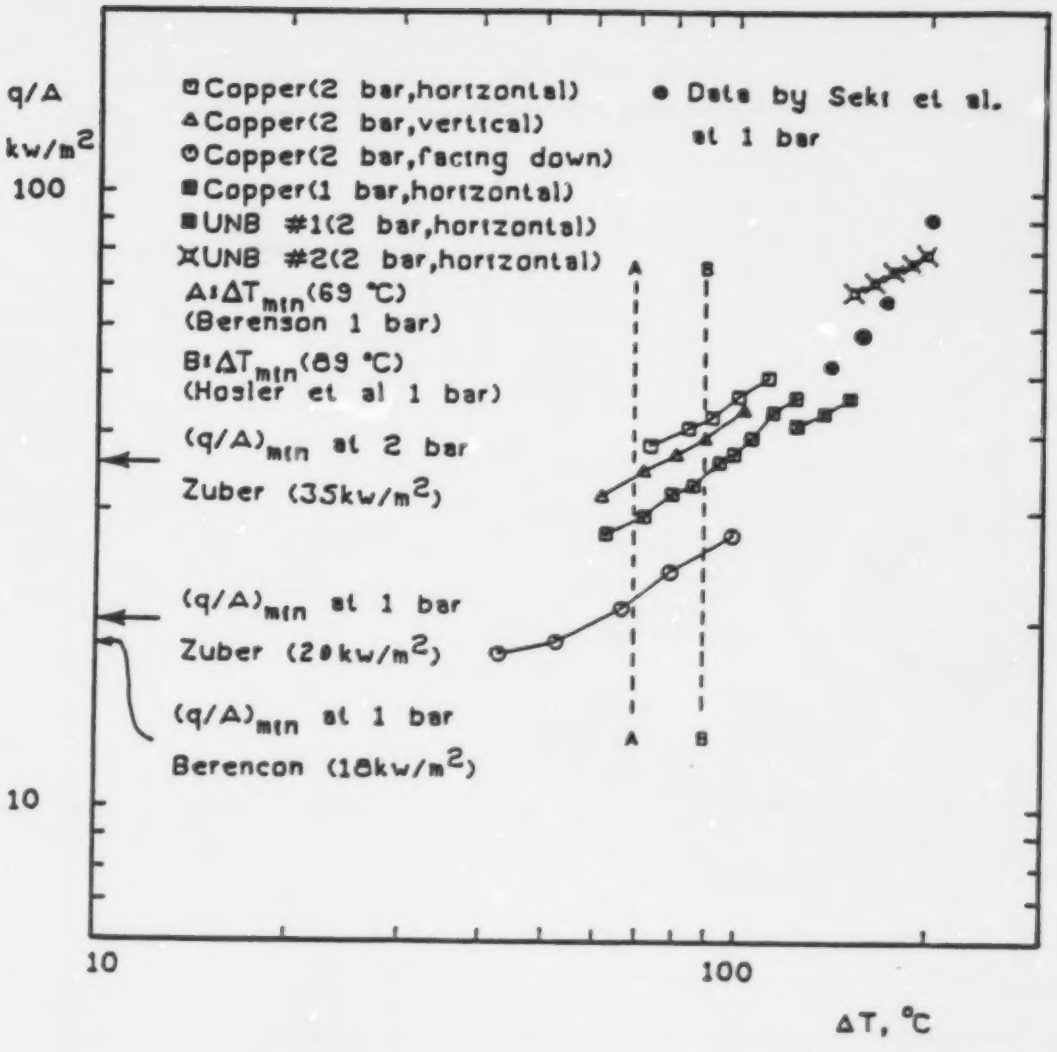

Figure 37. Comparison of the present results with available data and predictions in film boiling region.

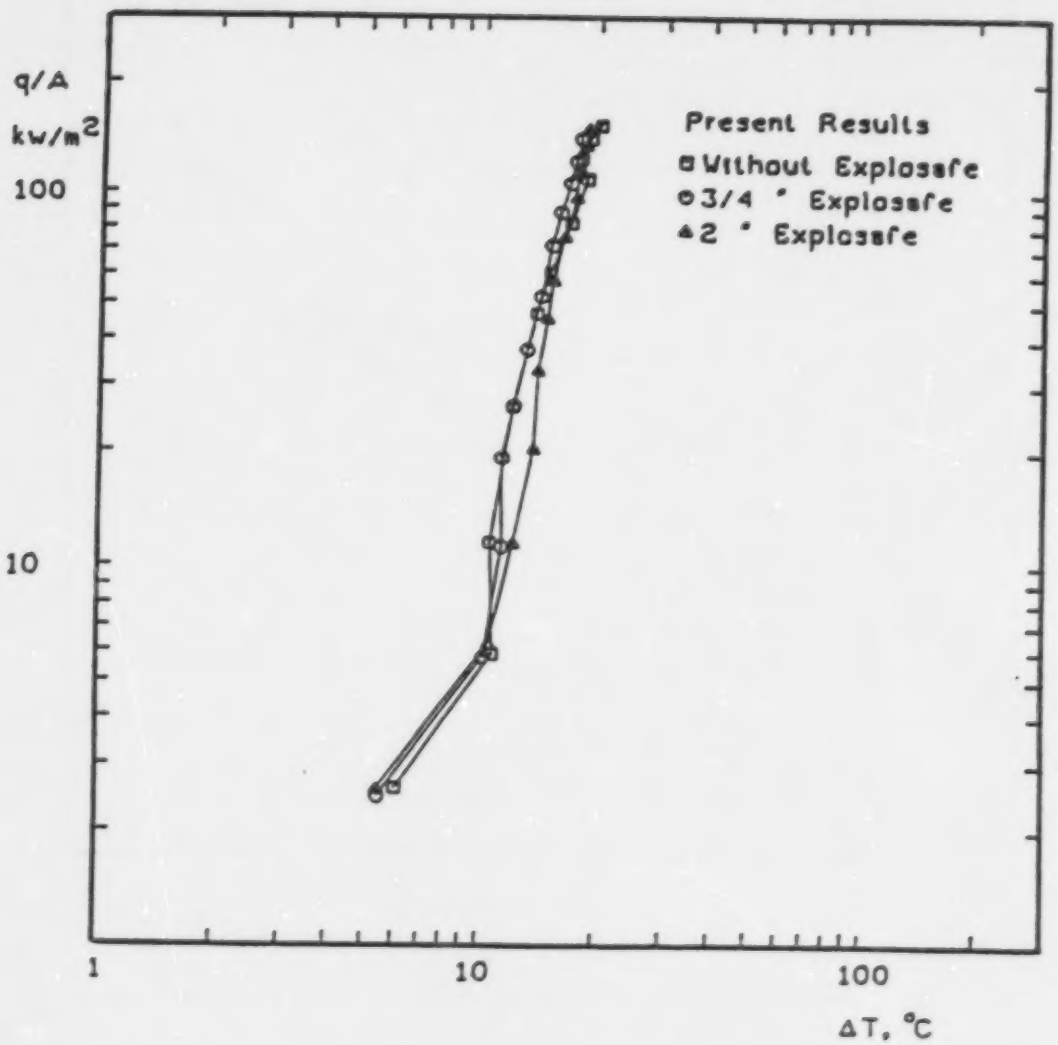

Figure 38. Effect of Explosafe

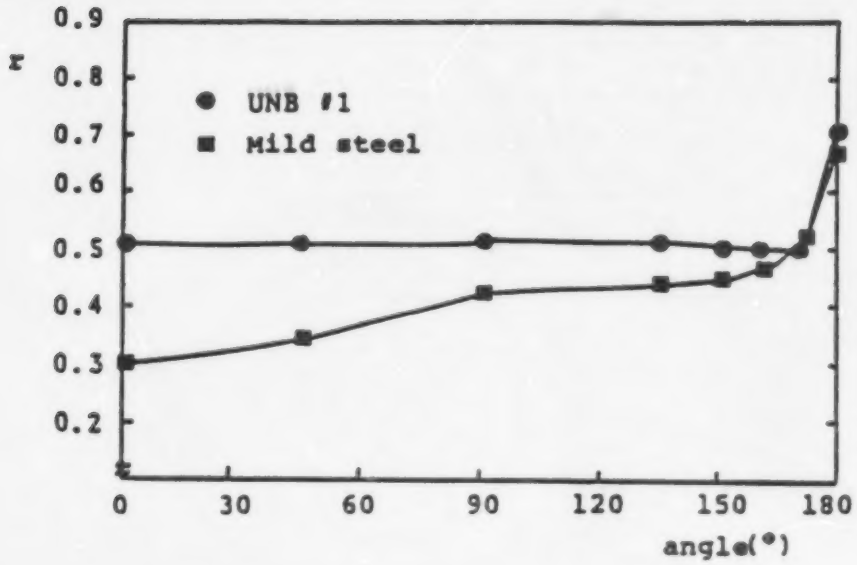

Figure 39. Variation of the exponent 'r' in Rohsenow equation

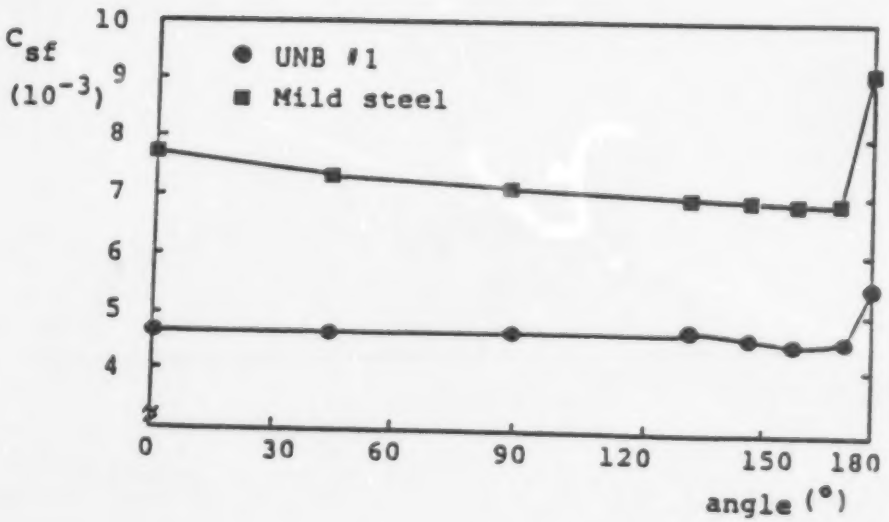

Figure 40. Variation of the constant 'C_{sf}' in Rohsenow equation.

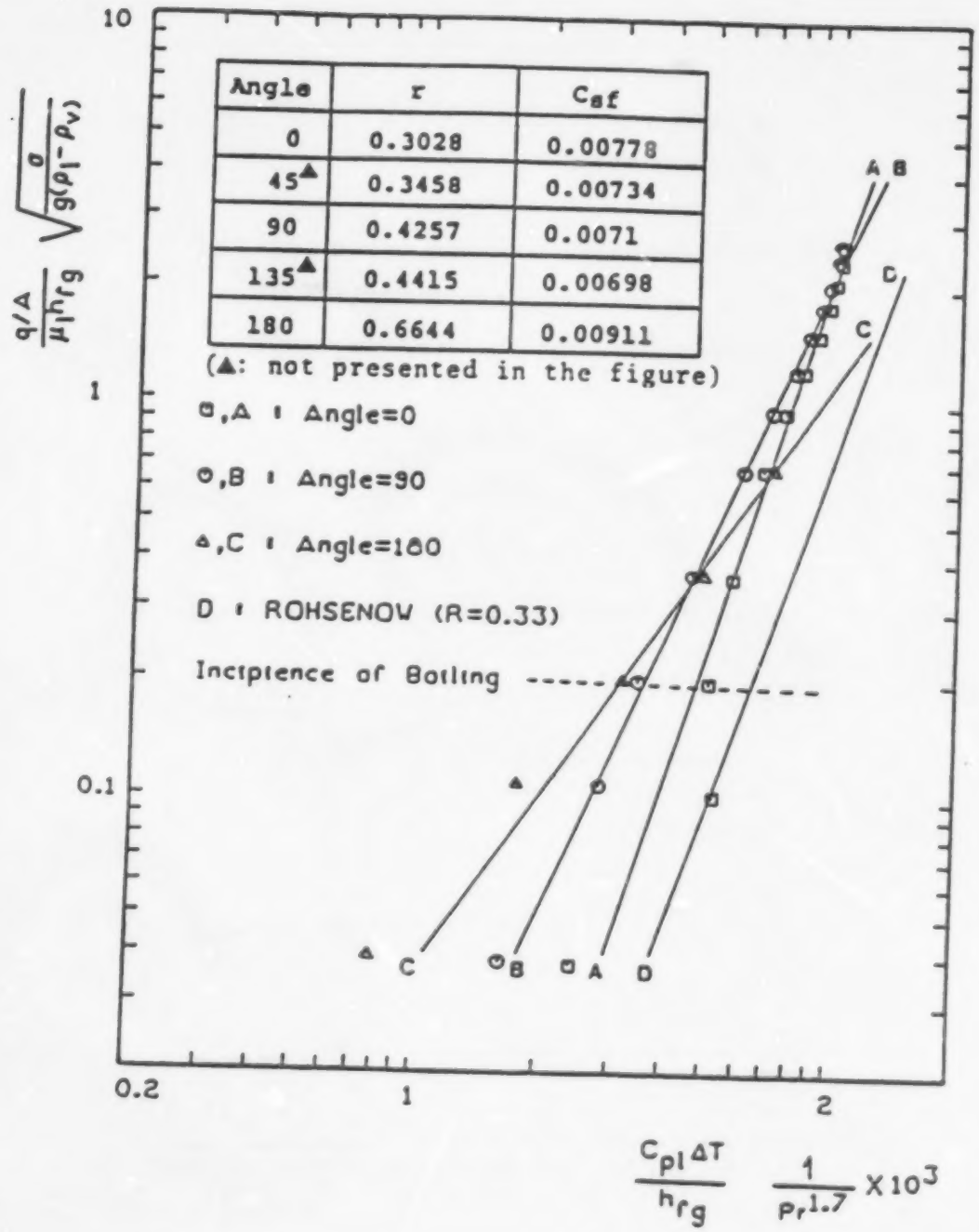

Figure 41. Correlation of data from mild steel surface using modified Rohsenow equation.

there is a thin layer of liquid at the wall interface which retards the heat flow toward the EXPLOSAFE and subsequently it is not sufficiently superheated to activate nucleation sites on its surface. This material layer reduces to ? to a thermal resistance which prevents the liquid from having good access to the surface so to wet it and sweep the heated fluid. As the thickness the thermal resistance of the EXPLOSAFE increases causing even poorer heat transfer to the liquid.

The effect of pressure in nucleate and film boiling was observed to follow accepted patterns.

All nucleate boiling results were correlated by the Rohsenow equation:

$$\frac{Cp_{\ell}\Delta T}{h_{fg}} = C_{sf}\left(\frac{q/A}{\mu_{\ell} h_{fg}} \sqrt{\frac{\sigma}{g(\rho_{\ell} - \rho_{v})}}\right)\left(\frac{r\, C_{\ell}\, \mu_{\ell}}{k}\right)^{s}$$

The uniqueness of this equation is that only one set of experimental values of q/A and ΔT is necessary to determine the coefficient 'C_{sf}' for given 'r' and 's' values. Once these coefficients are obtained, the behavior of a given liquid-surface combination can be determined for other values of ΔT.

Figures 39, 40 and 41 illustrate the results obtained. Complete details are to be found in [3].

3.2 Two-Phase Swelling Analysis

A model for the constant pressure two-phase swelling height based upon bubble rise dynamics has been proposed in [3].

In order to analyze the swelling phenomena the following two assumptions are made,

1) Bubble formation on the heated surface is evenly distributed over the surface.

2) The bubble rise velocity, V_b, is [3]

$$V_b = 1.18\left[\frac{\sigma g(\rho_\ell - \rho_v)}{\rho_\ell^2}\right]^{\frac{1}{4}}$$

The mass of the vapor generated by a given heat flux (kg/sec) is:

$$\dot{m}_v = \frac{Q}{h_{fg}}$$

where Q and h_{fg} are total heat input (watts) and latent heat of vaporization (J/kg) respectively.

The volumetric rate of vapor generation (m^3/sec):

$$w = \frac{\dot{m}_v}{\rho_v}$$

where ρ_v is the density of the vapor.

The increase in volume due to vapor holdup is:

$$\Delta V' = wt$$

The time, t, taken for the vapor bubbles moving with a constant velocity, V_b, to rise to the top of the height is

$$t = \frac{H}{V_b}$$

As seen in Figure 42 the height, H, is not constant but varies as a function of inclination angle θ, due to tank geometry. At the tank boundaries it is further assumed that:

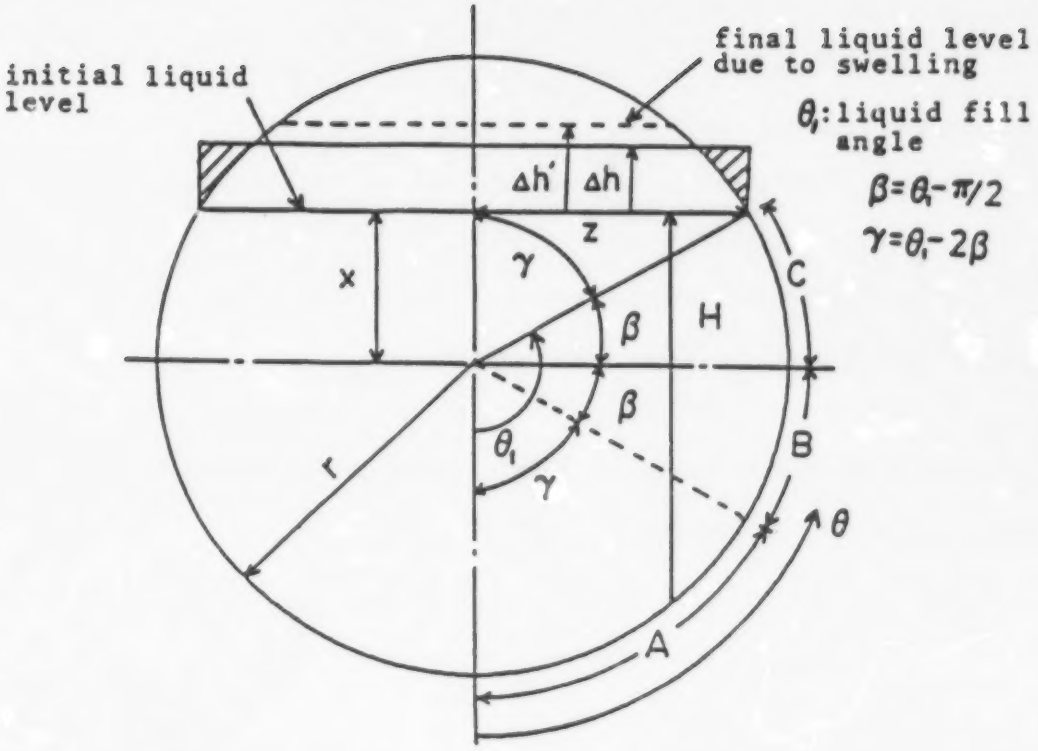

Figure 42. Idealized system for swelling

3) There are no boundary layer effects and bubbles formed at the region A in Fig. 43, $(0<\theta<\gamma)$, move vertically. In this region, the distance bubbles move can be expressed as:

$$H_1 = x + r \cos \theta \qquad (0 < \theta < \gamma)$$

where x, r, and θ represent the liquid height above the centerline of the tank, radius of the tank, and the inclination angle which is an independent variable in the equation. (Fig. 43a).

4) Bubbles formed at the region B, $(\gamma < \theta < \pi/2)$ move vertically and upon reaching the region C slide along the surface. (Fig. 43b)

In this region, the distance bubbles move can be expressed as:

$$H_2 = 2 r \cos \theta + e(\theta - \gamma)$$

5) Bubbles generated at the region $C\pi/2 < \theta < \theta_1)$, slide along the curved surface. The distance bubbles pass becomes:

$$H_3 = r(\theta_1 - \theta)$$

The heights as functions of A permit integration to evaluate an average height, H_{ave}, for the system. H_{ave} becomes

$$H_{ave} = \frac{\int_0^{\gamma} H_1 d\theta + \int_{\gamma}^{\pi/2} H_2 d\theta + \int_{\pi/2}^{\theta_1} H_3 d\theta}{\theta_1}$$

By substituting the values of H_{ave} and V_b, an average time, t_{ave}, can be calculated. With this information an initial increased volume due to boiling, $\Delta V'$ can be evaluated and subsequently a swelled height, Δh can be determined.

The actual swelled height is not Δh but $\Delta h'$ due to the cylindrical geometry of the tank. To account for the overhatched area (Fig. 42), integration is performed again to evaluate the actual swelled height, $\Delta h'$.

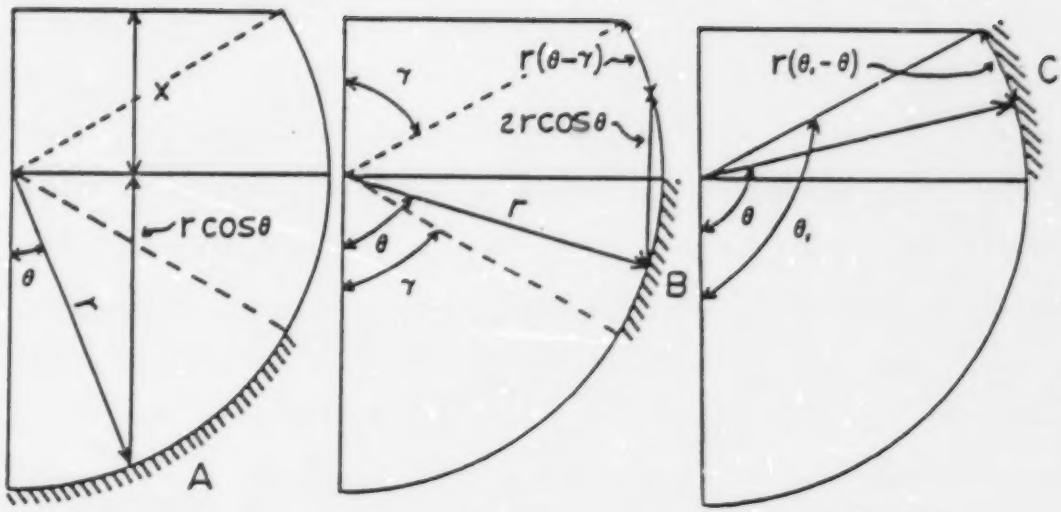

Figure 43. Heights at different regions.

The swelling analysis has been applied to the UNB tank with several different liquid fillings in order to compare with experimental data. A comparison is shown in Table 7 for 16 kW/m^2.

A less than satisfactory comparison can be made to experimental results obtained during the depressurization caused by PRV vent. Considerable more new work is necessary in order to accurately characterize and predict the two-phase void distribution and swell height caused by this pressure relief.

TASK 4. Alternate Protection Schemes.

The work in task 3 identified that enhanced boiling surfaces when coupled with geysering devices may substantially reduce tank vapour space wall temperatures. Continuing work in this area is therefore necessary. The provision of the 25 mm thick EXPLOSAFE annular pack at 40 kW/m^2 and the pool boiling tests with this surface did little to support the theory that circumferential conduction to the liquid space in the EXPLOSAFE results in heat transfer from the hot vapour space. In fact these measurements indicated that maintaining mechanical contact with the vapour space was difficult and hence heat transfer enhancement questionable with any EXPLOSAFE packing.

This work is reported in detail in Refs. [1,3] and [7].

TASK 5. Supporting Literature and Analyses.

Volumes 5, 6 [4, 5] include all the studies made and reported in earlier interim progress reports. These are as listed in Table 1. The Tables of Contents for all the Volumes which are summarized here appear as Appendix 1 of this document. Only sufficient detail will be given here to describe the major accomplishments of each item not reported previously.

Table 7. Comparison between the theoretical and experimental swelling heights for UNB tank with different tank fillings ($q/A = 16$ kw/m^2, at 2 bar)

Filling %	x (m)	θ_1 (°)	H_{ave} (m)	t_{mod} (sec)	Δh (m)	$\Delta h'$ (m)	Δh_{exp} (m)
75	0.0772	114	0.1648	1.56	0.025	0.03	0.015
55	0.015	95	0.1298	1.2	0.015	0.017	0.013
25	-0.0772	66	0.0735	0.67	0.0066	0.0074	0.009

5.1 Numerical Model

A numerical model, adapted from CALSPAN, has been translated into BASIC and is running on an HP85B with 32K memory and 128K RAM. Modifications to the programme to include external insulation, the termination of free convection by inclusion of a test on the Clausius-Clapeyron criteria, two-phase void development and swelling, subcooled and saturated nucleate boundary layer boiling and testing for possible film boiling with swelling have been partially completed. Figures 44 to 45 illustrate the programme logic and a computer simulation of an 1/5 scale unprotected test in Alberta, further development of this programme is necessary in order to validate the detailed sub models used and verify its application to a variety of experimental conditions.

5.2 Thermodynamic Properties

A FORTRAN subroutine "TDPROP" has been written whch calculates various thermodynamic properties of propane under the conditions of compressed liquid, saturated liquid and superheated vapour, and vapour (saturated or superheated) only.

The input to the subroutine are, the total mass of propane, the volume of the tank and the temperatures of the vapour and the liquid. From the input data the program determines the state of the fluid. The properties such as tank pressure, fluid density, enthalpy, internal energy, entropy, dP/dT, dP/dp, velocities of sound, and the latent heat (for liquids) are calculated for vapour and/or liquid as the case may be. The comptational range of TDPROP is:

231.07 K < TLIQ < 369.8 k

231.07 K < TVAP < 700 K

1.013 bar < P < 42.42 bar

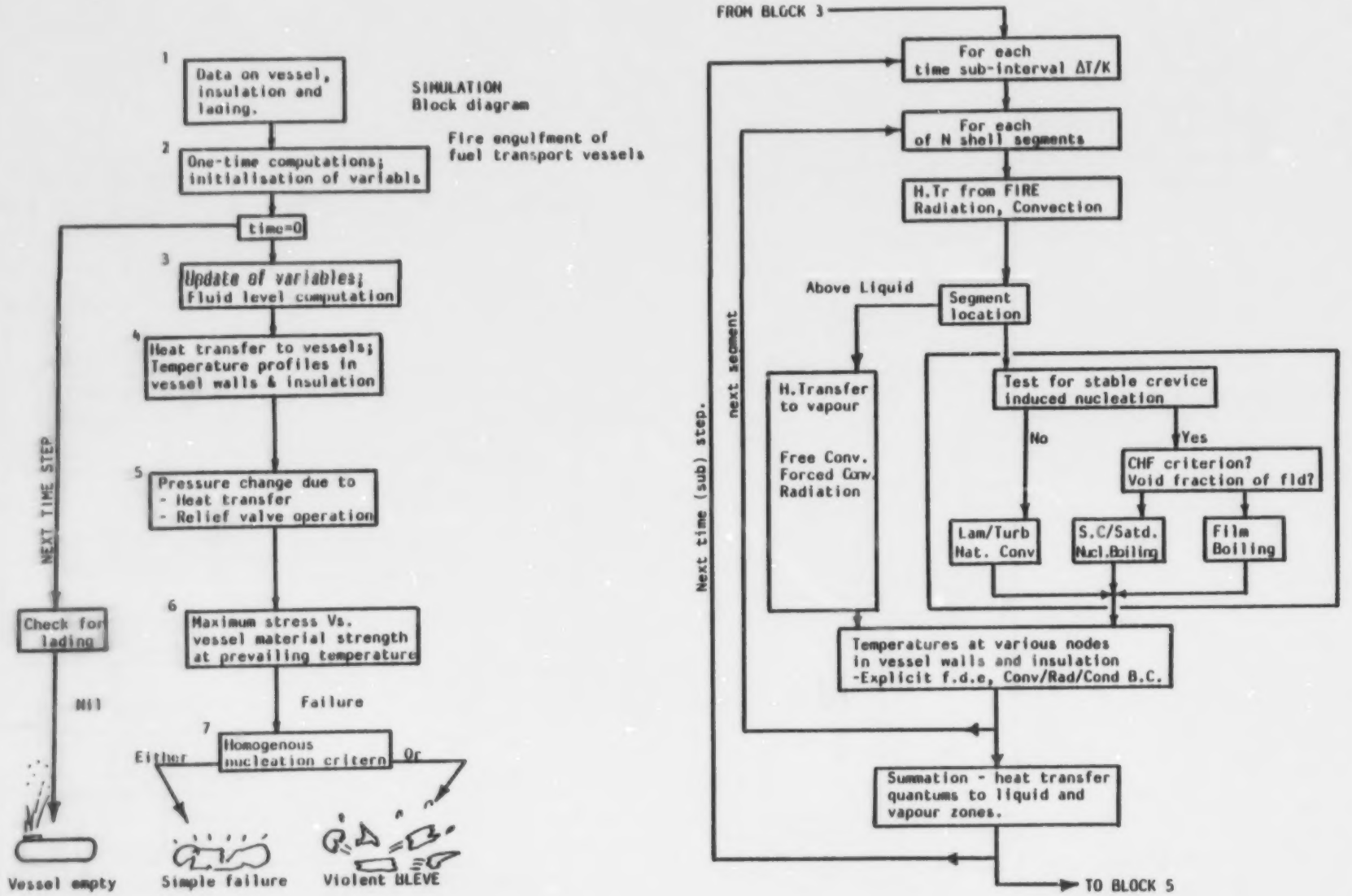

Fig. 44 Computer Simulation Model: Flow Diagram

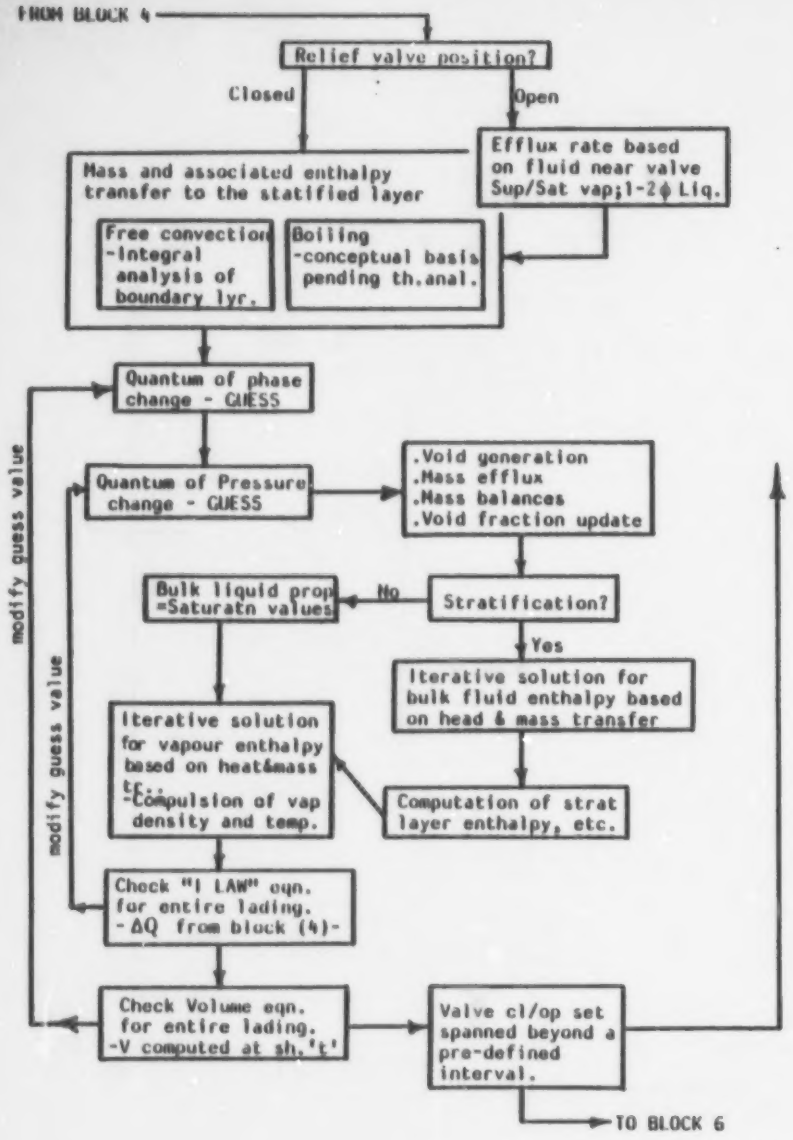
FROM BLOCK 4
Relief valve position?
Closed
Open
Efflux rate based on fluid near valve Sup/Sat vap;1-2ϕ Liq.
Mass and associated enthalpy transfer to the statified layer
Free convection -Integral analysis of boundary lyr.
Boiling -conceptual basis pending th.anal.
Quantum of phase change - GUESS
Quantum of Pressure change - GUESS
.Void generation
.Mass efflux
.Mass balances
.Void fraction update
Bulk liquid prop =Saturatn values
No
Stratification?
Yes
Iterative solution for bulk fluid enthalpy based on head & mass transfer
Iterative solution for vapour enthalpy based on heat&mass tf.. -Compulsion of vap density and temp.
Computation of strat layer enthalpy, etc.
Check "I LAW" eqn. for entire lading. -ΔQ from block (4)-
Check Volume eqn. for entire lading. -V computed at sh.'t'
Valve cl/op set spanned beyond a pre-defined interval.
TO BLOCK 6
modify guess value
modify guess value

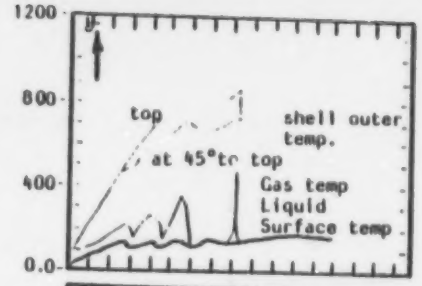

Uninsulated, horiz tank 2'ϕ; 12'long,laden with 970 lb propane. Valve set pi 280 psia, orifice .0027 sq.ft. Flame temp at time '0' on wd 1300°F around shell. --- 1/s scale test;Trans Canada report No TP2740,'80; R.D. Appleyard.

Shell temperatures

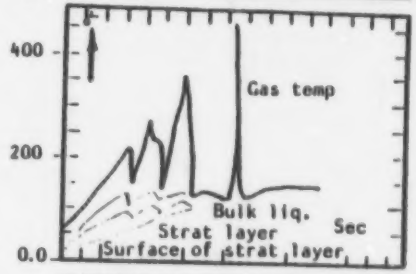

Fluid temperatures

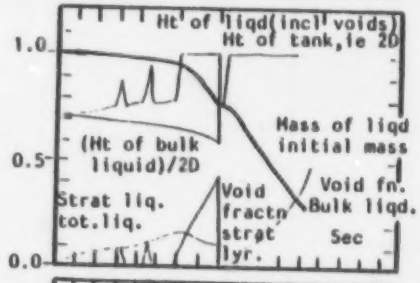

Mass of lading; fluid level; stratification %; void fractions.

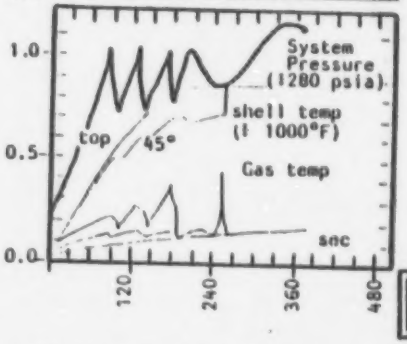

System pressure; temp.

SAMPLE PROGRAM
OUTPUT ... ON HP 85B ...

Fig 45 Computer Simulation Model: Flow Diagram Control and Results

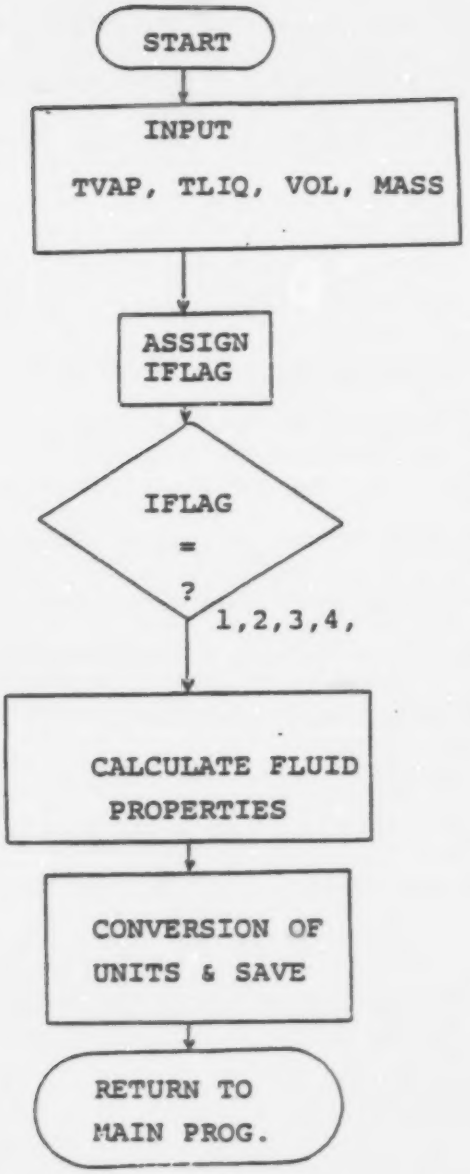

IFLAG=1 : SAT LIQ + SAT VAP
=2 : SAT LIQ + SUP. VAP
=3 : ONLY VAP
=4 : ONLY LIQUID

Figure 46. Flow Diagram of Subroutine TDROP

A flow diagram for the subroutine is shown as Figure 46.

In addition to the above the surface tension, thermal conductivity and viscosity can be computed from the function subprograms SURTEN, CONDUC, and VOSCOS. These routines do not include the critical region enhancement terms.

The complete program listings are given in Volume 5 of the Final Report [4].

5.3 Tank Car Geometry

A FORTRAN subroutine 'GEOM' analyzes the geometry of a cylindrical tank as a function of the angle of pitch with respect to the horizontal. The programme determines the wetted surface area (WSA) and the fire surface area (FSA); both necessary for analyzing the heat transfer to the tank's lading.

There are three possible shapes that the liquid (vapour) can assume with pitch angle. These are a truncated cylinder, a wedge, and a truncated wedge (Figure 47). General formulae for the volume, FSA, and WSA were developed for each shape. These formulae were then expressed such that each involved only one unknown dimension; that is the various dimensions were related in terms of the angle of pitch and the known tank dimensions. The one unknown dimension can thus be determined either explicitly or by employing an iterative scheme and the others demensions necessary to determine WSA and thus FSA can be evaluated.

The program listing is detailed in Volume 5 [4].

5.4 Cylindrical Surfaced Calorimeter

In order to visualize the fluid thermohydraulics under the effects of a torch fire a cylindrical surfaced calorimeter was constructed and preliminary testing conducted. The 101 mm diameter calorimeter was fitted to a 152 mm

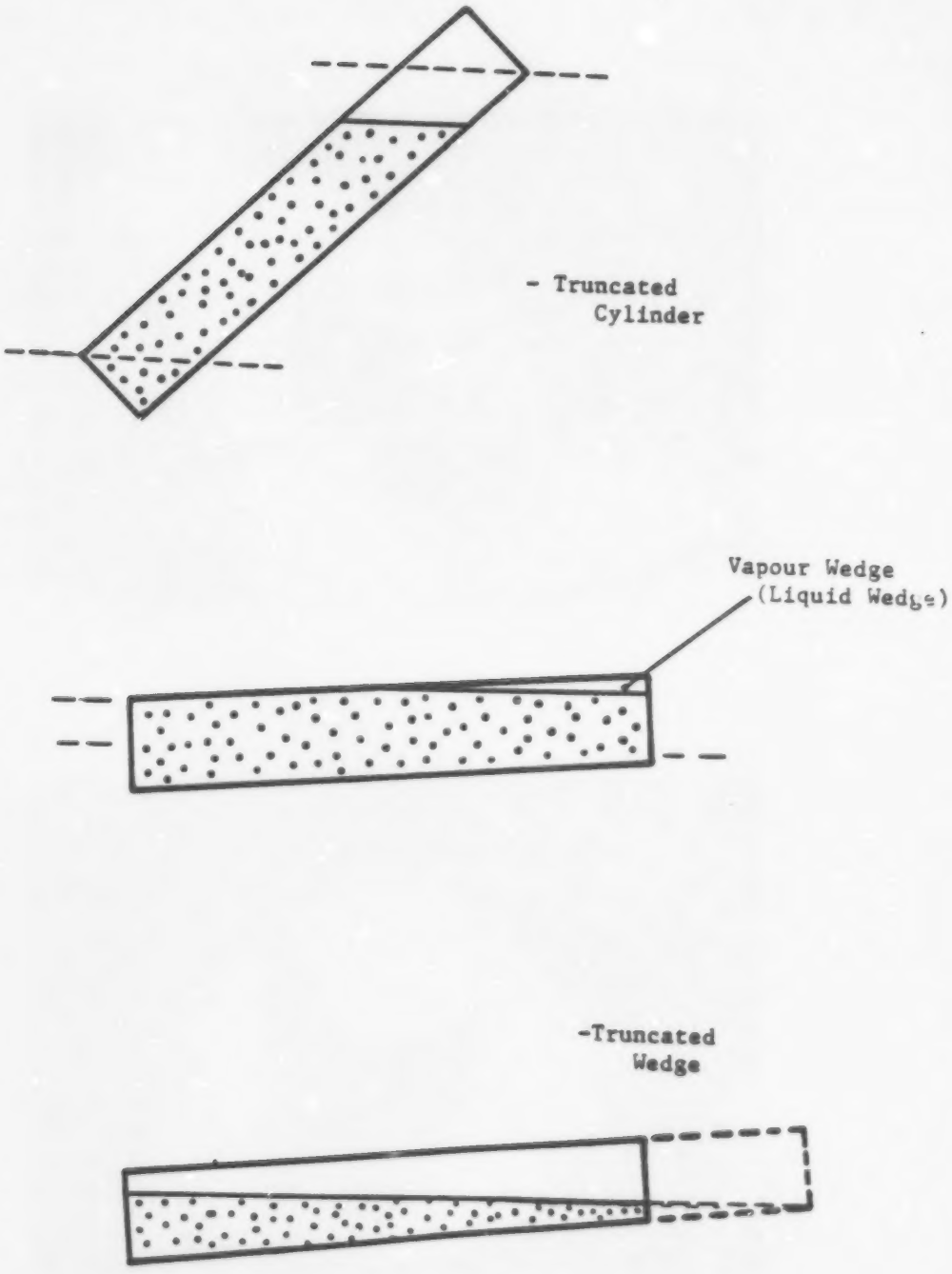

Figure 47. Tank Pitch Geometry as a Function of Fill

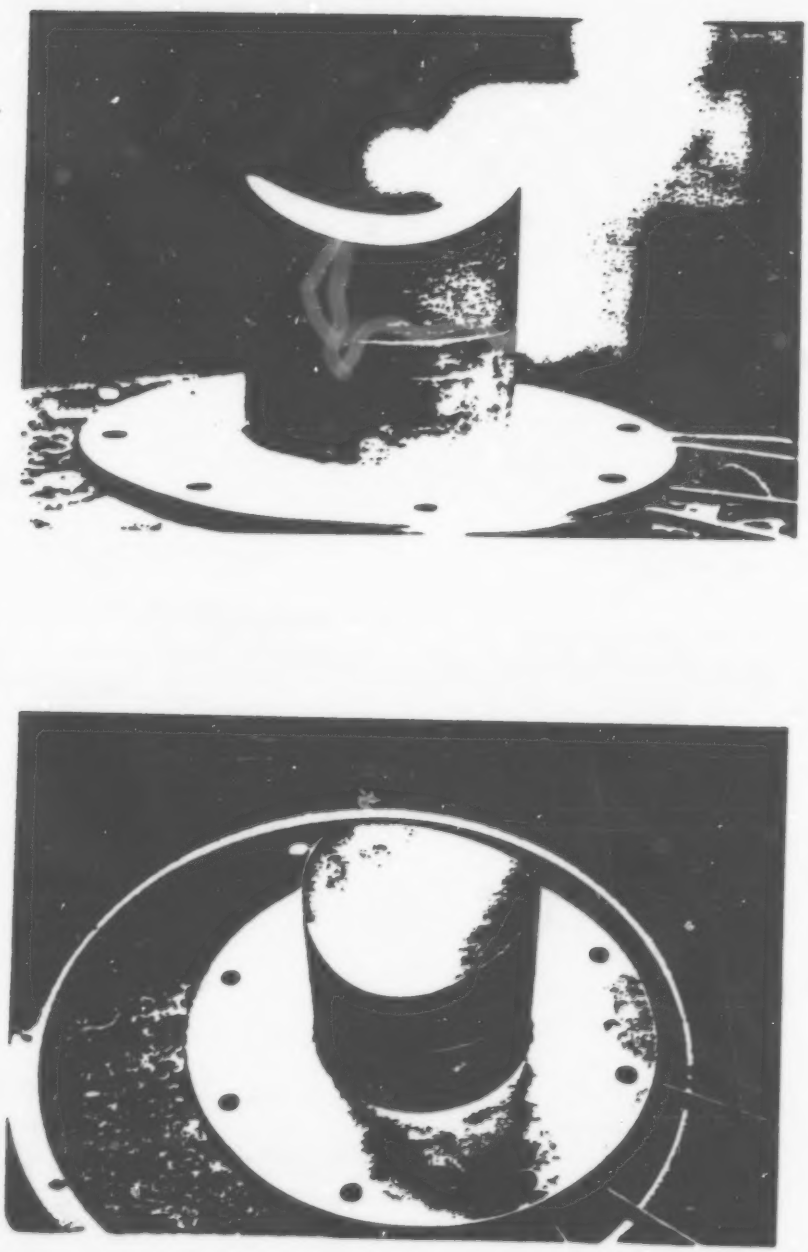

Figure 48. Views of Torch Fire Wall Heater

diameter by 101 mm Pyrex Tee vessel 305 mm long. Plexiglass end windows permitted flow and heat transfer visualization at local surface heat fluxes up to 570 kw/m^2 (Figure 48).

Initial testing with water with the calorimeter axis 25 degrees below horizontal indicated the formation of a statified layer which grew in thickness until the entire contents of the vessel demonstrated a profound anticlockwise motion with considerable bubble carry under resulting from the nucleate boiling occuring on the patch (Fig. 49).

This work was of a preliminary nature only and larger scale experiments coupled with analysis is required to quantify the phenomena.

5.5 Thermal Conductivity and Contact Conductance of Explosafe

The thermal conductivity of EXPLOSAFE, an expanded aluminum foil used to augment the heat transfer in a pressure vessel, was measured over a temperature range of 5°-70° C. Measurements were obtained with different styles, orientations and thicknesses of EXPLOSAFE. In addition, the thermal contact conductance for an EXPLOSAFE matrix and wall interface was determined for one particular style as a function of pressure and a simple correlation developed.

A guarded hot-plate apparatus with an on-line Microcomputer (Hewlett Packard-85) and the Hewlett Packard-3497 Data Acquisition System was used.

5.5.1 Experimental

The apparatus (Figure 50) consisted of a hot plate and two cold plates on either side of the hot plate. Two identical specimens of EXPLOSAFE were clamped between the hot and cold plates. A guard heater surrounded the hot plate along the edge to prevent heat loss through the edges. Cold fluid at a

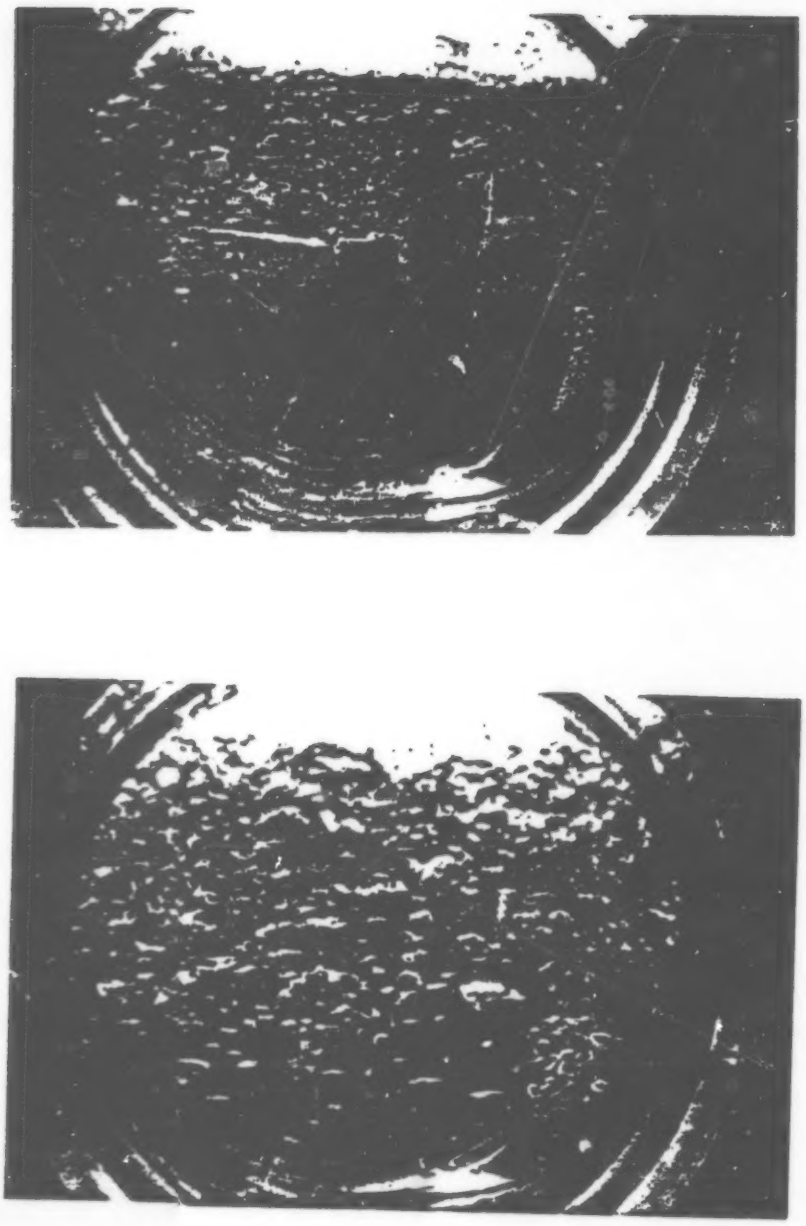

Figure 49. Views of Boilup on Torch Fire Wall Heater

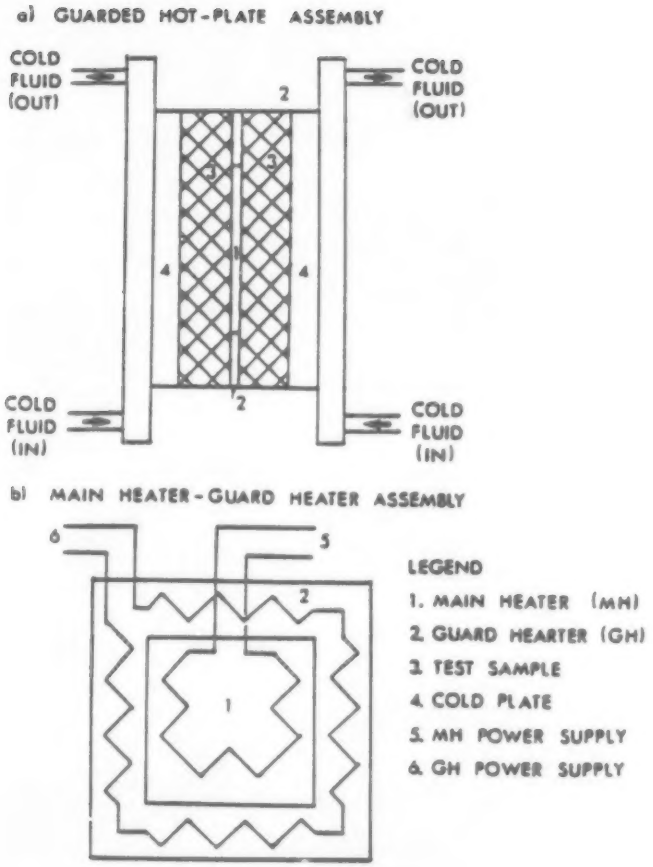

Fig. 50 Guarded hot-plate apparatus.

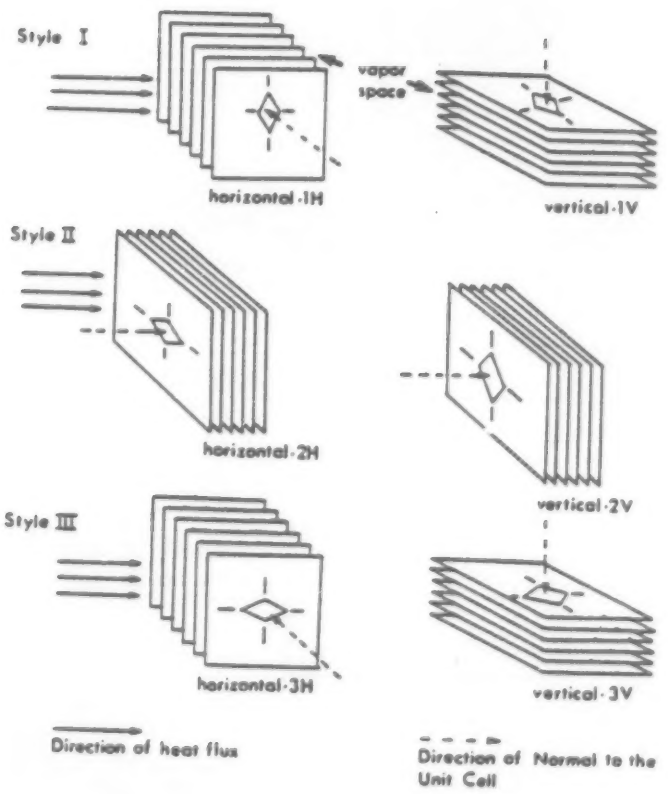

Fig. 51 EXPLOSAFE Styles and Orientations

controlled temperature was circulated through the cold plates. Four spring scales were affixed to the apparatus to measure the interfacial contact pressure between the hot/cold plates and the EXPLOSAFE sample. The temperatures of the guard heater, the main heater and the cold plates were suitably adjusted to obtain a desired temperature differenct (ΔT) or heat flux, Q, in the specimens. The steady state temperature difference across the EXPLOSAFE specimen and the heat flux were measured to determine the apparent thermal conductivity, λ_a, including the effect of contact conductance. An estimate of the true bulk thermal conductivity, λ_t, of the speciment was made after application of a thermal contact grease (Wakefield Thermal Compound 120-8) to the contacting surfaces. The thermal conductance was assumed to be infinite in this case due to near perfect contact established between the specimens and the hot/cold plates.

$$Q = \lambda_t A [(\Delta T_L/\Delta X_L) + (\Delta T_R/\Delta X_R)]$$

Using these results, the contact conductance, h_c, was calculated from the measurement in tests where thermal contact grease was not applied.

$$\frac{\Delta T_L}{\Delta X_L/\lambda_a} + \frac{\Delta T_R}{(\Delta X_R/\lambda_a)} = \frac{Q}{A} \quad \frac{\Delta T_L}{(2/h_c) + (\Delta X_L/\lambda_t)}$$

$$+ \frac{\Delta T_R}{(2/h_c) + (\Delta X_R/\lambda_t)}$$

5.5.2 Test Samples

EXPLOSAFE samples were supplied by the Vulcan Industrial Packaging Limited, Canada. The various styles (styles I, II, III) and orientations (V and H) in which they were tested, are shown in Figure 51. For styles I and II, V and H indicate the direction of the normal to the plane of the unit cell of the EXPLOSAFE mesh. For style III, V and H refer to the orientation of the major axis of the unit cell. Samples having thicknesses of 25 mm and 50 mm were tested.

5.5.3 Theoretical Predictions

A theoretical model was developed to predict the thermal conductivity of EXPLOSAFE for styles I and III. It was assumed that heat was transferred across the EXPLOSAFE thickness only by conduction through the aluminum foil. A theoretical value of the thermal conductivity, λ_{th}, was obtained from

$$\lambda_{th} \quad \lambda_{al} \quad \frac{\Delta X}{L_p} \cdot \frac{A_f}{A_e}$$

where $A_e = A_{vap} + A_l$

The path Length, L_p, and cross-sectional area, A_f, of the heat conduction path through the aluminum foil as well as the effective cross-sectional area, A_e, of EXPLOSAFE per conduction path as shown in Figure 52 were obtained from the test samples by direct measurement.

5.5.4 Result and Discussion

The apparent thermal conductivity, λ_a, of all the specimens was measured at mean temperatures of 5°-70°C (Figure 53).

True thermal conductivities for styles I and III were measured experimentally as well as estimated theoretically. The results are summarized in Table 8.

The apparent thermal conductivity, λ_a, as a function of pressure was measured for style III in the range of 1.69 to 4.65 kPa. An increase in λ_a with increasing pressure resulted due to improved contact conductance at the EXPLOSAFE-plate interface. Using the results of Figure 54, the thermal contact conductance was determined as a function of pressure.

$$h_c = 193.32 + 41.10\ P$$

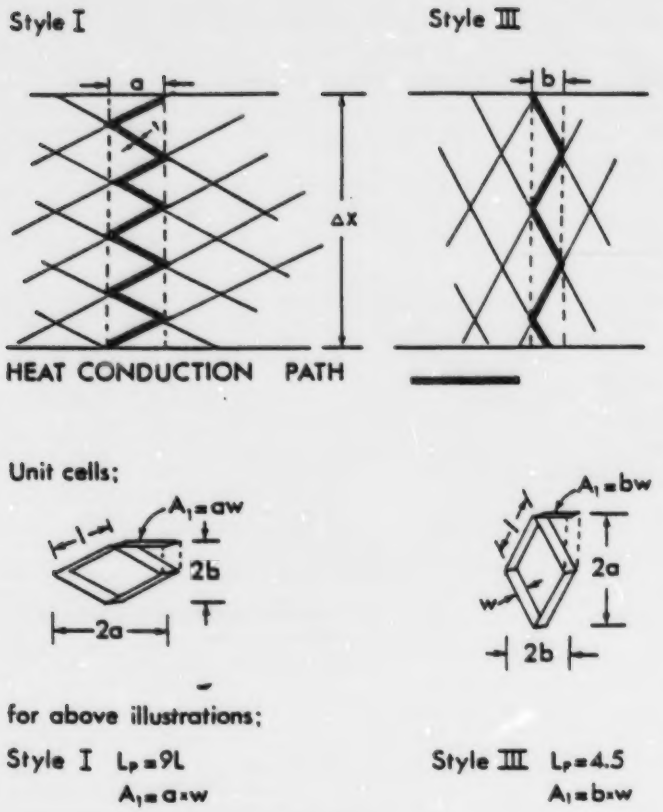

Figure 52. Heat transfer model for EXPLOSAFE

style	λ_t, W.m^{-1}.K^{-1}	
	Theoretical	Experimental
style I	0.409	0.45
style II	0.106[5]	0.20
style III	2.414	2.25 H 2.60 V

Table 8. True thermal conductivity of EXPLOSAFE

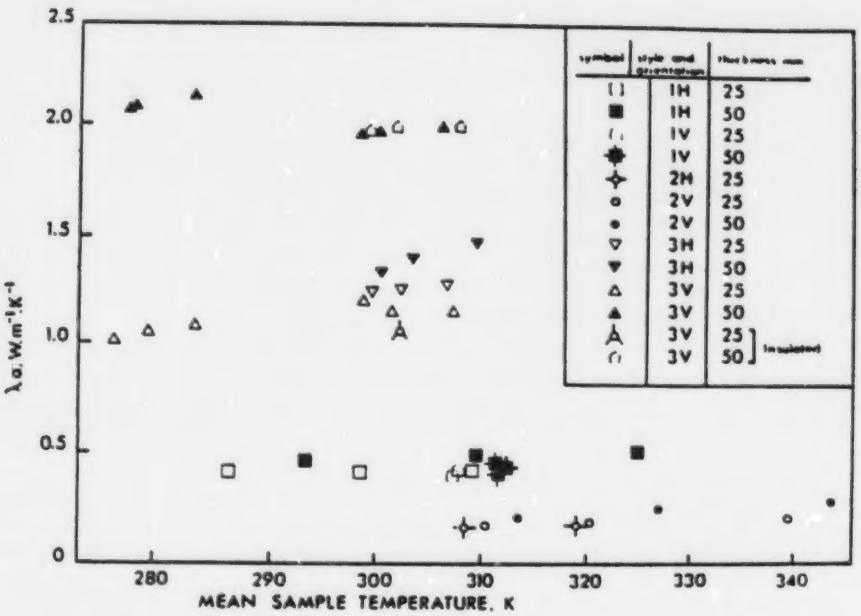

Figure 53. Apparent thermal conductivity of EXPLOSAFE

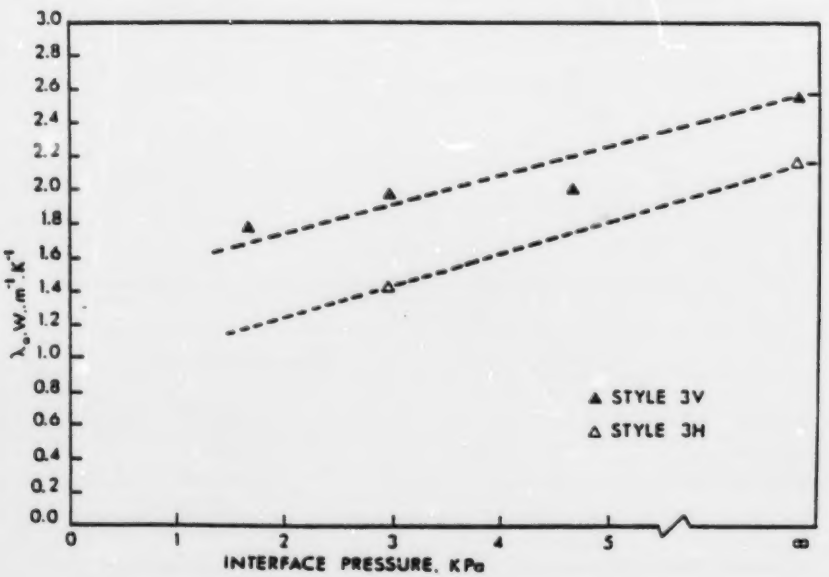

Figure 54. Apparent thermal conductivity of EXPLOSAFE as a function of pressure

TASK 6. Pool Fire - Flare Interaction.

Analysis of the radiation exchange factors between pool fires, the flare and the tank have been prepared for publication and presentation [5,6].

A series of tests (Table 9) was performed to determine the effect of a high velocity propane jet flare on the heat flux to a cylindrical surface within a pool fire.

Three steel pans of 30, 60, and 90 cm diameters were used to contain the pool fire.

Two calorimeters of 8 and 25 mm diameters were placed in the pool fire at different positions (Figures 55 and 56). The tops of the calorimeters were level with the propane nozzle tip which was 7.5 cm above the pool surface. The rate of heat transfer to the calorimeters was determined by the increase in enthalpy of the water passing through the calorimeters.

The water cooled propane burner was placed close to the center of the pan. The nozzle of the burner is removable and the appropriate size nozzle is used for the corresponding size pan. A calibrated rotameter was used to measure the propane flow rate.

In experiments 4 to 6, a radiometer was placed near the center of the pan to measure the local heat flux in the fire. The top of the radiometer was 7.5 cm above the pool surface.

Readings were taken on the calorimeter and the radiometer with a pool fire alone and with the propoane flare operating within the pool fire. This gives a direct comparison of the total flux to the calorimeter and the radiometer with the propane flare operating and not operating. The data of Table 9 indicate that the propane flare does not substantially alter the heat flux to the calorimeter or radiometer for the conditions under which the test was conducted.

Table 9

Heat Flux to Calorimaters and Radiometer in Propanal Pool Fire and Propane Flare Interaction Studies [6]

Diameter of calorimeter = 1"

Test #	Pan Size (ft)	Heat Flux Pool Fire (kw/m^2)	Heat Flux, Pool Fire & Propane Flare (kw/m^2)	% Change in Heat Flux	(SCFM) Propane Flow Rate	(SCFM) Target Propane Flow Rate	Water Flow Rate (kg/s)
1*	1	31.42	38.3	+22%	0.487	3.85	2.63×10^{-3}
2*	1	61.37	66.31	+ 8%	0.487	3.85	2.63×10^{-3}
3*	1	66.14	67.76	+ 2%	0.487	3.85	2.63×10^{-3}
4**	1	53.69	54.21	+ 1%	3.3	3.85	1.88×10^{-3}
5**	2	25.73	25.28	- 1.75%	6.84	15.48	5.47×10^{-3}

Diameter of Calorimeter = 0.25"

Test #	Pan Size (ft)	Heat Flux Pool Fire (kw/m^2)	Heat Flux, Pool Fire & Propane Flare (kw/m^2)	% Change in Heat Flux	(SCFM) Propane Flow Rate	(SCFM) Target Propane Flow Rate	Water Flow Rate (kg/s)
1*	1	46.63	49.68	+ 6.5%	0.487	3.85	2.03×1^{-3}
2*	1	79.68	75.68	- 5%	0.487	3.85	1.73×10^{-3}
3*	1	88.06	87.25	- 1%	0.487	3.85	1.75×10^{-3}
4**	1	--- ***	--- ***		3.3	3.85	2.07×10^{-3}
5**	2	59.29	52.63	-11%	6.84	15.48	2.47×10^{-3}

Radiometer

Test #	Pan Size (ft)	Heat Flux Pool Fire (kw/m^2)	Heat Flux, Pool Fire & Propane Flare (kw/m^2)	% Change in Heat Flux	(SCFM) Propane Flow Rate	(SCFM) Target Propane Flow Rate
4	1	23.82	22.57	-5.27%	3.3	3.85
5	2	53.21	53.80	+1.10%	6.84	15.48

* See Figure I in Appendix for positions of the equipments in the pool fire.

** See Figure II in Appendix for positions of the equipments in the pool fire.

*** See Table II in Appendix for experimental data.

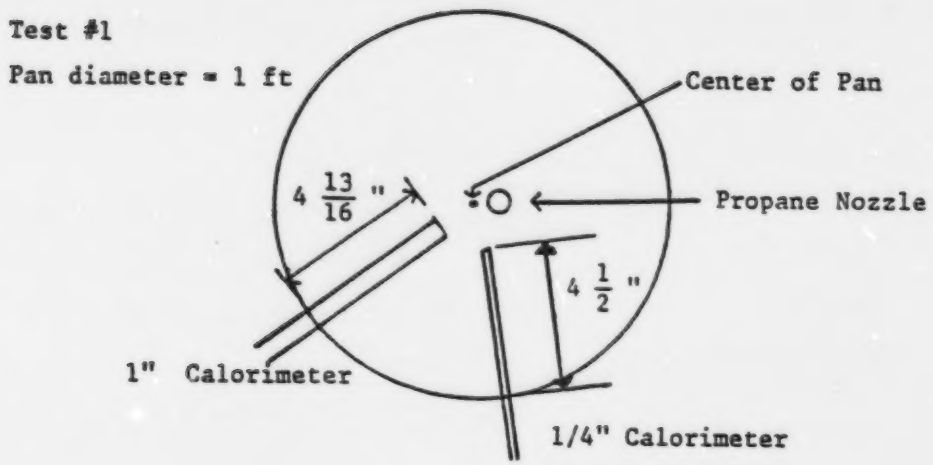

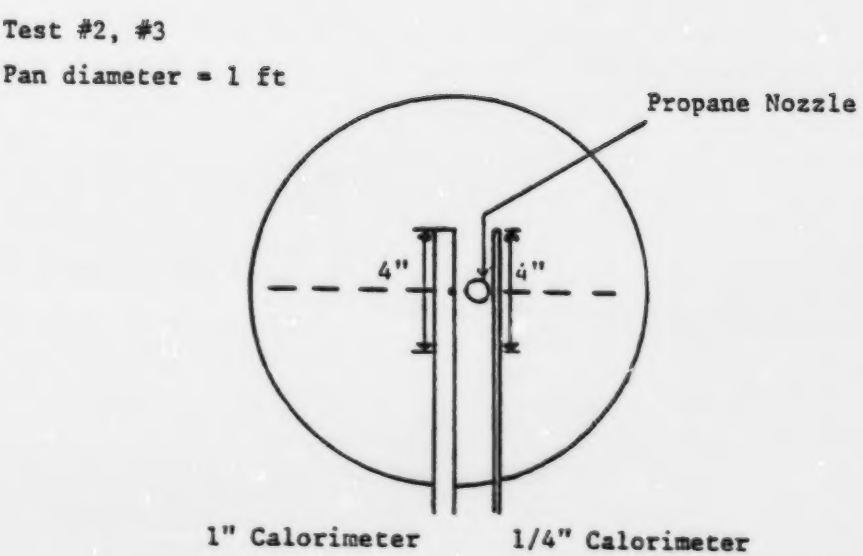

Figure 55. Top view of the positions of the equipments in the pool fire for tests 1 to 3.

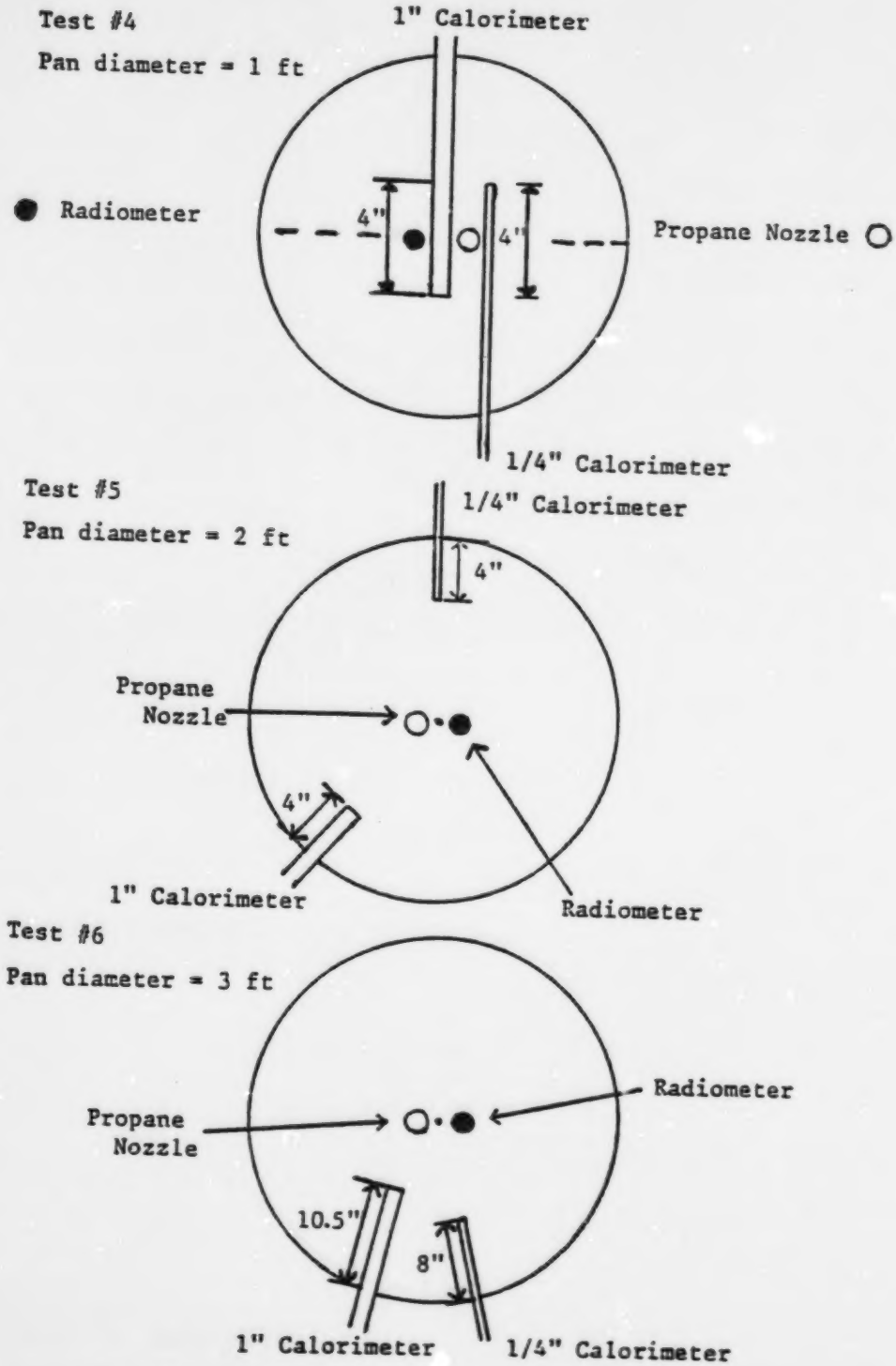

Figure 56. Top view of the postions of the equipments in the pool fire for tests 4 to 6.

TASK 7. R12 Test Programme

Preliminary to conducting tests with R12 the inner stainless steel tank (Task 1) had been remachined to reduce the wall thickness to 3 mm. Rescheduling of the experimental programme for the continuing Phase II tests and student thesis requirements has necessitated postponing these tests indefinitly.

TASK 8. Audio Visual Presentation of Results

A 3/4 VHS video cassette record of all the tests has been prepared (Volume 8a)[7]. Audio visual material, obtained from various sources (CBC, AAR, AFPA) is to be incorporated into a final video tape production describing the background to the TDC support programme and to summarize the results of all phases of the programme.

TASK 9. Test Data Presentation

All test data for the experiments listed in Table 3 has been provided in the form of computer data printouts and plots of all experimental parameters as functions of time in Volume 8b [7].

Conclusions

An experimental facility has been developed, reported, and utilized for the experimental investigation of the thermal hydraulic behaviour and response tanks containing pressure liquefied fluids when exposed to simulated accidental fire conditions. Aspects of this study have addressed the experimental observation of pressurized fluid behaviour with heat addition and pressure relief, the analysis and experimental verification of free convection thermal stratification of the liquid contents, the effects of

orientation and surface preparation on the boiling process, the pool fire - flare interaction, vapour space heat transfer, internal protection, and ancilliary subjects.

Specific conclusions summarized from the work reported may be stated as:

1. An experimental facility to test and observe thermohydraulic response of externally heated pressure liquified fluids has been designed, constructed, tested and utilized in an ongoing programme of experiments to simulate fire accidents with such tanks protected by pressure relief valves and other systems.
2. The internal pressure of the lading in such tanks is set by the liquid surface temperature and any low boiling point impurity vapour or noncondensable gas ballast. The temperature stratification in the liquid results from the wall heat transfer over only a portion of the liquid wetted wall; an unstable region, located at the bottom of the cylinder results in the heating of the cooler core liquid. Analysis of this phenomena has been conducted with and without EXPLOSAFE.
3. Experiments, conducted to determine the effects of inclination and heat flux on heat transfer from plain, specially prepared, and EXPLOSAFE covered surfaces in liquid R11 indicate that at moderate to high heat fluxes inclination does not significally influence nucleate pool boiling over that for horizontal surfaces. In the film boilup region however significant reductions in heat transfer occur with downward facing surfaces. Explosafe layers were found to diminish heat transfer from surfaces in the nucleate boilup regions for all angles of inclination.
4. Preliminary analysis of the two phase swelling resulting from the pool boilup of partially liquid filled cylinders has been conducted.

5. Tests conducted with a 25 and 50 mm thick EXPLOSAFE pack in the test vessel revealing little or no advantage to this method of tank protection. Liquid space heat transfer was slightly impeded through vapour space temperatures were somewhat reduced.
6. Enhanced boiling surfaces, specially prepared by the spraying of molten metal on the interior of tanks results in a porous metal coating with extremly high heat transfer potenial at very small temperature differences. These surfaces appear to have promise for the protection of the inside surfaces of tanks. Such interiors, especially when utilized with the geysering systems proposed in this work, could result in significant cooling of the critical vapour space.
7. The thermal conductivity and contact conductance of EXPLOSAFE has been determined for a variety of configurations with 25 and 50 mm sample thickness.
8. Preliminary measurements of the radiant exchange between a small scale pool fire and a high pressure propoane flare indicates that the heat flux to surfaces within the pool are not significantly altered by the presence of the flare.

In addition to the above significant specific conclusions are made in the supporting volumes accompaning this summary report.

Recommendations

As a result of the work reported here continuation of TDC support is recommended in a programme of studies designed to further use experimental facility developed here. The areas requiring further study are:

1. Subcooled and saturated two-phase boundary layer development and stratification.
2. The effects of PRV orientation, heat flux, lading fill and orifice diameter on pressure relief and thermal-hydraulics.
3. The use of high heat flux interior surfaces for internal fluid cooling of the tank vapour space.
4. Vapour space heat transfer with swelling and pressure relief, and
5. Tank car thermal response computer modeling.

REFERENCES

1. N.U. Aydemir, J.E.S. Venart and A.C.M. Sousa, Transient Natural Convection in a Partially Filled Horizontal Cylinder, Final Report, Volume 2, TP 7514E, Transportation Development Center, Transport Canada

2. G. Qureshi, J.E.S. Venart, A.C.M. Sousa and F.R. Steward, Experimental Determination of the Heat Transfer in the Vapour Space of a Partially Filled Horizontal Cylinder, Final Report, Volume 3, TP 7515E, Transportation Development Center, Transport Canada

3. D.S. Jung, J.E.S. Venart and A.C.M. Sousa, Pool Boiling Heat Transfer: The Effects of Enhanced Surfaces and Inclination, Final Report, Volume 4, TP 7516E, Transportation Development Center, Transport Canada

4. J.E.S. Venart, A.C.M. Sousa, F.R. Steward, et al, Supporting Studies, Final Report, Volume 5, TP 7518E, Transportation Development Center, Transport Canada

5. Published Papers, Final Report, Volume 6, TP 7519E, Transportation Development Center, Transport Canada

6. F.R. Steward and S. Wong, Pool Fire - Flare Interactions, Final Report, Volume 7, TP 7520E, Transportation Development Center, Transport Canada

7. J.E.S. Venart, A.C.M. Sousa and F.R. Steward, Tank Simulator Test Data, Final Report, Volume 8, TP 7521E, Transportation Development Center, Transport Canada

APPENDIX A

APPENDIX A.1

TP 7514E

TANK CAR THERMAL RESPONSE ANALYSIS: FINAL REPORT, VOLUME 2 TRANSIENT NATURAL CONVECTION IN A PARTIALLY FILLED HORIZONTAL CYLINDER

N.U. Aydemir, J.E.S.Venart, A.C.M.Sousa

TABLE OF CONTENTS

		PAGE
I	INTRODUCTION	1
	1.1 Objectives	1
	1.2 The Physical Phenomena	5
	1.3 The Mathematical Model	10
	1.4 Possible Solutions of the Governing Equations of Motion	13
II	INTEGRAL ANALYSIS	15
	2.1 Introduction	15
	2.2 Analysis	16
	2.3 An Exact Solution of the Integral Equations of Motion	20
III	A THERMAL STRATIFICATION MODEL	28
	3.1 Introduction	28
	3.2 A Model for Thermal Stratification	31
	3.3 Approximate Analysis of Hydrodynamic Stability of a Boundary Layer on a Concave Surface	33
	3.4 Final Describing Equations	36
	3.5 Modifications of Flow Properties for a Porous Boundary Layer	38
	3.6 Effects of External Stratification on the Boundary Layer	39
	3.7 Results and Discussion	41
IV	FINITE DIFFERENCE SOLUTIONS	46
	4.1 Introduction	46
	4.2 The Difficulties Associated With the Geometry and A Possible Approach	47
	4.3 The Boundary Conditions	53
	4.4 Discretization in the ζ-η Plane; Disadvantages and Advantages	58
	4.5 Solution Method and Algorithm	59
	4.6 Test Runs	61
	4.7 Heat Lines	78
	4.8 Conclusions	84
REFERENCES		88
APPENDIX A	PERTURBATION SOLUTIONS FOR EXTERNAL STRATIFICATIONS	91
APPENDIX B	TRANSFORMED EQUATIONS OF MOTION	95
APPENDIX C	DISCRETIZED EQUATIONS	97
APPENDIX D	COMPUTATIONAL FLOW CHART	99

APPENDIX A.2

TP 7515E

TANK CAR THERMAL RESPONSE ANALYSIS: VOLUME 3 EXPERIMENTAL DETERMINATION OF THE HEAT TRANSFER IN THE VAPOUR SPACE OF A PARTIALLY FILLED HORIZONTAL CYLINDER

G. Qureshi, J.E.S. Venart, A.C.M. Sousa,
F.R. Steward

TABLE OF CONTENTS

		PAGE
I	INTRODUCTION	1
	1.1 Introduction	1
	1.2 Literature Review	5
	1.2.1 Heat Transfer in Partially Filled Horizontal Cylinders	7
	1.2.2 Geysering Systems	7
II	EXPERIMENTAL FACILITY	9
	2.1 The Test Section	9
	2.1.1 The Horizontal Cylinder	10
	2.1.2 The Heating System	11
	2.1.3 Weighing System for Mass Flow Measurements	12
	2.1.4 Thermocouple Assembly	12
	2.1.5 Pressure Transducer	13
	2.1.6 Video-recording Unit	14
	2.1.7 Expected Accuracy of Measurements	14
	2.2 Design of the Pressure Relief Valve	15
	2.3 Test Program and Experimental Procedure	19
III	EXPERIMENTAL RESULTS	22
	3.1 Wall and Vapour Temperature Profiles in the Vapour Space of the Unprotected Tank	22
	3.1.1 76% Liquid Fill	23
	3.1.2 58% Liquid Fill	25
	3.1.3 23% Liquid Fill	26
	3.1.4 Effect of the Valve Orifice Area on Wall and Vapour Temperature Profiles	28
	3.2 Wall and Vapour Temperature Profiles in the Vapour Space of the Explosafe Equipped Tank	29
	3.2.1 76% Liquid Fill	30
	3.2.2 58% Liquid Fill	31
	3.2.3 23% Liquid Fill	32
IV	HEAT TRANSFER MODELS AND CORRELATIONS	34
	4.1 General Model for the Heat Transfer in the Vapour Space of a Tank With and Without Explosafe	34
	4.1.1 The UNB Tank	35
	4.1.2 Full and One-Fifth Scale Tanks	37
	4.1.3 One-Fifth Scale Tank (NOVA)	38
	4.2 Model for the Heat Transfer in the Vapour Space of the UNB Tank Using an Alternate Method	39

4.3 Analysis of Vapour Space Heat Transfer Results..... 41
4.3.1 Unprotected Tanks..... 41
4.3.2 Explosafe Equipped Tanks..... 44
4.4 Correlation Development..... 45

V ALTERNATE PROTECTION METHOD..... 50
5.1 Description of the Problem 50
5.2 Purpose of This Work 52
5.3 Geyser Prediction Model and Correlation 52
5.4 Optimisation of the Diameter and the Critical Heat Flux 54
5.5 Heat Transfer Models for Geyser and non-Geyser Heat Flux..... 55
5.5.1 Without Geysering..... 56
5.5.2 Geysering Situation..... 57
5.6 System Designs for Geysers..... 59

VI CONCLUSIONS AND RECOMMENDATIONS..... 61
6.1 Conclusions..... 61
6.2 Recommendations..... 63

REFERENCES 66
FIGURES 68

APPENDICES
I (a) Flow Diagram for the Experimental Scanning Program. 111
(b) Listing of the Experimental Scanning Program..... 112
II(a) Flow Diagram for the Plotting Program.. 116
(b) Listing of the Plotting Diagram..... 117
III Thermocouple Layout and Experimental Data..... 120
III.1 Heat Transfer in the UNB Vessel Using an Alternate Method..... 140
III.2 Heat Transfer in the Vapour Space of an Unprotected Vessel..... 141
III.3 Sample Calculations..... 144
III.3.1 Conduction Heat Transfer in the Vapour Space..... 144
III.3.2 Radiation Heat Transfer From the Vapour Space Wall to the Liquid Surface in the UNB Vessel..... 145
III.3.3 Heat Transfer Coefficient..... 148
III.3.4 Nusselt and Fourier Numbers.... 153
III.3.5 Convection Heat Transfer in the Vapour Space of the UNB Vessel (an alternate method)..... 155
III.3.6 Verification of the Assumption T_w(outer surface) = T_w(inner surface)..... 161

APPENDIX A.3

TP 7516E

TANK CAR THERMAL RESPONSE ANALYSIS: VOLUME 4 POOL BOILING HEAT TRANSFER: THE EFFECTS OF ENHANCED SURFACES AND INCLINATION

D.S. Jung, J.E.S.Venart, A.C.M.Sousa

TABLE OF CONTENTS

		PAGE
I	INTRODUCTION	1
	1.1 Introduction	1
	1.2 Study Objectives	3
II	LITERATURE REVIEW	5
	2.1 Introduction	5
	2.2 Effect of Surface Orientation	8
	2.3 Boiling Phenomena from Enhanced Surfaces	13
	2.4 Effect of Swelling	15
III	EXPERIMENTS	17
	3.1 Apparatus	17
	3.2 Experimental Procedure	31
	3.3 Instrumentation and Data Acquisition Procedures	33
IV	ANALYSIS OF SWELLING	37
	4.1 Analysis	37
	4.2 Results and Discussion	41
V	RESULTS AND DISCUSSION	45
	5.1 Experimental Results	45
	5.2 Discussion	55
	5.2.1 Single Phase Natural Convection.	55
	5.2.2 Hysteresis Effects in Incipient Boiling	61
	5.2.3 Nucleate Boiling	66
	5.2.4 Film Boiling	80
	5.2.5 Effect of Explosafe	88
	5.2.6 Effect of Pressure	90
	5.2.7 Evaluation of Constants in Rohsenow Correlation and Their Variation	92
VI	CONCLUSIONS AND SUGGESTIONS FOR FUTURE WORK.	102
	6.1 Conclusions	102
	6.2 Suggestions for Future Work	107
REFERENCES		110
APPENDIX A	MANUFACTURING PROCEDURE FOR UNB #2 SURFACE	113
APPENDIX B	DETAILED FLOW DIAGRAM OF THE SOFTWARE AND LISTINGS OF COMPUTER PROGRAM	114
APPENDIX C	HEAT LOSS CALCULATION METHOD AND POSSIBLE ERROR	120

APPENDIX A.4

TP 7518E

TANK CAR THERMAL RESPONSE ANALYSIS: VOLUME 5

SUPPORTING STUDIES

J.E.S.Venart, A.C.M.Sousa, F.R. Steward, et al

TABLE OF CONTENTS

		PAGE
I	DRAFT MANUSCRIPT "Transient Laminar Free Convection in Horizontal Cylinders".....	1-1
II	DRAFT MANUSCRIPT "Three Dimensional Formulation of the Radiant Heat Flux Variation in a Cylinder Engulfed in Flames".....	2-1
III	DRAFT MANUSCRIPT "Nucleate and Film Pool Boiling in R11: The Effects of Inclination Angle and Surface Enhancement".....	3-1
IV	COMPUTER PROGRAMME "Rail Tank Car Geometry".....	4-1
V	STUDY PAPER "Design, Construction and Testing of a Cylindrically Surfaced Calorimeter.....	5-1
VI	STUDY PAPER "Report on the Significance of Flare Radiation of Railway Cars Containing LPG"..	6-1
VII	STUDY PAPER "Report on Pool Fire Experiments Related to Tank Car Modelling".....	7-1
VIII	COMPUTER PROGRAMME "Development of Computer Code to Determine the Thermodynamic and Transport Properties of propane".....	8-1

APPENDIX A.5

TP 7519E

TANK CAR THERMAL RESPONSE ANALYSIS:

VOLUME 6

PUBLISHED PAPERS

TABLE OF CONTENTS

		PAGE
I	DISCUSSION: Paper I (A.F. Roberts) Fire and Explosion Loss Prevention and Safety Promotion in the Process Industries Proc. Sept. 12-16, (1983) Harrogate, IChemE.....	1-
II	ABSTRACT: "Thermal Modelling of LPG Rail Tank Cars - Exposed to a Fire Environment". 4th Int. Conf. on Mathematical Modeling, Zurich, (Aug. 15-17, 1983) p. 164-5.....	1-14
III	PAPER: "Thermal Conductivity and Contact Conductance of EXPLOSAFE", Proc. 18th Int. Thermal Conductivity Conf., Rapid City, South Dakota (Oct. 1983) in press.....	1-11
IV	ABSTRACT: "The Physical Behaviour of LPB Tank Cars under Accident Conditions", Comb. Inst. Can. Sect. Techn. Mtg. UNB *May, 1984.	1-5
V	ABSTRACT: "Radiative View Factors Associated with Rail Tank Car Fires", Comb. Inst. Com. Sect. Tech. Mtd., UNB, (May, 1984).....	1-6
VI	PAPER: "Experiments on the Physical Modeling of LPG Tank Cars under Accident Condition", Int. Symp. "Transport and Storage of LPG and LNG", Proc. Vol. 1 Royal Flemish Soc. of Engineers, Drugge (7-9th May 1984), p. 385-390.....	1-6
VII	PAPER: "Physical Behaviour of Pressure Liquefied Fuel Tanks in Fire Accidents". Proc. CSME 1984 Annual Conf. (May, 1984), Halifax, N.S., pp. 349-371.....	1-23
VIII	PAPER: "Transient Thermal Stratification in Heated Partially Filled Horizontal Cylindrical Tanks", ASME/AIChE National Heat Transfer Conference, Niagara Falls, N.Y., (Aug. 5-8, 1984), ASME Paper 84-HT-60.....	1-9
IX	PAPERS: "Incident Radiation from an Engulfing Pool Fire to a Horizontal Cylinder, Part I..	1-28
	"Incident Radiation From a Flare to a Horizontal Cylinder, Part II".....	1-31
	Fire Safety Journal (in press - accepted Feb. 6, 1984)	

APPENDIX A.6

TP 7520E

TANK CAR THERMAL RESPONSE ANALYSIS: VOLUME 7

POOL FIRE - FLARE INTERACTIONS

F.R. Steward, S. Wong

TABLE OF CONTENTS

		PAGE
I	INTRODUCTION	1
II	APPENDIX.....	4
III	SAMPLE CALCULATIONS.....	5

LIST OF FIGURES

PAGE

FIGURE 1 Top View of the Positions of the Equipment in the Pool Fire for Tests 1 to 3..... 7

FIGURE 2 Top View of the Positions of the Equipment in the Pool Fire for Tests 1 to 3..... 8

LIST OF TABLES

PAGE

TABLE I Heat Flux to Calorimeters and Radiometer in Proposal Pool Fire and Propan Flare Interaction Studies..... 3

TABLE II Experimental Results of Test #4..... 6

APPENDIX A.7

TP 7521E

TANK CAR THERMAL RESPONSE ANALYSIS:
VOLUME 8

TANK SIMULATOR TEST DATA

J.E.S.Venart, A.C.M. Sousa, F.R. Steward

TABLE OF CONTENTS

	PAGE
TEST DATA NUMBER 5	1
TEST DATA NUMBER 6	36
TEST DATA NUMBER 7	69
TEST DATA NUMBER 13	103
TEST DATA NUMBER 14	138
TEST DATA NUMBER 15	171
TEST DATA NUMBER 16	204
TEST DATA NUMBER 17	234
TEST DATA NUMBER 18	266
CHANGE OF LIQUID LEVEL WITH TIME	298
TEST 15	299
TEST 16	300
TEST 17	301